Characterisation of a Novel Subtilase Cytotoxin from Shiga Toxigenic *Escherichia coli*

Damien Christopher Chen Sau Chong

A thesis submitted in fulfilment of the requirements
for the degree of Doctor of Philosophy

School of Molecular and Biomedical Science
Discipline of Microbiology and Immunology
The University of Adelaide
Australia 5005

October 2008

Chapter 3

Intracellular Trafficking

3.1 Introduction

Typically, the substrates for the various A subunits of AB_5 toxins are essential components of the host cell biosynthetic or regulatory machinery located in the cytosol, necessitating translocation of the A subunit across a membranous barrier in order to engage its target. For toxins such as diphtheria toxin and the anthrax toxins, cell entry involves internalisation into endosomes, with the low pH of this compartment triggering direct translocation of the enzymatic component of the toxin into the cytosol (Sandvig and van Deurs, 2002). For AB_5 toxins such as Stx and Ctx, trafficking is more complex. After binding to their respective glycolipid receptors via pentameric B subunits, they are internalised by receptor-mediated endocytosis. The toxin-receptor complexes then enter a retrograde transport pathway and traffic via the TGN and Golgi to the ER (Sandvig *et al.*, 1992; Sandvig and van Deurs, 2002; Lencer and Tsai, 2003). The B subunits of both Stx and Ctx are essential and sufficient for this trafficking. Retro-translocation of the A subunits from the ER lumen to the cytosol is then achieved by subversion of the protein-translocation channel Sec61 (Lencer and Tsai, 2003; Yu and Haslam, 2005).

SubAB is the only toxin known to target a eukaryotic chaperone protein or a component of the ER. It is also the only AB toxin whose specific substrate is not located in the cytosolic compartment. For this reason, the uptake and trafficking of SubAB within target cells was investigated, and its behaviour compared with those of Ctx and Stx.

3.2 Results

3.2.1 Investigation of SubAB Trafficking by Electron Microscopy

Visualisation of SubAB trafficking in Vero cells was initially examined by TEM. This involved incubating a flask of cells with SubAB, washing away unbound toxin, dehydrating the cell pellet in a graded series of ethanol changes and embedding in LR White resin. Sections were mounted on grids and SubAB was detected by immunogold using murine anti-SubA and viewed by TEM as described in Section 2.17.4. Sections cut from LR White cell pellets contained cells that appeared to be damaged or sheared with a complete absence of gold particles. Despite altering the sample preparation procedure, including pelleting, dehydration and resin infiltration conditions, cells continued to present a damaged morphology.

An alternative approach was to grow Vero cells in Transwells, processing the polycarbonate membrane insert as before and detecting SubAB by immunogold labelling (Figure 3.1a). While Vero cells appeared to be normal, immunolabelling was non-specific as gold particles appeared outside the cell (red circles). Furthermore, the labelling technique did not show SubAB accumulation at any point on the cell surface or in subcellular compartments but rather, the toxin was evenly distributed within the cell (blue circles). Cells grown in Transwells were also incubated with SubAB conjugated to peroxidase (SubAB-POD) and reacted with DAB. While SubAB-POD occasionally produced a weak signal on the surface of some cells there was no evidence of its internalisation (Figure 3.1b). A TLC toxin overlay assay (described in Section 2.10.5) comparing the GGS affinities of SubAB-POD with native SubAB confirmed that conjugation with POD abolished the affinity of SubAB for the GGS species (R_f = 0.347 and 0.396) determined in Section 4.2.1 (Figure 3.2). Hence, a different approach was sought to investigate the subcellular trafficking of SubAB.

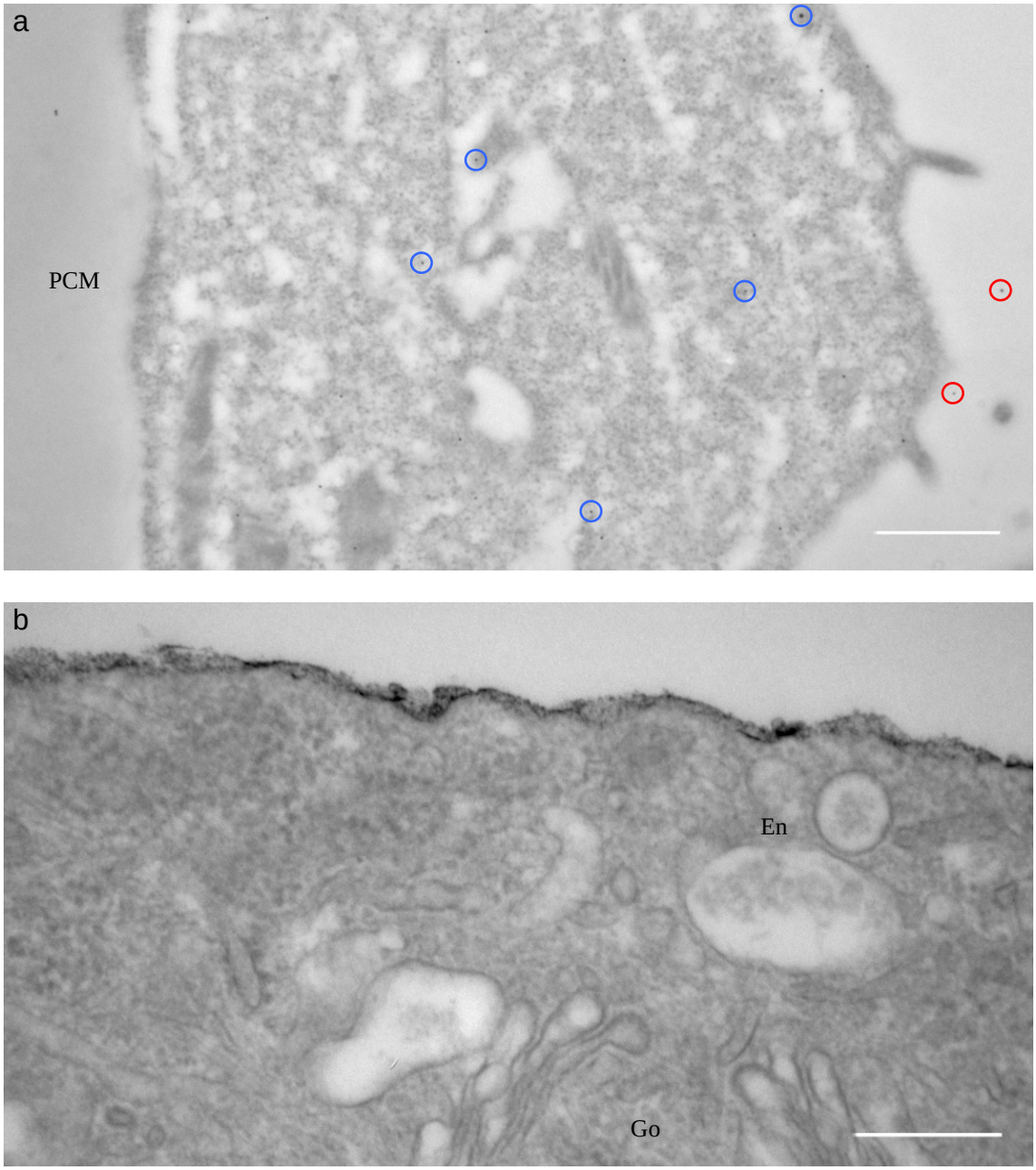

Figure 3.1: Visualisation of SubAB by TEM.

Vero cells grown in Transwells were incubated with 5 µg.ml^{-1} SubAB for 1 h, mounted onto grids and SubAB was detected by immunogold labelling (circles) using mouse anti-SubA antiserum (a). Red circles indicate non-specific, extracellular labelling. Alternatively, Vero cells were incubated with 5 µg.ml^{-1} SubAB-POD for 1 h then processed for DAB cytochemistry and heavy metal staining (b) En: endosome; Go: Golgi; PCM: polycarbonate membrane. Sections were viewed by transmission electron microscopy. Scale bars = 500 nm.

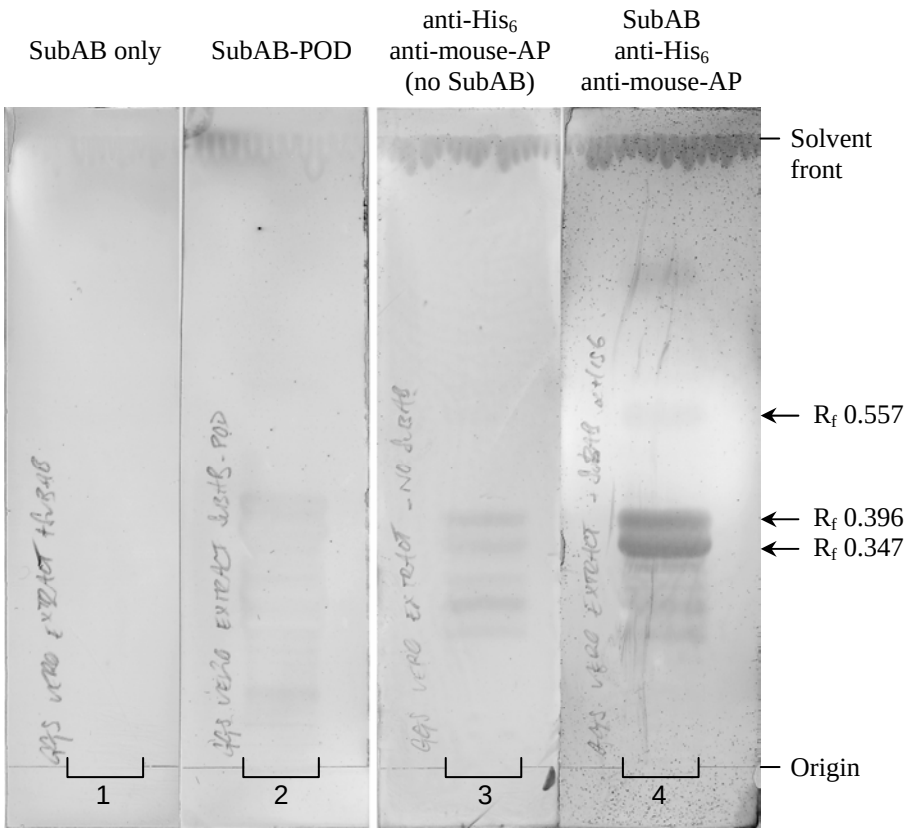

Figure 3.2: Binding specificity of SubAB-POD.

Vero cell GGS extracts were run on TLC plates in chloroform:methanol:0.2% (w/v) $CaCl_2$ (60:35:8), and sprayed with PIBM. Lanes 1 and 2 were incubated with 1 µg.ml^{-1} SubAB and SubAB-POD, respectively and developed with 4-chloro-1-naphthol. Lanes 3 and 4 were incubated with or without 1 µg.ml^{-1} SubAB, then probed with mouse anti-His_6 followed by anti-mouse-AP and were developed using X-phosphate.

3.2.2 Affect of Fluorochrome and SubA Presence and Activity on Trafficking

As multiple attempts at visualising SubAB trafficking by TEM were unsuccessful, an alternative approach was employed in which the intracellular transport of fluorescently-labelled SubAB was observed in relation to fluorescent toxins and subcellular markers. These were labelled with dextran-TR, Tf-TR, Caveolin-EGFP, WGA-TR, anti-Golgin-97, anti-BiP, ER-Tracker Red, LysoTracker DND-99 and MitoTracker CMXRos as described in Section 2.14.3. Fluorescent co-localisation of SubAB-OG with organelle markers (usually TR) was indicated by yellow co-incidental pixels acquired by dual-laser confocal microscopy.

To address the possibility of the fluorochrome labelling altering cell specificity or trafficking of SubAB, Vero cells were initially incubated in media containing SubAB-OG labelled at various dye:protein molar ratios (MR) using the OG Protein Labeling Kit (Section 2.14.2). The SubAB-OG labelled using an MR of 20:1 was not internalised by Vero cells (Figure 3.3), while SubAB-OG (MR = 4:1) produced a signal that was insufficient to acquire (not shown). However, SubAB-OG (MR = 8:1) was internalised by Vero cells, and provided an acceptable signal strength with minimal

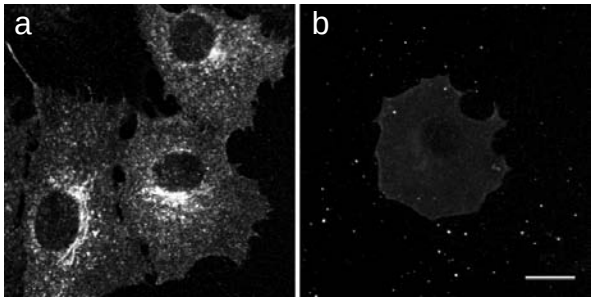

Figure 3.3: Affect of dye:protein ratio on SubAB trafficking.

Vero cells were co-incubated for 30 min with 1 μg.ml^{-1} of either SubAB-OG (MR = 8) (a) or SubAB-OG (MR = 20) (b). Unbound proteins were washed off with PBS and cells were incubated for a further 30 min. Formalin fixed cells were then viewed by laser confocal microscopy (60 × oil objective). Scale bar = 25 μm.

fluorochrome labelling to reduce its impact on the function of native SubAB. Hence, this ratio was standardised for all subsequent fluorochrome labelling reactions.

To determine whether the type of fluorochrome used affected trafficking, Vero cells were co-incubated with both SubAB-OG and SubAB-TR (Section 2.15.2). The two species were observed to completely co-localise, demonstrating that their cellular specificity and trafficking pathways were identical (Figure 3.4a). Furthermore, the enzymatic activity of SubA did not affect cellular uptake or trafficking, as incubation of Vero cells with the inactive mutant toxin $SubA_{A272}B$ labelled with OG resulted in the same staining pattern as SubAB-TR (Figure 3.4b). Likewise, subcellular transport of SubB-OG was identical to that of SubAB-TR (Figure 3.4c). Thus, SubB is sufficient to direct uptake and trafficking, and neither the enzymatic activity of SubA nor the presence of the A subunit is required or impacts in any obvious way on cellular uptake and trafficking.

The affect of fluorochrome labelling on the cytotoxic capacity of SubAB was also investigated. Vero cells were seeded in a 96-well microtitre plate and incubated for three days with serially diluted SubAB or SubAB-OG (described in Section 2.9). Both native SubAB and SubAB-OG were highly toxic for Vero cells, with identical specific activities of 10^{10} $CD_{50}.mg^{-1}$. That is, 0.1 pg of either SubAB or SubAB-OG is sufficient to kill at least 50% of the ~3×10^4 Vero cells present in a microtitre plate well. This indicates that cytotoxic activity of SubAB was not diminished by fluorochrome labelling. Accordingly, SubAB-OG (MR = 8:1) was used throughout these trafficking studies.

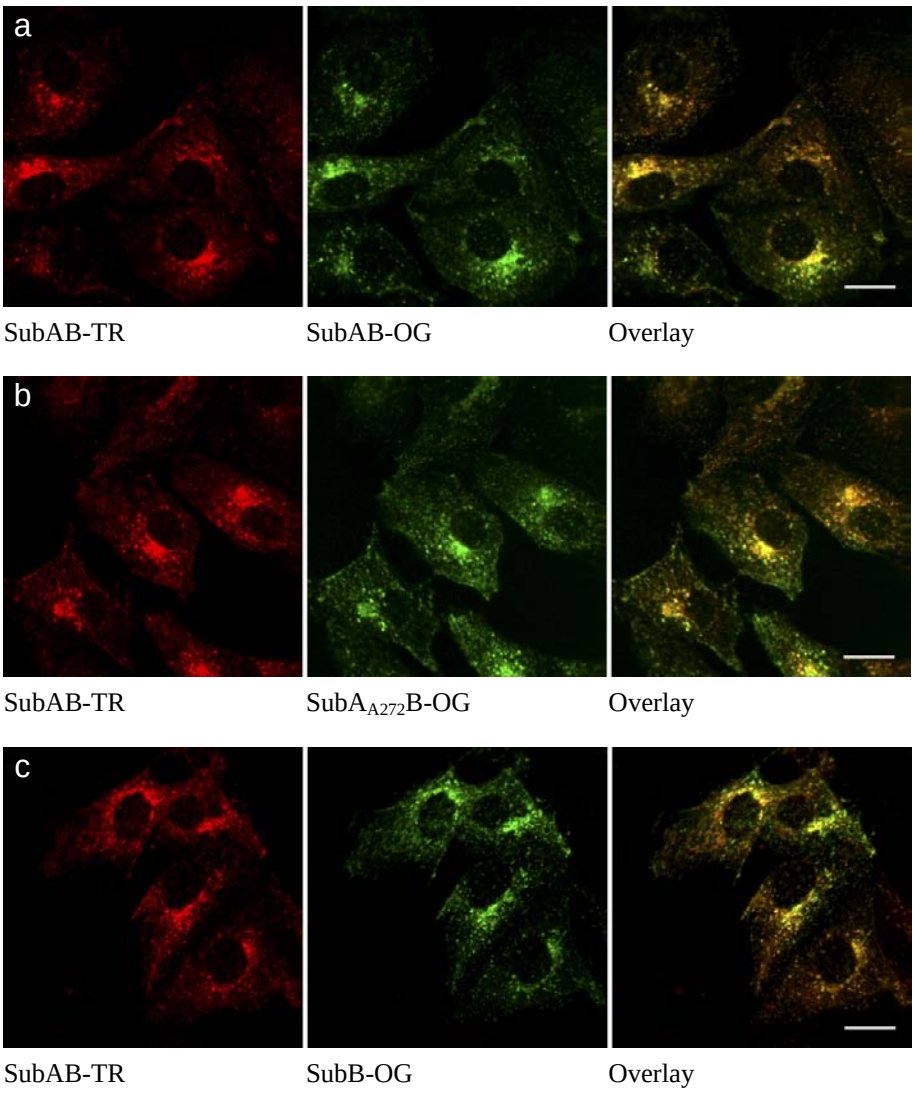

Figure 3.4: Affect of fluorochrome labelling and SubA$_{A272}$ on SubB trafficking.

Vero cells were co-incubated for 30 min with 1 µg.ml^{-1} SubAB-TR and SubAB-OG (a), SubA$_{A272}$B-OG (b) or 0.5 µg.ml^{-1} SubB-OG (c). Unbound proteins were washed off with PBS and cells were incubated for a further 30 min. Formalin fixed cells were then viewed by dual-laser confocal microscopy (60 × oil objective). Scale bars = 25 µm.

3.2.3 SubAB Trafficking in Various Cell Lines

HCT-8, HeLa and N2A cells were assessed for their ability to bind and internalise SubAB-OG. Cells were exposed to SubAB-OG for 30 min and compared to results obtained using Vero cells (Figure 3.5). When compared to Vero cells (Figure 3.5d), a limited amount of toxin bound to the HCT-8 cell surface with negligible internalisation. Similarly, despite more SubAB-OG adhering to the outer membrane of HeLa cells than HCT-8 cells, toxin uptake was not clearly demonstrated. Curiously, while SubAB-OG was trafficked in N2A cells, it was rarely observed and presented with a very weak signal. Accordingly, Vero cells were used throughout this study unless otherwise indicated.

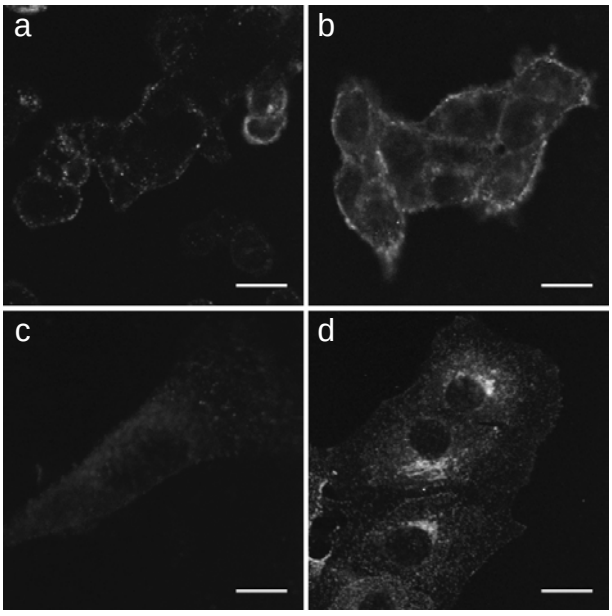

Figure 3.5: Variation in SubAB-OG binding and trafficking in different cell lines.

HCT-8 (a), HeLa (b), N2A (c) and Vero cells (d) were exposed to 1 $\mu g.ml^{-1}$ SubAB-OG for 30 min then formalin fixed. Samples were viewed by laser confocal microscopy (60 × oil objective). Scale bars = 25 µm.

3.2.4 Fluorescence Co-trafficking with CtxB and StxB

To investigate the uptake and intracellular trafficking pathway of SubAB, the transport of fluorescent SubAB in Vero cells was initially compared to that of other AB_5 toxins by confocal fluorescence co-localisation. The retro-translocation pathways of Stx (Sandvig *et al.*, 1992) and Ctx holotoxins (Lencer and Tsai, 2003) have been previously characterised and shown to be identical to that of their respective B pentamers (Fujinaga *et al.*, 2003; Khine *et al.*, 2004). When Vero cells were co-incubated with SubAB-OG and either StxB-TR or CtxB-AF594, there were marked differences in tropism for individual cells (Figure 3.6). Some cells bound and internalised SubAB or CtxB or StxB alone, while others took up both or neither of the toxins to which they were exposed. For Vero monolayers treated with SubAB-OG and StxB-TR, examination of multiple fields (>100 cells examined) indicated that 20.7% of the cells bound SubAB alone, 16.2% bound StxB alone, 35.2% bound both toxins, and 27.9% remained unstained. For monolayers treated with SubAB-OG and CtxBAF594, 18.9% of cells bound SubAB alone, 47.8% bound CtxB alone, 27.0% bound both toxins, and 6.3% remained unstained. In cells that simultaneously internalised two toxins, fluorescence co-localisation was prevalent in juxtanuclear regions and occasional puncta. However, there was also evidence of differential staining of puncta demonstrating that whilst intracellular trafficking pathways appeared to be similar for SubAB and CtxB (63.2% overlap) or StxB (64.2% overlap), they were not identical.

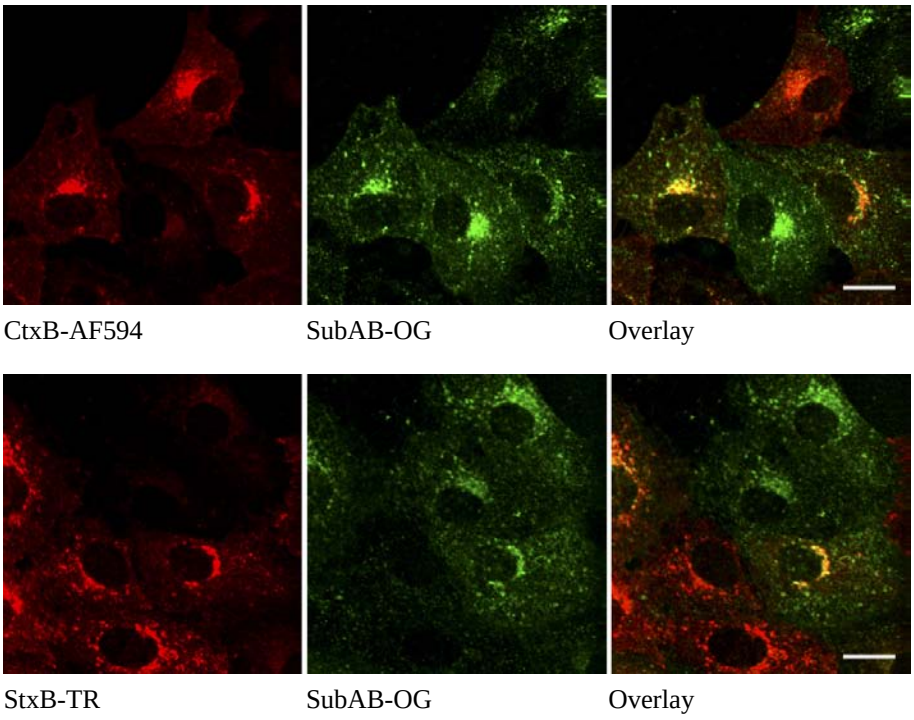

Figure 3.6: Co-trafficking of SubAB with CtxB and StxB.

Vero cells exposed to 1 μg.ml^{-1} SubAB-OG were co-incubated with 0.5 μg.ml^{-1} StxB-TR or 0.5 μg.ml^{-1} CtxB-AF594 for 30 min. Unbound proteins were washed off with PBS and cells were incubated for a further 30 min. Formalin fixed cells were then viewed by dual-laser confocal microscopy (60 × oil objective). Scale bars = 25 μm.

3.2.5 Fluorescence Co-localisation with Subcellular Markers

To further examine the trafficking route of SubAB within Vero cells after a 1 h incubation, the co-localisation of SubAB-OG with various fluorescent organelle markers was investigated (Figure 3.7). Although SubAB-containing vesicles co-localised with the fluid phase endosome marker dextran-TR (88.7% overlap) and Tf-TR, which is endocytosed via clathrin-coated vesicles (56.1% overlap), negligible co-localisation of SubAB-TR with caveolae was noted in transfected Vero cells expressing Caveolin-1-EGFP (3.7% overlap). Similarly, transport of SubAB-OG to lysosomes labelled with LysoTracker DND-99 was rarely observed (2.0% overlap). This was not unexpected, since trafficking of AB_5 toxins to lysosomes results in toxin degradation, and typically occurs only in non-sensitive cell types (Sandvig and van Deurs, 1996).

Translocation via the TGN and Golgi was confirmed by co-localisation with WGA-TR (93% overlap). Similarly, immunofluorescent labelling of Golgin-97, a membrane protein localised to the Golgi's cytoplasmic face (Verma *et al.*, 2000), in Vero cells exposed to SubAB-OG revealed translocation to the juxtanuclear Golgi apparatus (88.7% overlap). Co-localisation with immunolabelled BiP showed toxin association with its intracellular substrate and by inference, its transport to the ER compartment (32.5% overlap). Trafficking to the ER was also confirmed by directly labelling the ER with ER-Tracker Red in cells exposed to SubAB-OG (27.7% overlap). Co-localisation of the toxin with mitochondria labelled with MitoTracker CMXRos was not observed (~1% overlap).

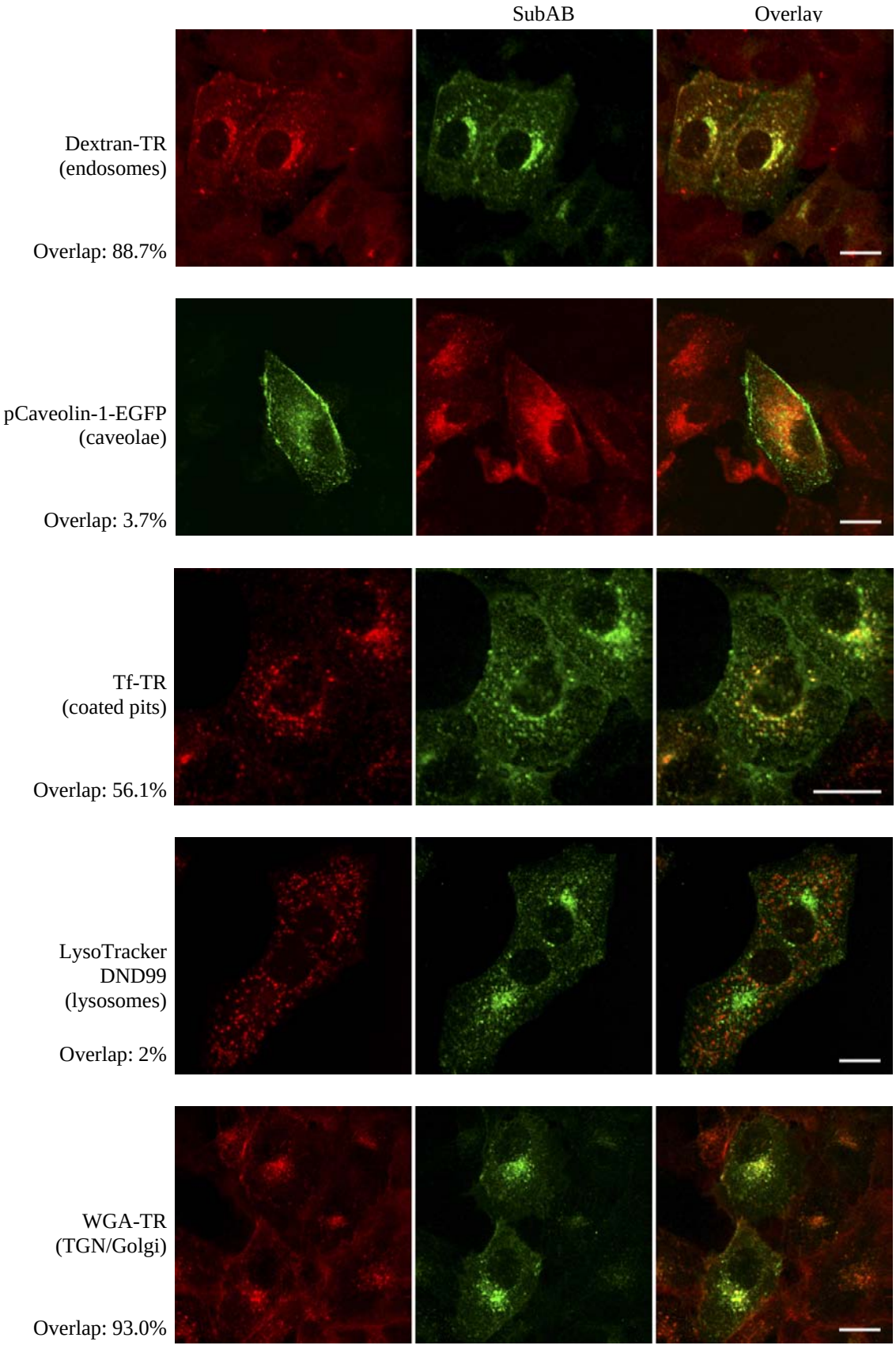
SubAB
Overlay
Dextran-TR
(endosomes)
Overlap: 88.7%
pCaveolin-1-EGFP
(caveolae)
Overlap: 3.7%
Tf-TR
(coated pits)
Overlap: 56.1%
LysoTracker
DND99
(lysosomes)
Overlap: 2%
WGA-TR
(TGN/Golgi)
Overlap: 93.0%

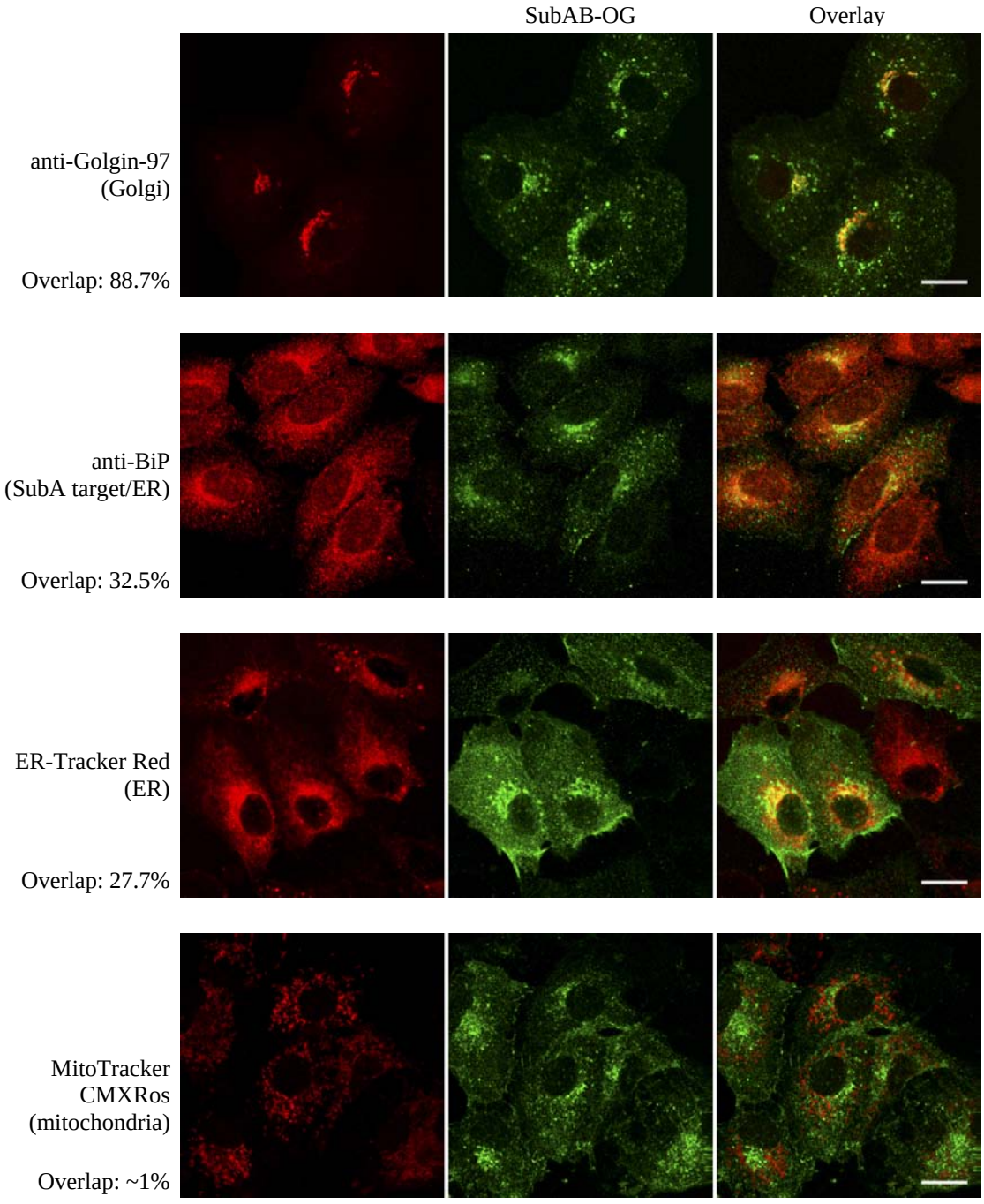

Figure 3.7: Subcellular localisation of SubAB.

Vero cells were exposed to 1 μg.ml^{-1} SubAB-OG/-TR for 30 min. Unbound proteins were washed off with PBS and incubated for a further 30 min in media supplemented with 50 μg.ml^{-1} Dextran-TR, 5 μg.ml^{-1} Tf-TR, 100 nM LysoTracker DND-99, 5 μg.ml^{-1} WGA-TR, or 400 nM MitoTracker, as indicated. Alternatively, cells were transfected with pCaveolin-1-EGFP using Lipofectamine 2000 and selected with geneticin. For immunofluorescence, cells were formalin fixed and permeabilised with Triton X-100, treated with anti-Golgin-97 or anti-BiP, and detected using AF594-conjugated anti-mouse and anti-goat secondary antibodies, respectively. Samples were viewed by dual-laser confocal microscopy (60 × oil objective except for Tf-TR: 100 × oil). Scale bars = 25 μm.

While time-lapse live cell imaging was not possible with immunolabelled organelles, the distribution of SubAB-OG was examined at an earlier timepoint of 5 min for comparison with respect to selected subcellular markers used in Figure 3.7 (Figure 3.8). In Vero cells that internalised SubAB-OG after a 5-min exposure, the toxin was observed in clathrin-coated vesicles as indicated by its co-localisation with Tf-TR (40% overlap). However, at this same timepoint, SubAB-OG did not appear to co-localise with anti-Golgin-97 or anti-BiP (both exhibited ~1% overlap), indicating that detectable levels of toxin had yet to arrive at the Golgi nor the ER, respectively.

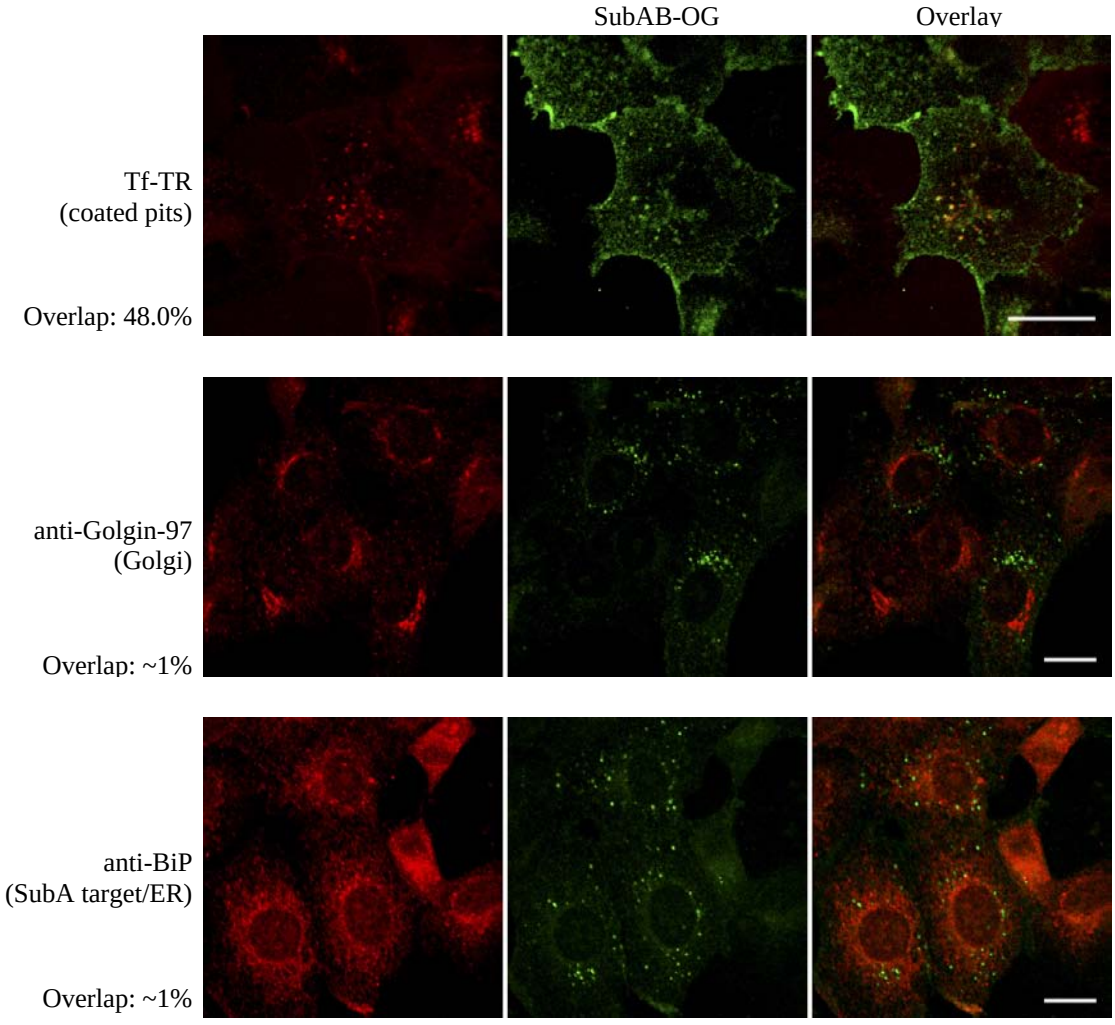

Figure 3.8: Subcellular localisation of SubAB after 5 min.

Vero cells were exposed to 1 μg.ml^{-1} SubAB-OG, with 5 μg.ml^{-1} Tf-TR where indicated for 5 min. For immunofluorescence, cells were formalin fixed afetr exposure to 1 μg.ml^{-1} SubAB-OG, permeabilised with Triton X-100, treated ith anti-Golgin-97 or anti-BiP, and detected using AF594-conjugated anti-mouse and anti-goat secondary antibodies, respectively. Samples were viewed by dual-laser confocal microscopy (60 × oil objective, except for Tf-TR: 100 × oil). Scale bars = 25 μm.

3.2.6 Inhibition of Trafficking

Further information on the intracellular trafficking pathway of SubAB in comparison with CtxB and StxB was obtained by subjecting Vero cells to a variety of pre-treatments reported to obstruct retrograde transport. Cells were then exposed to SubAB-OG, CtxB-AF594 or StxB-TR for 3 h and examined for evidence of disruption of trafficking. To establish if SubAB-OG was internalised by a passive or an active mechanism, cells were subjected to a 4°C temperature block to diminish host cell metabolic activity (Figure 3.9).

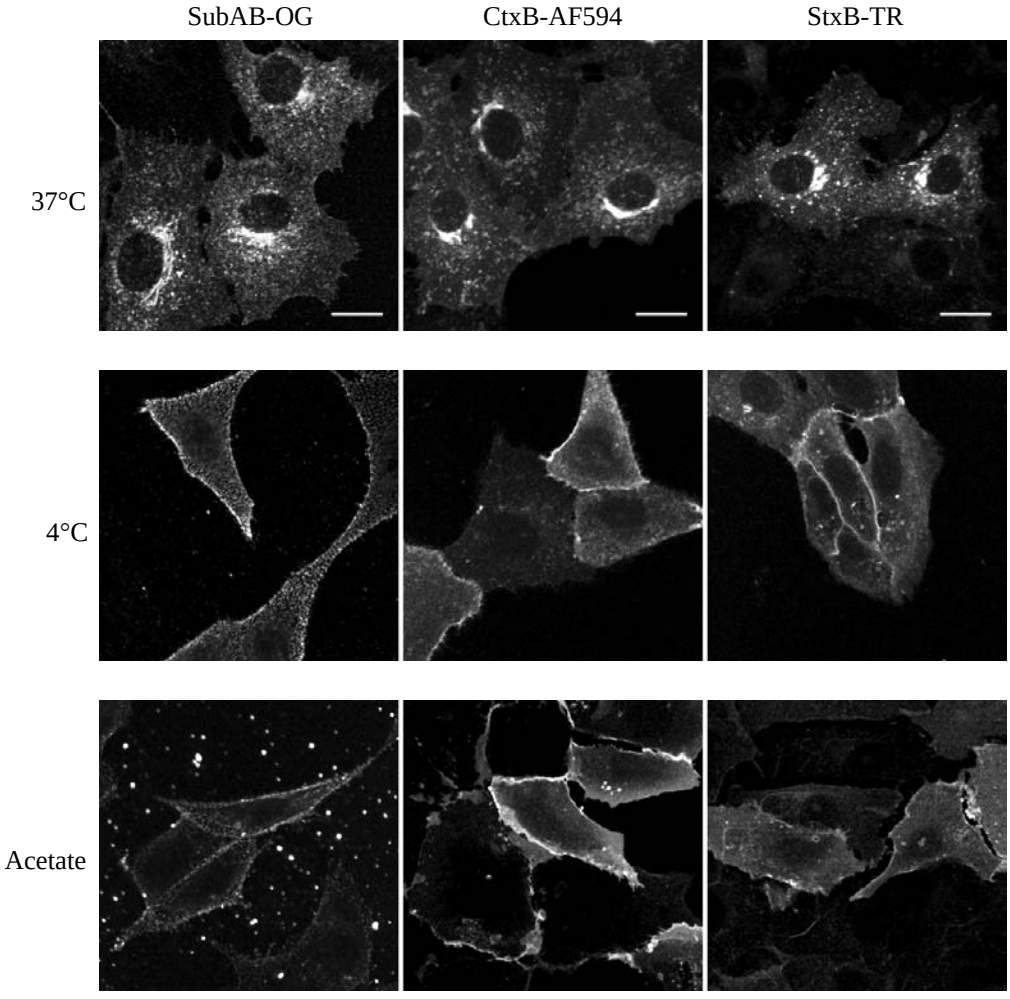

Figure 3.9: Inhibition of trafficking with a temperature block and acetate.

Vero cells were pre-incubated for 30 min at 4°C or in media supplemented with 60 mM acetate, and then exposed to 1 μg.ml^{-1} SubAB-OG, 0.5 μg.ml^{-1} CtxB-AF594, or 0.5 μg.ml^{-1} StxB-TR for 3 h, while maintaining inhibitory conditions. Samples were viewed by laser confocal microscopy (60 × oil objective). Scale bars = 25 μm.

Binding of SubAB-OG to the Vero cell surface was independent of the incubation temperature. However, unlike control cells grown at 37°C, those incubated at 4°C did not internalise SubAB-OG indicating that toxin entry occurs via an active mechanism. Lowering the cytosolic pH with media supplemented with acetate is known to prevent invagination of the plasma membrane and subsequent vesicle formation (Khine *et al.*, 2004). SubAB-OG accumulated on the surface of cells treated with 60 mM acetate. These data indicate that in normal cells, SubAB is actively internalised within membrane-bound vesicles. Similar effects were observed for CtxB-AF594 and StxB-TR. Targeting of vesicles containing SubAB-OG to distinct crescent-shaped Golgi was no longer apparent in the presence of nocodazole, which depolymerises microtubules in an energy-dependent manner (De Brabander *et al.*, 1976; Turner and Tartakoff, 1989), indicating SubAB-OG may exploit a microtubule-dependent endosomal pathway. Similar redistributions were also noted with CtxB-AF594 and StxB-TR in nocodazole-treated cells (Figure 3.10a). However, the drug has been reported to dissociate the Golgi apparatus (Lippincott-Schwartz *et al.*, 1990), and trafficking of SubAB-OG to the fragmented Golgi continued in the presence of nocodazole as demonstrated by fluorescence co-localisation with immunolabelled Golgin-97 (Figure 3.10b).

Treatment of cells with the drug CPZ inhibits clathrin-dependent endocytosis by inducing the loss of coated pits from the cell surface (Wang *et al.*, 1993; Orlandi and Fishman, 1998) and did not prevent SubAB-OG uptake at concentrations up to 10 $\mu g.ml^{-1}$ (Figure 3.11). When employed at concentrations above 10 $\mu g.ml^{-1}$, CPZ clearly prevented internalisation of SubAB-OG. However, at such concentrations the compound also had a cytopathic effect on Vero cells, characterised by rounding of cells and detachment from the substrata (Figure 3.11d).

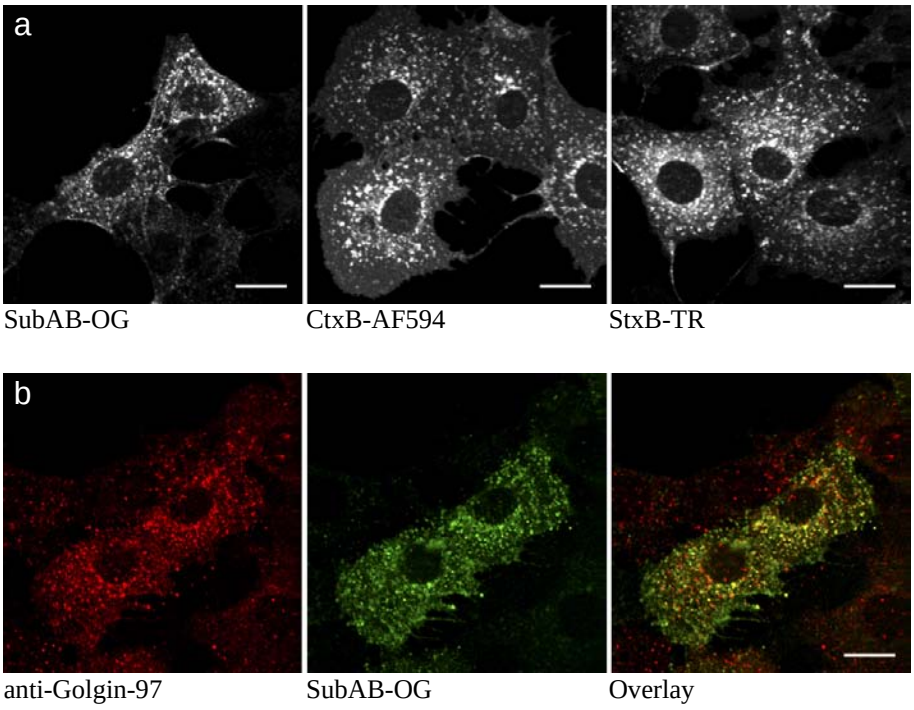

Figure 3.10: Inhibition of trafficking with nocodazole.

Vero cells were pre-incubated for 30 min in media supplemented with 1.5 µg.ml^{-1} nocodazole, and then exposed to 1 µg.ml^{-1} SubAB-OG, 0.5 µg.ml^{-1} CtxB-AF594, or 0.5 µg.ml^{-1} StxB-TR for 3 h, while maintaining inhibitory conditions (a). For immunofluorescence co-localisation (b), nocodazole-treated samples exposed to SubAB-OG were formalin fixed and permeabilised. Golgi were labelled with anti-Golgin-97 and detected with anti-mouse-AF594. Samples were viewed by dual-laser confocal microscopy (60 × oil objective). Scale bars = 25 µm.

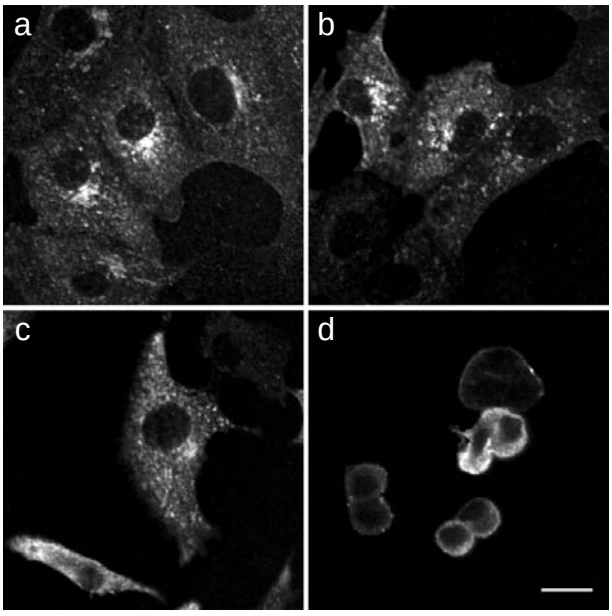

Figure 3.11: Affect of CPZ on SubAB-OG trafficking in Vero cells.

Vero cells were pre-incubated for 30 min in normal growth media (a) or supplemented with 7.5 µg.ml^{-1} (b), 10 µg.ml^{-1} (c) or 12.5 µg.ml^{-1} CPZ (d), and then exposed to 1 µg.ml^{-1} SubAB-OG for 3 h, while maintaining inhibitory conditions. Samples were viewed by laser confocal microscopy (60 × oil objective). Scale bar = 25 µm.

To investigate clathrin-mediated endocytosis further, Vero cells were pre-treated with PAO, which inhibits clathrin-dependent endocytosis by reacting with vicinal sulfhydryls to form stable ring structures (Bates *et al.*, 2000; Takano *et al.*, 2004). PAO had no effect on cell viability at the dose employed. In cells treated with PAO, surface accumulation of SubAB-OG was evident, indicating that endocytosis of SubAB-OG is mediated by a clathrin-dependent pathway. In contrast, PAO did not block internalisation of either CtxB-AF594 or StxB-TR, although there was some perturbation of retrograde transport in both cases (Figure 3.12a). Furthermore, to determine if PAO specifically inhibits clathrin-dependent internalisation, the trafficking of Tf-TR was observed in PAO-treated Vero cells (Figure 3.12b). Tf-TR accumulated on the cell surface in the presence of PAO and there was extensive co-localisation with SubAB-OG

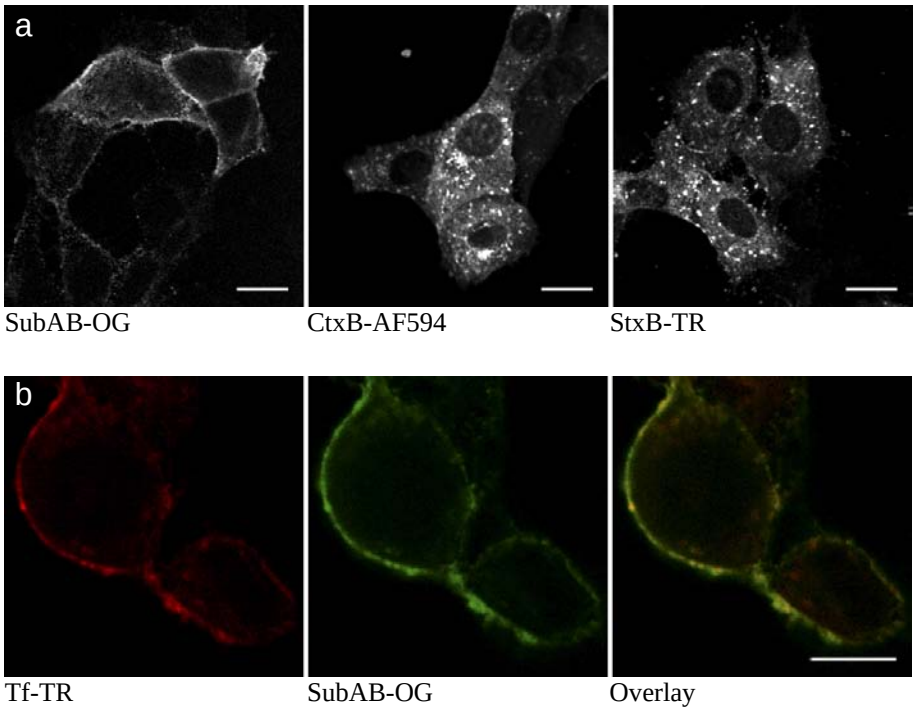

Figure 3.12: Affect of PAO on SubAB-OG trafficking in Vero cells.

Vero cells were pre-incubated for 30 min in normal growth media supplemented with 1.25 µM PAO, and then exposed to 1 µg.ml^{-1} SubAB-OG, 0.5 µg.ml^{-1} CtxB-AF594, or 0.5 µg.ml^{-1} StxB-TR for 3 h, while maintaining inhibitory conditions (a). For fluorescence co-localisation (b) PAO-treated samples were co-incubated with SubAB-OG and 5 µg.ml^{-1} Tf-TR. Samples in were viewed by laser confocal microscopy (a: 60 ×, b: 100 × oil objectives). Scale bars = 25 µm.

(86.7% overlap), confirming that under our experimental conditions, PAO is a specific inhibitor of clathrin-dependent internalisation.

Treatment with filipin, which binds cholesterol and inhibits caveolae formation (Rothberg *et al.*, 1992), did not prevent SubAB-OG uptake at 0.75 μg.ml^{-1} (Figure 3.13b). Although filipin concentrations above 0.75 μg.ml^{-1} disrupted Golgi targeting (Figure 3.13c) and ultimately internalisation of SubAB-OG (Figure 3.13d), such concentrations clearly affected cell morphology and viability.

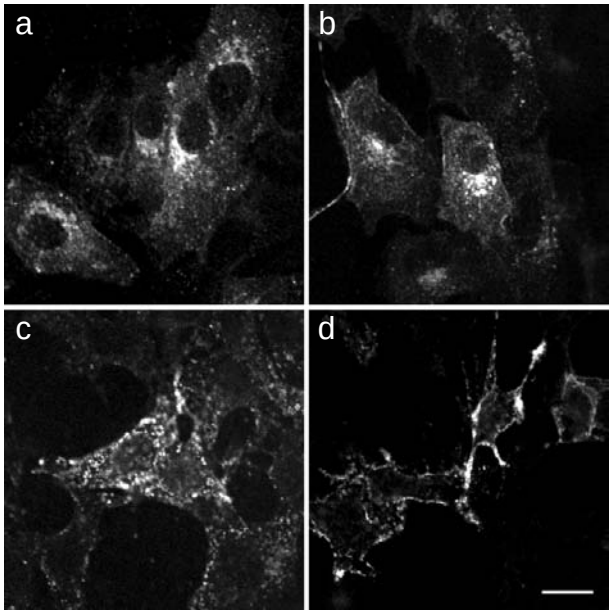

Figure 3.13: Affect of filipin on SubAB-OG trafficking in Vero cells.

Vero cells were pre-incubated for 30 min in normal growth media (a) or supplemented with 0.75 μg.ml^{-1} (b), 1 μg.ml^{-1} (c) or 1.25 μg.ml^{-1} (d) filipin, and then exposed to 1 μg.ml^{-1} SubAB-OG for 3 h, while maintaining inhibitory conditions. Samples were viewed by laser confocal microscopy (60 × oil objective). Scale bar = 25 μm.

To investigate this further, cells were depleted of cholesterol by pre-treatment with genistein and/or MβCD (Le and Nabi, 2003); these treatments had no effect on cell viability at the doses employed. Genistein and MβCD, singly or in combination, had minimal impact upon SubAB-OG trafficking. In contrast, MβCD caused marked surface accumulation of CtxB-AF594, while both MβCD and genistein affected targeting of StxB-TR to the Golgi (Figure 3.14).

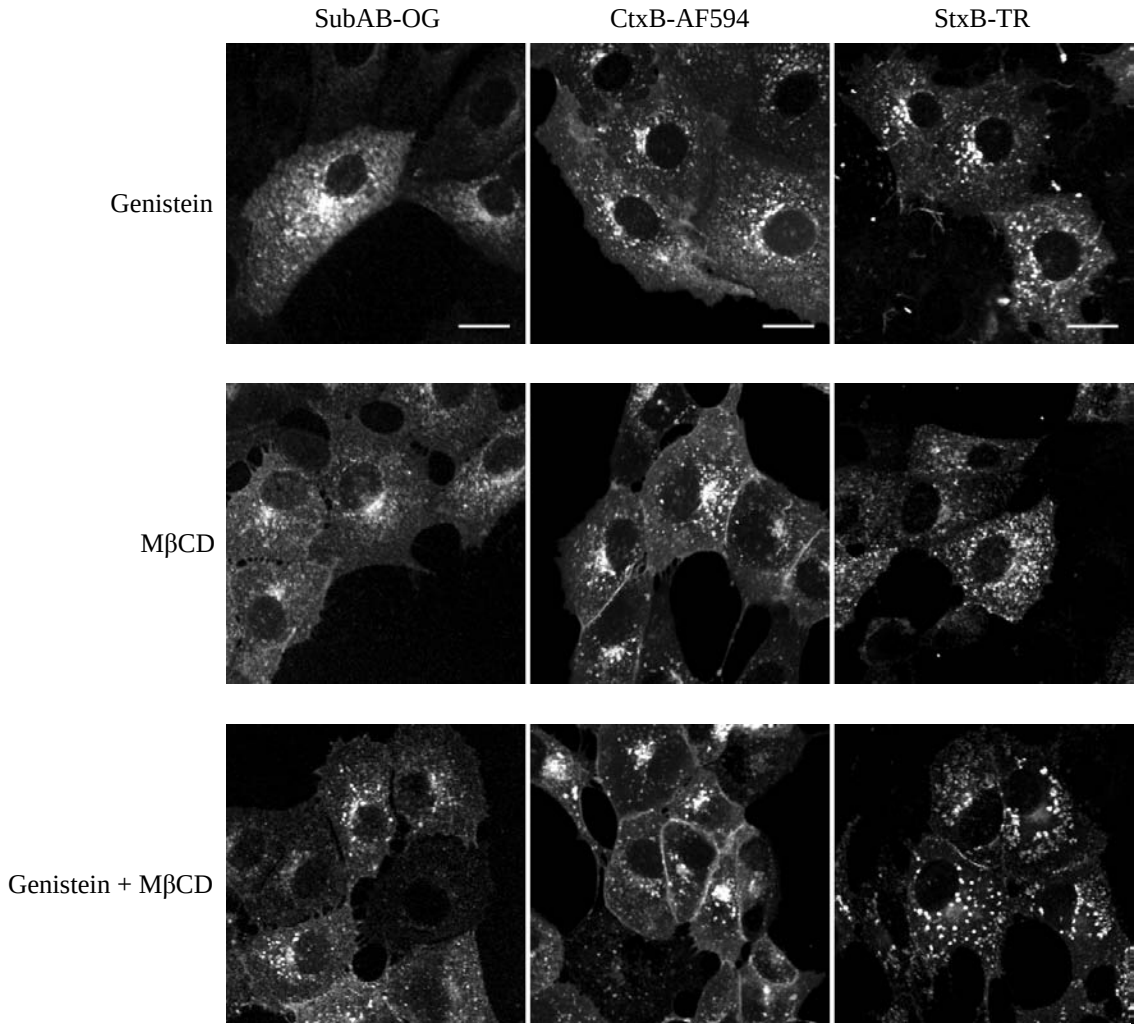

Figure 3.14: Inhibition of trafficking by cholesterol depletion.

Vero cells were pre-incubated for 30 min in media supplemented with 100 μg.ml^{-1} genistein and/or 5 mM MβCD, and then exposed to 1 μg.ml^{-1} SubAB-OG, 0.5 μg.ml^{-1} CtxB-AF594, or 0.5 μg.ml^{-1} StxB-TR for 3 h, while maintaining inhibitory conditions. Samples were viewed by laser confocal microscopy (60 × oil objective). Scale bars = 25 μm.

The Golgi-disrupting agent BFA reversibly fuses endosomes with the TGN and the *trans*-, *medial*- and *cis*-Golgi cisternae with the ER (Lippincott-Schwartz *et al.*, 1991; Donta *et al.*, 1993). In this study, compared to SubAB-OG trafficking in normal cells (Figure 3.9), BFA treatment caused all three labelled toxins to accumulate within collapsed Golgi bodies (Figure 3.15a), which were identified by labelling with WGA-TR (Figure 3.15b). These were distinct from the crescent-shaped Golgi observed in control cells grown at 37°C (Figure 3.9).

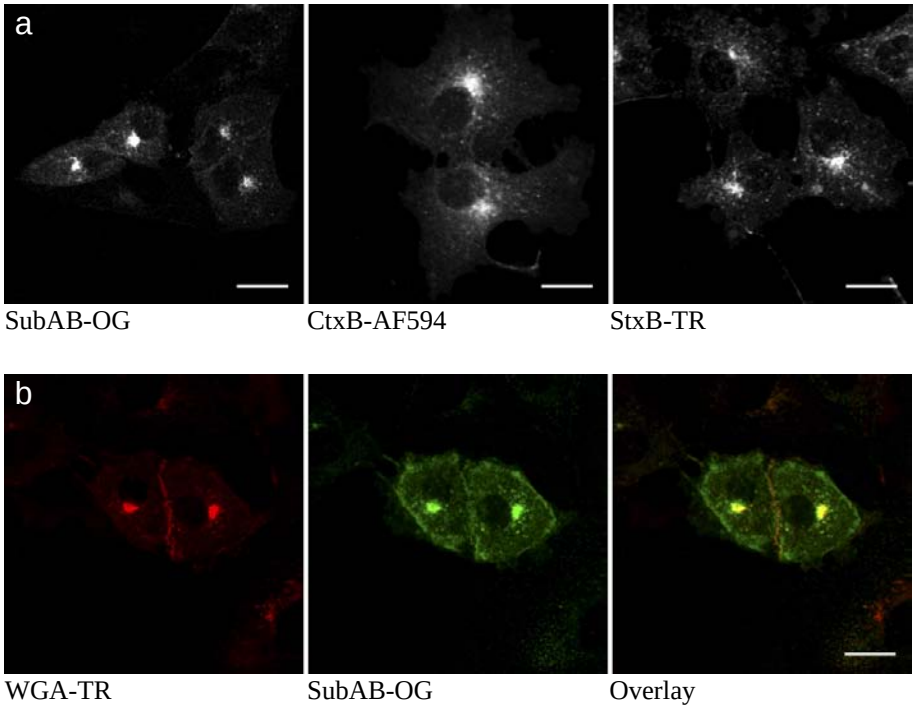

Figure 3.15: Inhibition of trafficking by Golgi disruption.

Vero cells were pre-incubated for 30 min in media supplemented with 0.5 µg.ml^{-1} BFA, and then exposed to 1 µg.ml^{-1} SubAB-OG, 0.5 µg.ml^{-1} CtxB-AF594, or 0.5 µg.ml^{-1} StxB-TR for 3 h, while maintaining inhibitory conditions (a). For fluorescence co-localisation (b), BFA-treated samples exposed to SubAB-OG were co-incubated for 30 min with 5 µg.ml^{-1} WGA-TR to label TGN/Golgi. Samples were viewed by dual-laser confocal microscopy (60 × oil objective). Scale bars = 25 µm.

3.2.7 Inhibition of Cytotoxicity

Previous studies with Ctx showed that in the presence of inhibitors, trace amounts of toxin may still be delivered to its target despite being unable to visualise such trafficking by fluorescence microscopy (Massol *et al.*, 2004). This indicates that prevention of toxin uptake does not necessarily correlate with the abrogation of cytotoxicity. To determine whether any of the inhibitors employed in Section 3.2.6 were capable of completely blocking retrograde transport of native SubAB to the ER, cleavage of its substrate BiP was assessed by Western blotting. This is an extremely sensitive measure of arrival of toxin in the ER compartment, as it has been previously shown that less than 1 $ng.ml^{-1}$ exogenous SubAB is sufficient to degrade all of the BiP in Vero cell monolayers within 60 min (Paton *et al.*, 2006a).

While nocodazole and filipin were capable of altering the distribution of SubAB-OG within Vero cells, neither compound protected BiP from cleavage by the toxin, as evidenced by complete loss of the intact 72-kDa BiP species, and appearance of its 28-kDa C-terminal cleavage product (Figure 3.16). This also indicated that the Golgi retained its ability to retrotranslocate SubAB to the ER despite the organelle's fragmentation in the presence of nocodazole. Similarly, genistein and MβCD treatments were unable to prevent BiP cleavage, indicating SubAB internalisation is not caveolae-/lipid raft-sensitive. However, incubation of Vero cells at 4°C, or at 37°C in the presence of either acetate, CPZ, PAO or BFA, completely blocked SubAB-mediated cleavage of BiP. Despite the inability to observe SubAB-OG trafficking in HeLa and N2A cells (Figure 3.5), SubAB-mediated BiP cleavage was evident in these cells in the absence of inhibitors (Figure 3.17). These cell lines were similarly protected against SubAB-mediated BiP cleavage with PAO and BFA, but not genistein and MβCD. Thus, metabolic activity, formation of membrane-bound vesicles, clathrin-dependent

endocytosis and a functional Golgi, respectively, are essential for SubAB-mediated trafficking and cytotoxicity.

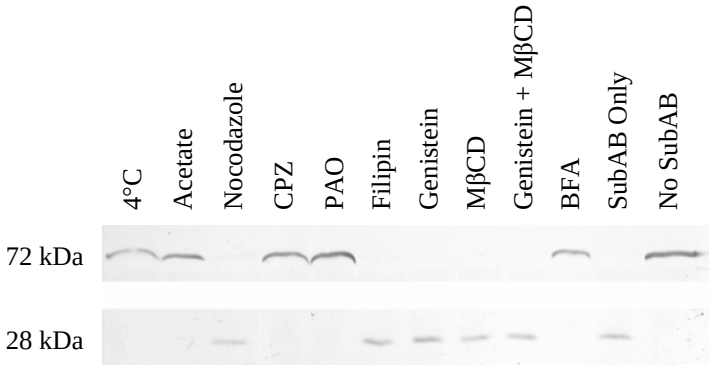

Figure 3.16: Inhibition of SubAB-mediated cytotoxicity in Vero cells.

Vero cells were pre-incubated for 30 min at 4°C or at 37°C in media supplemented with 60 mM acetate (pH ~5), 1.5 $\mu g.ml^{-1}$ nocodazole, 12.5 $\mu g.ml^{-1}$ CPZ, 1.25 µM PAO, 1.25 $\mu g.ml^{-1}$ filipin, 100 $\mu g.ml^{-1}$ genistein, 5 mM MβCD or 0.5 $\mu g.ml^{-1}$ BFA, and then exposed to 1 $\mu g.ml^{-1}$ SubAB-OG for 3 h, while maintaining inhibitory conditions. Cells were solubilised with 2 × LUG, separated by SDS-PAGE and transferred onto nitrocellulose. Membranes were probed with anti-BiP and detected with anti-Goat-AP. 72 kDa = native BiP; 28 kDa = C-terminal fragment of BiP cleaved by SubAB.

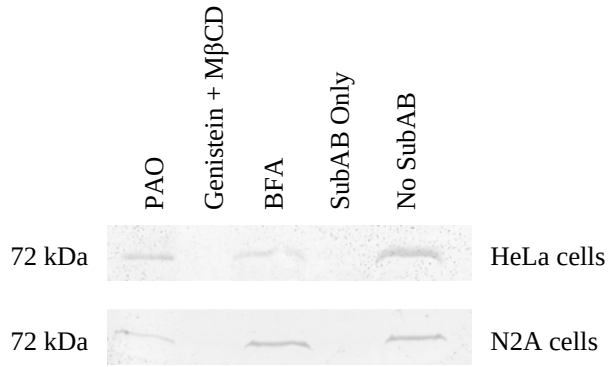

Figure 3.17: Inhibition of cytotoxicity in HeLa and N2A cells.

HeLa and N2A cells were pre-incubated for 30 min in media supplemented with 1.25 µM PAO, 100 $\mu g.ml^{-1}$ genistein and 5 mM MβCD, or 0.5 $\mu g.ml^{-1}$ BFA, and then exposed to 1 $\mu g.ml^{-1}$ SubAB-OG for 3 h, while maintaining inhibitory conditions. Cells were solubilised with 2 × LUG, separated by SDS-PAGE and transferred onto nitrocellulose. Membranes were probed with anti-BiP and detected with anti-Goat-AP. Only 72 kDa bands (native BiP) are shown from both cell lines.

3.2.8 Cell Cycle-Dependent Internalisation

The preferential binding and uptake of SubAB, StxB and CtxB observed in Vero cells (Figure 3.6) prompted analysis of internalisation of SubAB-OG, CtxB-AF595 and StxB-TR with respect to the cell cycle, by immunolabelling cell cycle phase markers (Figure 3.18). Examination of multiple fields indicated that most cells in G1 phase (63%, indicated by nuclear Cyclin E (Ohtsubo *et al.*, 1995)) internalised SubAB-OG, as were cells in early S phase (identified by limited BrdU incorporation), constituting 30.5% of all cells migrating through S phase. The remaining 69.5% that were further into S phase (indicated by high BrdU labelling) exhibited limited SubAB-OG internalisation, as did cells expressing cytoplasmic Cyclin B1 (G2 phase (Takizawa and Morgan, 2000)). Mitotic chromosome configurations were labelled with anti-PH3 to identify cells traversing M phase. Mitotic cells also demonstrated negligible SubAB-OG uptake. In contrast, CtxB-AF594 was internalised by cells in S through M phases and by approximately 68% of cells in G1 phase (Figure 3.19) while uptake of StxB-TR occurred preferentially by cells migrating through G1 phase (57% of cells labelled) (Figure 3.20).

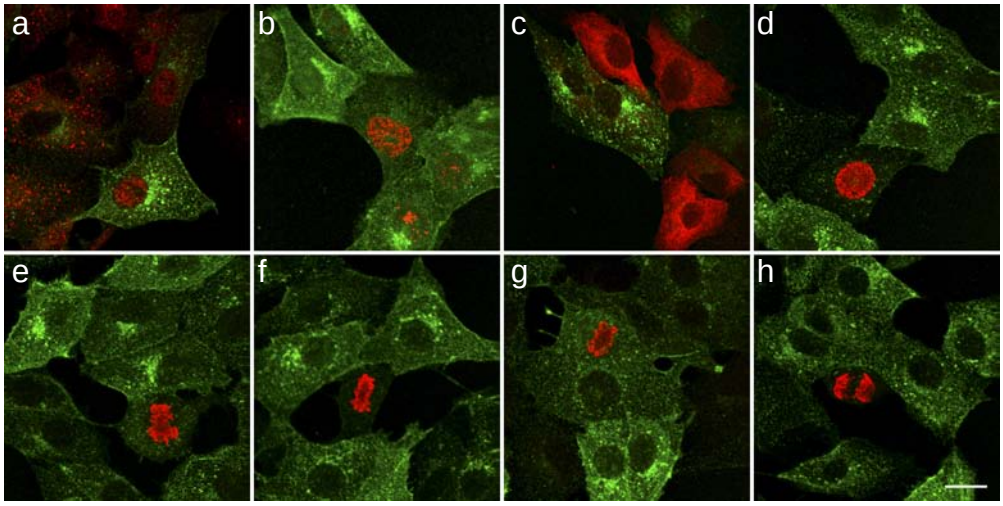

Figure 3.18: Cell cycle-dependent internalisation of SubAB-OG.

Vero cells were exposed to 1 µg.ml^{-1} SubAB-OG for 30 min. For S phase labelling, medium was supplemented with 20 µg.ml^{-1} BrdU. DNA was denatured using HCl and neutralised with Borax buffer. Cells were formalin fixed, permeabilised, and reacted with anti-BrdU, which was detected with anti-mouse-AF594. Nuclear Cyclin E and cytosolic Cyclin B1 indicate cells traversing G1 and G2 phase, respectively while chromosome configurations of cells in M phase are identified with anti-PH3. Anti-Cyclin E, -Cyclin B1 and -PH3 were detected with anti-rabbit-AF594. Cell cycle markers indicate cells in G1 (a), S (b), G2 (c), prophase (d), prometaphase (e), metaphase (f), anaphase (g), and telophase (h). Samples were viewed by dual-laser confocal microscopy (60 × oil objective). Scale bar = 25 µm.

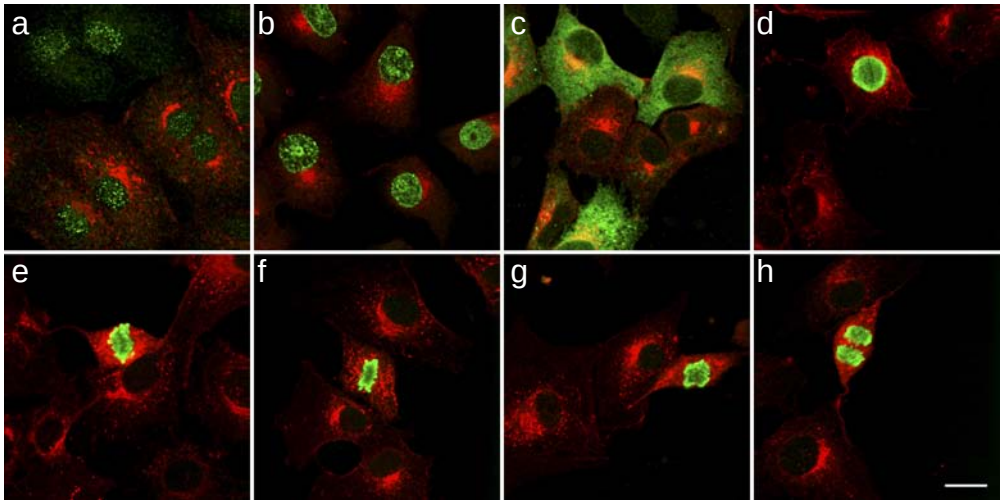

Figure 3.19: Cell cycle-dependent internalisation of CtxB-AF594.

Vero cells were exposed to 0.5 µg.ml^{-1} CtxB-AF594 for 30 min. For S phase labelling, medium was supplemented with 20 µg.ml^{-1} BrdU. DNA was denatured using HCl and neutralised with Borax buffer. Cells were formalin fixed, permeabilised, and reacted with anti-BrdU, which was detected with anti-mouse-AF488. Nuclear Cyclin E and cytosolic Cyclin B1 indicate cells traversing G1 and G2 phase, respectively while chromosome configurations of cells in M phase are identified with anti-PH3. Anti-Cyclin E, -Cyclin B1 and -PH3 were detected with anti-rabbit-AF488. Cell cycle markers indicate cells in G1 (a), S (b), G2 (c), prophase (d), prometaphase (e), metaphase (f), anaphase (g), and telophase (h). Samples were viewed by dual-laser confocal microscopy (60 × oil objective). Scale bar = 25 µm.

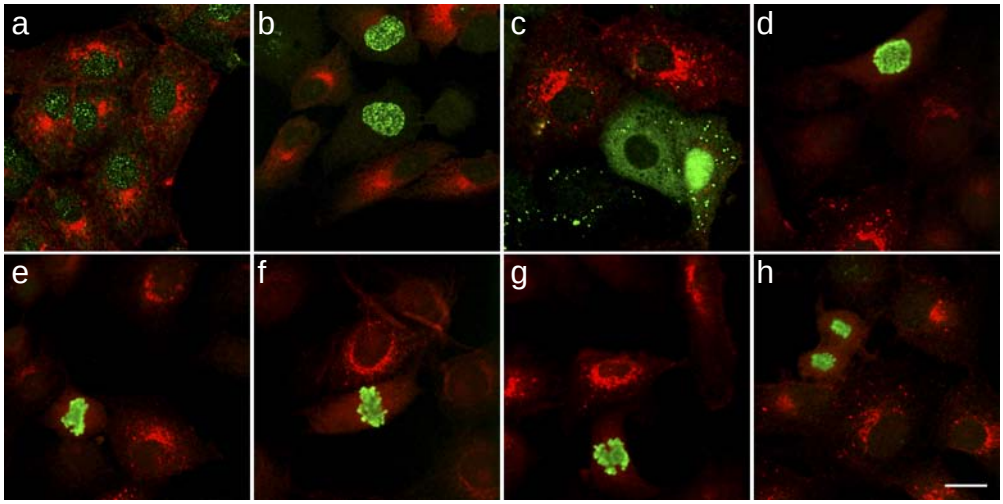

Figure 3.20: Cell cycle-dependent internalisation of StxB-TR.

Vero cells were exposed to 0.5 µg.ml^{-1} StxB-TR for 30 min. For S phase labelling, medium was supplemented with 20 µg.ml^{-1} BrdU. DNA was denatured using HCl and neutralised with Borax buffer. Cells were formalin fixed, permeabilised, and reacted with anti-BrdU, which was detected with anti-mouse-AF488. Nuclear Cyclin E and cytosolic Cyclin B1 indicate cells traversing G1 and G2 phase, respectively while chromosome configurations of cells in M phase are identified with anti-PH3. Anti-Cyclin E, -Cyclin B1 and -PH3 were detected with anti-rabbit-AF488. Cell cycle markers indicate cells in G1 (a), S (b), G2 (c), prophase (d), prometaphase (e), metaphase (f), anaphase (g), and telophase (h). Samples were viewed by dual-laser confocal microscopy (60 × oil objective). Scale bar = 25 µm.

3.3 Discussion

SubAB is the prototype of a distinct family of bacterial AB_5 cytotoxins, differing from the other AB_5 families in terms of its A subunit enzymatic activity, in which SubA is a serine protease, whereas Ctx, LT and Ptx are ADP-ribosylases, and Stx is an RNA *N*-glycosidase. It is also unique in that its only known substrate (BiP) is not located in the cytosol, but rather is a resident ER chaperone indicating that its transport need not progress beyond the ER. Additional differences exist between SubAB and either Ctx or Stx in terms of target cell receptor specificity, illustrated in this chapter by the differential binding of labelled toxins to Vero cells, and differential effects of the cell cycle on display of the respective receptors. These differences raised the possibility of distinct intracellular trafficking routes. Accordingly, the uptake and intracellular trafficking of SubAB has been investigated in detail, in comparison with CtxB and StxB.

As the subcellular transport of AB protein toxins, including those of ricin and Stx, have previously been demonstrated using TEM (van Deurs *et al.*, 1986; Sandvig *et al.*, 1992), visualisation of the SubAB trafficking pathway was initially attempted using electron microscopy. However, the repeated pelleting and resuspension of Vero cells in the protocol described in Section 2.17.4 may have contributed to the significant cell damage initially observed. To address this issue of cellular shearing, Vero cells were grown and treated in Transwell membrane inserts before embedding and labelling with immunogold. Despite the inherent restriction of only being able to view monolayer cross-sections, cells grown in Transwells presented with a far healthier morphology than those collected as a cell pellet. However, the presence of gold particles outside the cell indicated that immunogold labelling of SubAB was not specific (Figure 3.1a) and was most likely due to the use of crude rabbit anti-SubA antisera. The protocol may

benefit from the use of affinity-purified anti-SubA antisera, but this was unavailable at the time.

Another approach utilising electron microscopy involved the amalgamation of cell monolayers grown in Transwells (Soriani *et al.*, 2006) and SubAB-POD, which was subsequently detected by DAB cytochemistry in a similar manner to Sandvig *et al.* (1992) (Figure 3.1b). It was shown that the occasional binding of SubAB-POD to the Vero cell surface and lack of internalisation was due to the altered glycolipid receptor affinity of the toxin conjugate. As illustrated by TLC toxin overlay assays in Figure 3.2, native SubAB recognises the species with R_f values of 0.347 and 0.396 in Vero cell GGS extracts, whereas conjugation of SubAB to POD abolishes this receptor binding specificity. This may be explained by the presence of the large (40 kDa) NH_2-reactive POD which potentially labels each SubAB holotoxin with multiple POD molecules. Indeed, it has been demonstrated that conjugation of horseradish POD to ricin can prevent toxin trafficking to the Golgi cisternae in MCF-7 and Vero cells if more than one POD molecule was conjugated to the toxin (van Deurs *et al.*, 1986). Furthermore, the direct labelling of ricin with gold also abrogated Golgi transport and as the transport route of native SubAB had yet to be elucidated, there were no means of determining if monovalent labelling of SubAB with either POD or gold affected toxin trafficking. Hence, while visualisation of SubAB trafficking by TEM would have been desirable, the lack of affinity-purified antisera for immunolabelling and the altered trafficking potentially caused by conjugating SubAB with either POD or gold prompted the use of a different approach to investigate its intracellular transport route.

Given the adverse affects of conjugating large molecules to SubAB, an alternative approach was to directly label SubAB and $SubA_{A272}B$ with OG and TR fluorochromes, which are much smaller in terms of molecular size. It was determined

that labelling with too high a dye:protein MR can prevent SubAB trafficking, similar to the effect observed with POD, above. However, optimal labelling of SubAB was achieved using a dye:protein MR of 8:1. Furthermore, a comprehensive set of fluorescence co-localisation experiments demonstrated that with this MR, neither specific cytotoxicity, nor trafficking were affected by either OG or TR dyes. Neither did the enzymatic activity or the presence of the A subunit itself affect subcellular transport.

Accumulation of SubAB-OG, CtxB-AF594 and Stx-TR on the surface membrane of Vero cells incubated at 4°C, or in the presence of acetate, demonstrates that all are actively internalised by membrane-bound vesicles. However, incomplete co-localisation (approximately 65% overlap) of SubAB with either CtxB-AF594 or StxB-TR in cells that internalised both toxins (Figure 3.6), suggested that subsequent transport occurs via a retrograde pathway that is similar, but not identical to other AB_5 toxins. In particular, the distinct co-localised and non-co-localised puncta indicate differences in the endocytic mechanisms exploited. Co-localisation of SubAB-OG was seen with Tf-TR, a marker for clathrin-coated vesicles, indicating that uptake occurs via a clathrin-dependent pathway. Supporting this result was the observation that, unlike CtxB and StxB, endocytosis of SubAB was totally inhibited in the presence of the clathrin inhibitor PAO. PAO caused surface accumulation of SubAB-OG and the clathrin-dependent endocytosis marker Tf-TR, and also completely prevented cleavage of BiP in SubAB-treated Vero cells. Thus, not even traces of toxin were internalised and transported to the ER. A similar effect was also seen using CPZ, another clathrin inhibitor, although this also had general cytotoxic effects on Vero cells and thus, was not assessed for its affects on the intracellular transport of Ctx or Stx.

In contrast to the affect of PAO, SubAB was less susceptible than CtxB or StxB to inhibition of trafficking by genistein and/or MβCD, which deplete cholesterol and

cholesterol-associated caveolae. A comparable redistribution of toxin was noted in the presence of another cholesterol inhibitor, filipin. However, this appeared to be cytotoxic to Vero cells with gross alterations to cell morphology. Neither genistein nor MβCD had a significant impact on trafficking of SubAB-OG, either alone or in combination, nor could these compounds prevent complete cleavage of BiP in cells treated with active toxin. Similar findings were also obtained for HeLa and N2A cells, despite the inability to observe any internalised SubAB-OG. PAO was able to protect both cell types from SubAB-mediated BiP cleavage whilst genistein and MβCD were not, indicating that the toxin exploits a clathrin-dependent (cholesterol-independent) endocytic route. The negligible fluorescence co-localisation of SubAB-TR with Caveolin-1-EGFP in transfected Vero cells is also consistent with the above findings. In contrast, MβCD caused marked surface accumulation of CtxB-AF594, while both MβCD and genistein affected targeting of StxB-TR to the Golgi. These results support previous studies which demonstrate that transport from the plasma membrane of Ctx and Stx can occur via a cholesterol-dependent endocytic route (Falguieres *et al.*, 2001; Kovbasnjuk *et al.*, 2001; Wolf *et al.*, 2002; Lencer and Saslowsky, 2005). These findings imply that there are clear differences in the extent to which internalisation and subcellular trafficking of the three AB_5 toxins are dependent upon association with lipid rafts.

Despite the variation of transport routes from the plasma membrane, all three toxins converged at a juxtanuclear region, identified as the TGN/Golgi by labelling with WGA-TR and anti-Golgin-97. Although nocodazole fragments the Golgi apparatus, it does not disrupt its function, and previous studies have shown it had no effect on Golgi transport of vesicular stomatitis virus G protein (Rogalski and Singer, 1984). Accordingly, nocodazole did not abrogate SubAB transport or toxin-mediated cleavage

of BiP. Moreover, collapse of the Golgi, TGN and possibly recycling endosomes by treatment with BFA caused accumulation of all three labelled toxin species in this organelle, and importantly, completely prevented cleavage of BiP in SubAB-treated cells. This also correlates with previous studies that have shown BFA to block Ctx and Stx transport beyond the Golgi (Orlandi *et al.*, 1993; Mallard *et al.*, 1998).

Unlike Ctx and Stx, whose catalytic A subunits must exit the ER to access their cytosolic targets, SubAB-OG became associated with its intracellular substrate BiP in the ER lumen, presumably terminating its intracellular journey in that compartment. However, to address the possibility of BiP being an imprecise marker of the ER due to its role as a chaperone, ER-Tracker Red was also used. While SubAB does not possess an ER-targeting KDEL motif like those found in Ctx and the related LT (Lencer and Tsai, 2003), its localisation to the ER was nevertheless confirmed. This was unsurprising, as deletion of the KDEL motif in Ctx and its absence in Stx toxin does not abolish transport to the ER (Sandvig *et al.*, 1992; Fujinaga *et al.*, 2003), although in the case of Ctx, it improves transport efficiency (Lencer *et al.*, 1995). The studies involving co-localisation of SubAB-OG with subcellular markers showed that trafficking occurred rapidly, with substantial co-localisation with Tf-TR, a clathrin marker, within 5 min and subsequent co-localisation with Golgi and ER markers within 30 min of addition of toxin. This is consistent with previous reports that cleavage of BiP could be detected in Vero cells within 20 min (Paton *et al.*, 2006a).

These data provide robust support for the conclusion that SubAB undergoes clathrin-dependent (cholesterol-independent) retrograde transport, via early endosomes and the Golgi network, to the ER. This disagrees with recent findings which suggested that SubAB may be translocated to the cytoplasm from an early endosomal compartment, because Cy3-labelled SubAB co-localised with EEA1, an early endosome

marker, but not with β-COP or GM130, which were employed as markers of the Golgi apparatus even after 30 min (Morinaga *et al.*, 2007). Given the sub-cellular location of the substrate of SubAB, this seemed counter-intuitive. The reason for this discordance may reside in the fluorescent conjugation of SubAB in which Morinaga *et al*. (2007) used a different labelling procedure and did not present evidence that this did not affect toxin trafficking. Indeed, in the present study, it was demonstrated that too high a dye:protein MR almost completely inhibited trafficking of labelled toxin (Figure 3.3). In this study an optimal dye:protein MR of 8:1 was used and this was shown to have no effect on trafficking or specific cytotoxicity of the labelled product.

An interesting observation in the present study was the marked heterogeneity in terms of toxin uptake by individual Vero cells in monolayers exposed to SubAB-OG and co-incubated with either CtxB-AF594 or StxB-TR. This clearly demonstrates that the three toxins engage distinct receptors. For CtxB and StxB, the preferred receptors are the glycolipids GM_1 and Gb_3, respectively (Merritt and Hol, 1995), whereas data from the glycan array in Section 4.2.3 indicate the SubB receptor possesses a high affinity for glycan conjugates with a distal Neu5Gcα(2→3)Galβ disaccharide or even Neu5Gcα alone. In addition to influencing early trafficking events, the differential target specificity may also influence signal transduction events that may initiate from B subunit-receptor interactions.

Differential internalisation of SubAB-OG by Vero cells in a non-synchronous cell population led to the hypothesis that its uptake was influenced by the cell cycle phase, as previously reported for Ctx and Stx in Vero cells (Pudymaitis and Lingwood, 1992; Majoul *et al.*, 2002). Immunolabelling of cell cycle phase markers revealed that Vero cells traversing G1 and early S phases internalised SubAB-OG to a greater extent than those migrating through the remainder of the cycle. Although it has recently been

shown that SubAB induces cell cycle arrest (G0/G1 phase) in Vero and HeLa cells by downregulating Cyclin D1, this was only evident in cells that were incubated with toxin for more than 20 h (Morinaga *et al.*, 2008). In contrast, StxB-TR was predominantly internalised during G1 phase, while CtxB-AF594 uptake occurred throughout the cell cycle except for some cells in G1. It should be noted that SubAB-OG was bleached in the detection of BrdU (an S phase marker) as this procedure involved treating cells with concentrated HCl to denature DNA (Section 2.15.4). Accordingly, the signal was resuscitated with anti-OG-AF488. However, as CtxB-AF594 and StxB-TR appeared to be more resistant to low pH, they did not require signal retrieval.

Curiously, previous studies on cell cycle-dependent uptake of Stx and Ctx conflict with the findings of the current study, as well as with each other. Pudymaitis and Lingwood (1992) report maximal sensitivity to Stx during early S phase, while Majoul *et al*. (2002) report that this occurs during G2 phase and mitosis for Stx, and G1 phase for Ctx. It should be noted, however, that although clear cell cycle-dependent differences in gross uptake of SubAB-OG were observed by fluorescence microscopy, there was a low-level baseline internalisation by all cells in non-synchronised cultures. Furthermore, the specific enzymatic activity of SubAB is such that this basal level of toxin uptake is sufficient to cause complete degradation of BiP in Vero cell monolayers.

Bacterial protein toxins have proven to be useful as tools in cell biology, providing insight into cellular processes and subcellular transport routes. In this study the internalisation and retrograde trafficking of SubAB to its ER-resident target BiP, by an exclusively clathrin-dependent pathway has been demonstrated. At present, the reason for the inability of SubAB to engage alternative transport routes from the plasma membrane to the ER, such as those exploited by both Ctx and Stx in Vero cells, is unknown. However, a key factor may relate to the relative capacity of toxin-receptor

complexes to associate with lipid rafts. The apparently absolute specificity of SubAB for BiP (Paton *et al.*, 2006a), and its rapid retrograde transport to the ER compartment, makes SubAB a powerful tool for examining the role of BiP in important cellular functions. These include mediating correct folding of nascent secretory proteins, regulating ER stress signalling, and targeting terminally mis-folded proteins to the Sec61 apparatus for degradation by the proteasome (Gething, 1999; Hendershot, 2004). It is now believed that the catalytic subunits of Stx, Ctx and ricin are retro-translocated from the ER lumen into the cytosol by subversion of the Sec61 pathway, thereby enabling them to engage their respective substrates (Lencer and Tsai, 2003). Furthermore, at least for StxA, this is believed to occur following interaction with BiP and another chaperone HEDJ/ERdj3 (Yu and Haslam, 2005; Falguieres and Johannes, 2006). This latter finding is of particular interest given the fact that to date, SubAB has only been found to be produced by strains of *E. coli* that also produce Stx (Paton *et al.*, 2004; Paton and Paton, 2005). This raises the possibility that cleavage of BiP by SubAB may directly modulate entry of StxA into the cytosol, and hence the *in vivo* consequences of Stx intoxication in patients infected with a bacterial strain producing both toxins.

Chapter 4

Host Glycan Receptor

4.1 Introduction

Molecular recognition events have been shown to involve the interactions between protein ligands and their glycoconjugate receptors expressed on the target cell surface. Variations in the carbohydrate sequence, glycosidic linkages and branched structures permit the diverse glycosylation of these conjugates by host cells. Glycoconjugates are often targeted by pathogen-associated ligands (including bacterial toxins) and such discriminatory glycosylation of host tissues subsequently determines cell sensitivity, intracellular trafficking, tissue trophism and host specificity (Fishman, 1982; Lingwood *et al.*, 1987). As a result, much research has been directed towards the elucidation of a vast number of target glycan receptors and the pathogen-associated structures that recognise them.

The carbohydrate receptors recognised by AB_5 toxins are typically expressed in the context of glycolipids (Merritt and Hol, 1995). Binding to the cognate glycan receptor is mediated by the B subunit pentamer and is a critical step in initiating pathogenesis of disease, influencing subcellular trafficking and delivery of the enzymatic A subunit to its intracellular substrate (Sandvig and van Deurs, 2002; Lencer and Tsai, 2003). Furthermore, toxin binding can trigger signal transduction pathways and apoptotic cascades, which are distinct from the direct toxic effects on host cell machinery (Popoff, 1998; Cherla *et al.*, 2003; Fujii *et al.*, 2003; Smith *et al.*, 2003).

Previous studies have shown that SubAB can recognise the carbohydrate moiety of the GM_2 RMC, but that it may potentially bind other structures with greater affinity (Paton *et al.*, 2004). Although the SubB pentamer can bind the sialylated glycoprotein α2β1 integrin to cause vacuolation independently of SubA, this receptor has not been implicated in BiP cleavage and subsequent inhibition of protein synthesis (Yahiro *et al.*, 2006; Morinaga *et al.*, 2007). In this study, the intracellular trafficking pathway of

SubAB-OG was shown to be similar, but not identical, to those of CtxB-AF594 and StxB-TR by fluorescence co-localisation (Figure 3.6) and by the use of inhibitory conditions and compounds (Section 3.2.5). This indicates that the target receptor recognised by SubAB may also be distinct from those of Ctx and Stx (GM_1 and Gb_3, respectively). Elucidation of the oligosaccharide bound by SubAB will address a significant gap in our understanding of this fundamental step in toxin-mediated pathogenesis. For this reason attempts were made to determine the structure of the eukaryotic membrane glycan receptor recognised by SubAB.

4.2 Results

4.2.1 Putative Glycolipid Receptor Affinity

Identification of the glycoconjugate recognised by SubAB was first approached using a TLC toxin overlay assay, which has been previously used to demonstrate the carbohydrate affinities of Ctx and Stx (Magnani *et al.*, 1980; Lingwood *et al.*, 2000). Glycolipids were extracted from Vero cells, partitioned into neutral GSLs and acidic GGSs and loaded onto silica-coated TLC plates alongside purified GSL and GGS standards and separated by polarity by allowing a solvent front to migrate up the plate. Replicate chromatograms were then sprayed with orcinol to visualise total glycolipid composition, or overlaid with purified SubAB (carrying a His_6 tag at the C-terminus of SubB) to allow the toxin to bind its complementary carbohydrate receptor. SubAB bound to putative receptor species was subsequently labelled with anti-His_6 and detected with anti-mouse IgG-AP, as described in Section 2.10 (Figure 4.1). When compared with the intensity of the corresponding bands in the orcinol-sprayed plate, SubAB exhibited minimal binding to three species from the Vero cell GSL extract with R_f values of 0.033, 0.151 and 0.396 (Figure 4.1a). However, the toxin also had a much higher affinity for the purified Gb_4 standard.

On the chromatograms containing GGSs (Figure 4.1b), SubAB bound at least three glycolipids in the Vero cell extract (R_f = 0.347, 0.396 and 0.557) with the lower two bands exhibiting the highest affinities relative to the orcinol-sprayed plate. Weak binding was also observed with the GD_{1b} standard. Curiously, the toxin also recognised a species that migrated between GM_2 and aGM_1 (R_f = 0.629) in the track loaded only with purified aGM_1, GM_2 and GM_3. This species was presumably a minor contaminant or degradation product of one of the commercial GGS standards, although the precise

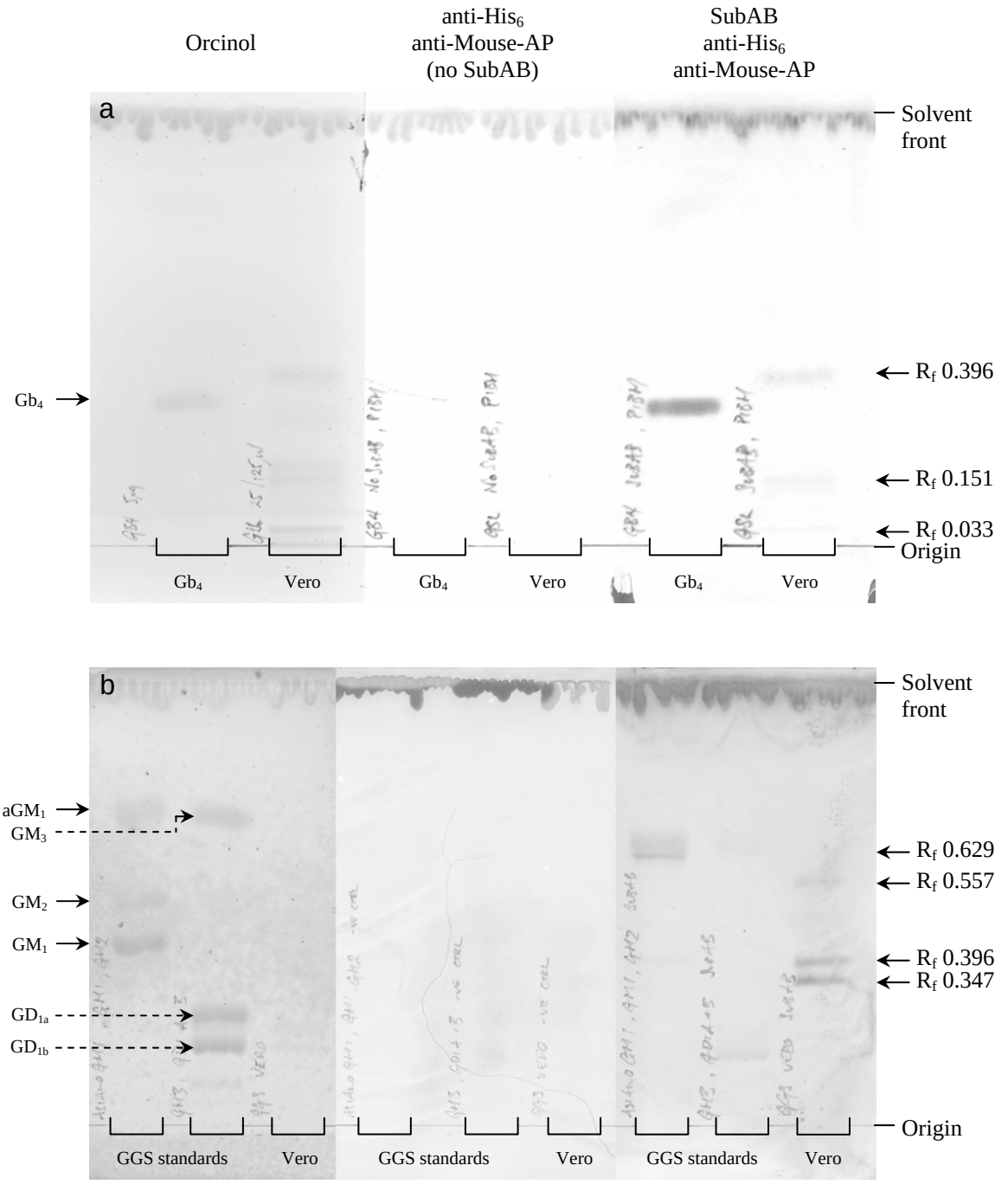

Figure 4.1: Host cell membrane glycolipid affinity of SubAB.

GSL (a) and GGS (b) standards and membrane extracts from Vero cells were loaded in triplicate and separated by TLC. Approximately 5 µg of purified GSL and GGS standards were also loaded for comparison. Chromatograms were sprayed with orcinol reagent to view total glycolipid composition or with PIBM, overlaid with or without 1 $\mu g.ml^{-1}$ SubAB, probed with anti-His_6 and detected with anti-Mouse IgG-AP. R_f values for a given species are calculated as the distance of migration divided by that of the solvent front with respect to the origin.

identity is unknown. This indicates that SubAB possesses a high affinity for Gb_4 and two GGS species expressed on Vero cells, which did not co-migrate with the available GGS standards. The silica regions corresponding to these bands of interest were scraped off a replicate chromatogram and analysed by MS. Unfortunately, negative ion MS, analysis performed by Istvan Toth (Molecular and Microbial Sciences School, University of Queensland), and MALDI MS analysis, performed by Peter Hoffmann (Adelaide Proteomics Centre, University of Adelaide), yielded inconclusive results.

4.2.2 Developing a Bacterial Receptor Mimic Construct Toxin Overlay Assay

In previous studies in our laboratory, a novel and highly effective probiotic was developed to treat the potentially fatal toxin-induced conditions arising from STEC infection (Paton *et al.*, 2000b). A non-pathogenic *E. coli* "platform strain" (CWG308) was engineered to express a chimeric LPS core with a tailor-made distal carbohydrate structure identical to the glycan domain of Gb_3. Recently, the range of bacterial RMCs has been expanded to include mimics of several GSL and GGS species (listed in Table 2.2), which have been used in this study because of their ability to neutralise bacterial AB_5 toxins.

To assess the capacity of SubAB to bind to this panel of RMCs, an LPS toxin overlay assay was developed, comparable to that of a TLC toxin overlay. Given that CtxB-POD specifically bound to GM_1 in toxin overlay chromatograms (results not shown) and that the GM_1 RMC exhibited a high avidity for Ctx *in vitro* and completely protected infant mice from challenge with virulent *V. cholerae* (Focareta *et al.*, 2006), Ctx-POD was employed as a positive control in validating an RMC toxin overlay assay. LPS isolated from CWG308 and GM_1 RMC strains were separated by SDS-PAGE, transferred onto PVDF and incubated with CtxB-POD (Figure 4.2). However, despite numerous attempts at altering the transferring and blotting conditions, CtxB-POD only

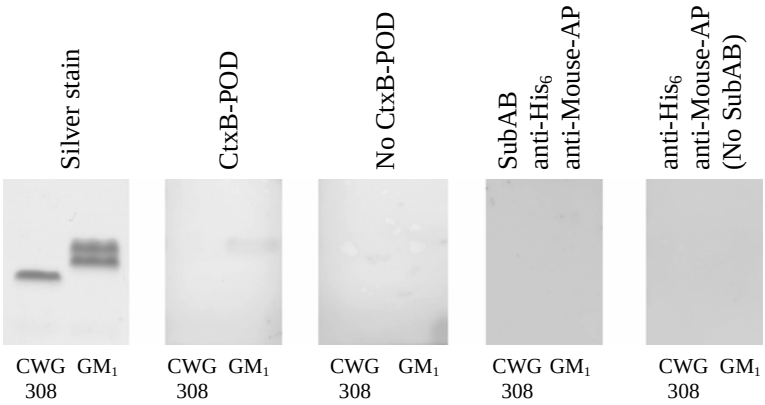

Figure 4.2: GM_1 RMC toxin overlay.

LPS isolated from *E. coli* CWG308 and CWG308:pJCP-GM_1 cultures were separated by SDS-PAGE, transferred onto PVDF and incubated with or without CtxB-POD or SubAB, which was then detected using anti-His_6 and anti-Mouse-AP.

demonstrated a weak affinity for the upper band of the GM_1 RMC LPS doublet indicating that the lower band was not a mimic of the carbohydrate moiety of GM_1. This lower band most likely comprises GM_2, as the terminal reaction does not necessarily go to completion. Furthermore, samples overlaid with SubAB (detected with anti-His_6) did not produce a discernable signal and was also the case when repeated with the complete panel of RMC extracts (not shown).

To increase the sensitivity of this assay, SubAB-OG was used in the RMC toxin overlay assay and binding was detected using a Bio-Rad Molecular Imager FX (Figure 4.3). Optimum OG labelling of SubAB was achieved by using a dye:protein molar ratio (MR) of 8:1 as detailed in Section 3.2.2. SubAB-OG did not appear to bind the carbohydrate structures of LPS extracts from CWG308, Gb_3 or Gb_4 RMCs. However, the toxin clearly bound to the two upper bands of GM_2 and GM_3, with weak associations with lactose (LgtE). The mobility of the GM_2 RMC middle band and the GM_3 RMC appear identical indicating that the incomplete terminal reaction of GM_2 results in an oligosaccharide lacking a distal GalNAcβ(1→4) linkage which would, therefore, possess the same glycan structure as that of the GM_3 RMC.

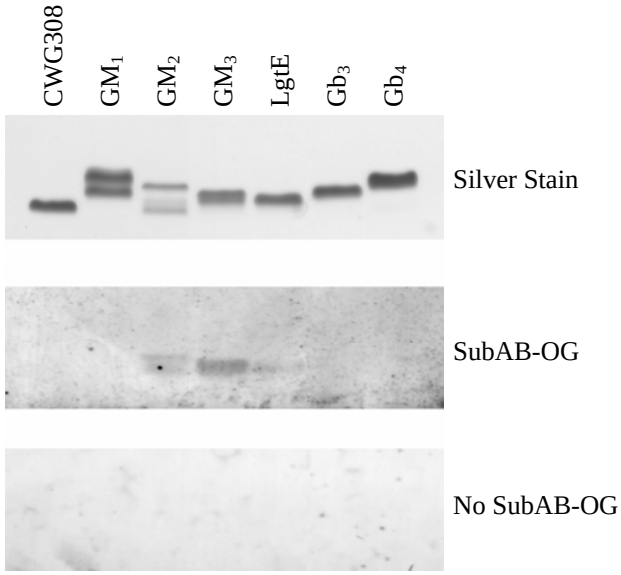

Figure 4.3: Complete RMC panel affinity of SubAB-OG.

LPS isolated from *E. coli* CWG308 and CWG308-based RMC cultures were separated by SDS-PAGE as indicated, transferred onto PVDF and incubated with or without SubAB-OG, which was detected using a fluorescence imager.

4.2.3 Analysis of SubAB Affinity by Glycan Array

As MS analyses of silica scrapings from TLC plates were unable to provide information on the putative glycolipid receptors for SubAB, and RMC analysis was limited by the existing repertoire of constructs, toxin receptor affinity was examined by glycan array analysis (performed by David Smith, CFG Core H, School of Medicine, Emory University, GA). Version 2.1 of the printed array consists of 285 oligosaccharides in replicates of six spotted onto Nexterion H slides (Schott AG, Mainz, Germany) and this was incubated with 100 $\mu g.ml^{-1}$ SubAB-OG. Toxin affinity is proportional to relative fluorescence units (RFU) and the ten species that bound with the highest intensities are listed in Table 4.1. The complete array plotted in Figure 4.4. A comprehensive list of all 285 glycans can be found in Appendix A sorted by glycan number (Table A.1) and by RFU with SubAB-OG (Table A.2).

Table 4.1: Glycan affinity of SubAB-OG (100 $\mu g.ml^{-1}$) by mean RFU.

#	Glycan Name	Mean RFU (n=4)*	STDEV	SEM	% CV
1	AGP	41519	1823	911	4
260	Neu5Gcα2-3Galβ1-4GlcNAcβ–Sp0	41467	15476	7738	37
2	AGP-A	36382	800	400	2
261	Neu5Gcα2-3Galβ1-4Glcβ–Sp0	31202	1458	729	5
258	Neu5Gcα2-3Galβ1-3GlcNAcβ-Sp0	30045	3164	1582	11
264	Neu5Gcα–Sp8	11973	8821	4411	74
3	AGP-βl	9830	1607	804	16
235	Neu5Acα2-3Galβ1-4GlcNAcβ1-3Galβ1-4GlcNAcβ1-3Galβ1-4GlcNAcβ–Sp0	5118	1064	532	21
227	Neu5Acα2-3Galβ1-4[6OSO3]GlcNAcβ-Sp8	4992	365	183	7
15	α-Neu5Ac–Sp11	4492	1293	647	29

* Although six spots are tested for each glycan, data are mean fluorescence for four spots, after discarding the two spots with the highest and lowest values. Sp#: spacer. Spacer structures can be found at http://www.functionalglycomics.org/. STDEV: standard deviation. SEM: standard error about the mean. CV: coefficient of variation.

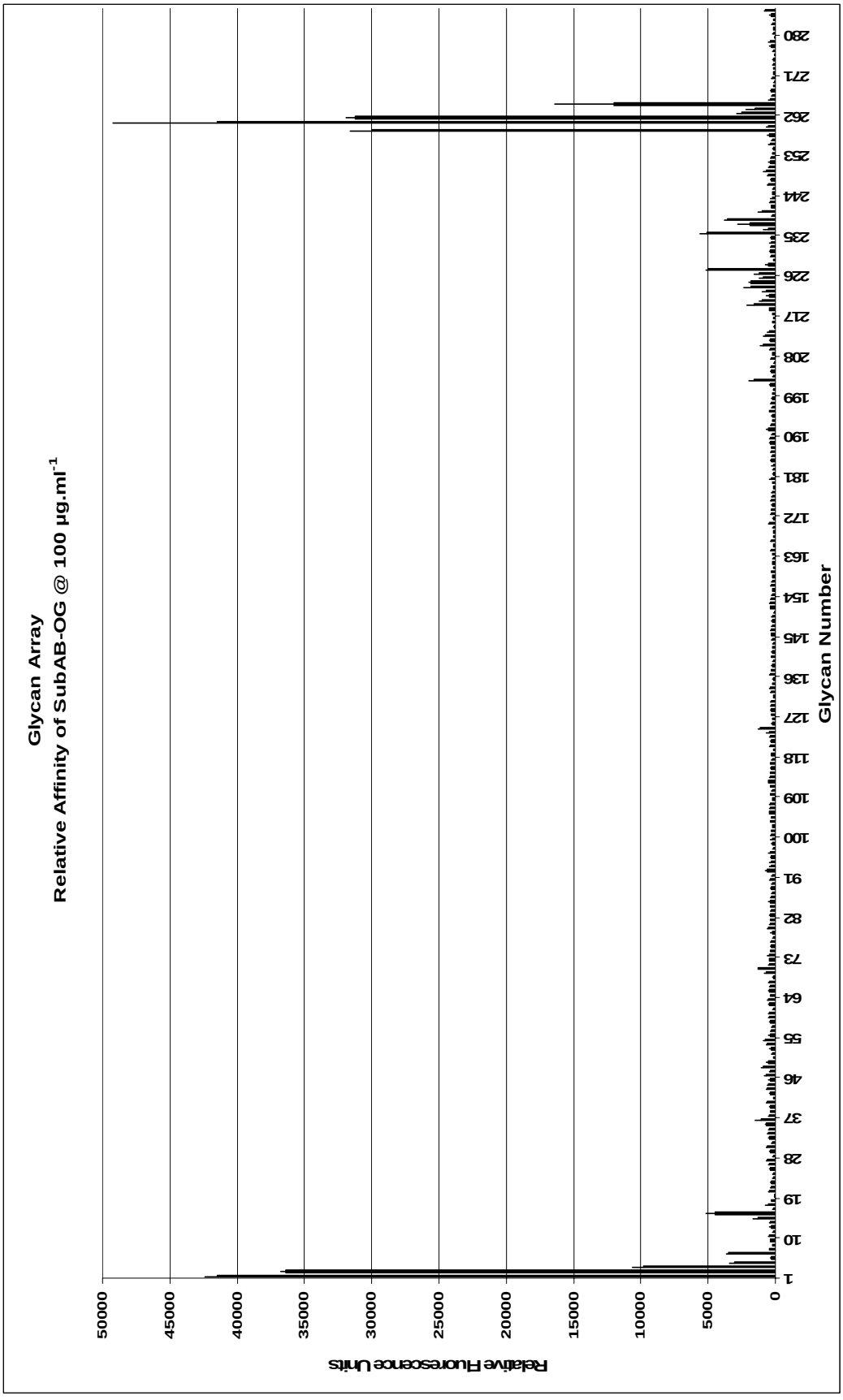

Figure 4.4: Relative affinity of SubAB-OG for the glycan array.

Printed arrays of 285 glycans (n = 4) were exposed to 100 µg.ml^{-1} SubAB-OG with mean RFU determined by David Smith (CFG, Core H).

The data show that SubAB exhibited a high affinity for glycans terminating in α(2→3)-linked N-glycolylneuraminic acid (Neu5Gc), which differs from oligosaccharides containing N-acetylneuraminic acid (Neu5Ac) by the addition of an OH group on the carbon of the acetyl group and is not normally expressed by human adults (Shaw and Schauer, 1988; Muchmore *et al.*, 1989). The toxin also bound the monosaccharide Neu5Gc (glycan #264) three- to four-fold stronger than Neu5Ac (#14 and #15). Neu5Gcα(2→3)Galβ(1→4)GlcNAcβ (#260), Neu5Gcα(2→3)Galβ(1→4)Glcβ (#261) and Neu5Gcα(2→3)Galβ(1→3)GlcNAcβ (#258) were the most efficiently bound glycans on the array, indicating that SubAB-OG does not appear to discriminate between the β(1→4) and β(1→3) linkage of the penultimate galactose. The addition of fucose to the oligosaccharide diminishes the receptors capacity to bind SubAB-OG as indicated by the low binding of SubAB-OG to Neu5Gcα(2→3)Galβ(1→4)[Fucα(1→3)]GlcNAcβ (#259) and Neu5Gcα(2→3)Galβ(1→3)[Fucα(1→4)]GlcNAcβ (#257). There are a number of glycans on the array terminating with Neu5Acα(2→3) and Neu5Acα(2→6) to which the toxin exhibits little or no affinity. The extended polylactosamine on structures #227, 235, 237 and 238 appear to compensate for the presence of Neu5Ac in these oligosaccharides.

Multivalent interactions may also be responsible for the high avidity for some structures with a distal Neu5Acα(2→3) residue. The binding to the serum glycoprotein α_1-AGP (glycan #1) is consistent with this idea since this glycoprotein is the most highly sialylated protein in serum (Kawasaki *et al.*, 1966; Hermentin *et al.*, 1992). Additionally, SubAB recognises the two fractions of this glycoprotein on the array, AGP-A (#2) and AGP-β1 (#3), with high affinity. AGP-A is a run-through fraction on a column of immobilised Con-A, which binds oligosaccharides with a high mannose

composition and AGP-β1 is the bound fraction which is eluted from the affinity column with mannose and has less sialic acid.

4.2.4 FCS as a Potential Source of Neu5Gc for SubAB

As human cells do not normally express Neu5Gc (Muchmore *et al.*, 1998) and as SubAB exhibited a high affinity for the heavily-sialylated serum protein α_1-AGP (Table 4.1), it is possible that FCS used in tissue culture may provide a source of Neu5Gc for human cells and promote SubAB entry. Consequently, uptake of Neu5Gc glycans from FCS may facilitate SubAB internalisation by human cells which are otherwise refractory. To address this possibility, attempts were made to adapt cell lines of human origin (HCT-8 and HeLa cells) to the synthetic media, VP-SFM (0% FCS). However, within three passages, cells either presented a severely altered morphology or had rounded up and detached from the substratum.

Since adaptation of human cells to serum-free media was unsuccessful, the glycolipid profiles of Vero cells grown in FCS and VP-SFM were compared by TLC toxin overlay assays to determine if SubAB binds preferentially to components of FCS-fed cells (Figure 4.5). Although the plate sprayed with orcinol demonstrated that there was a marked discrepancy in total GSL composition between Vero cells grown with and without FCS, there was no discernable difference in SubAB affinity for the GSL extracts. In contrast, the toxin bound two GGS species (R_f = 0.396 and 0.557) in extracts from cells grown with FCS that were not detected in those of serum-free Vero cells. Indeed, SubAB recognised only a single GGS species (R_f = 0.347) in extracts from cells grown in VP-SFM indicating that SubAB recognises at least two components whose expression is dependent on FCS in the medium (R_f = 0.396 and 0.557) that may be exploited as functional toxin receptors.

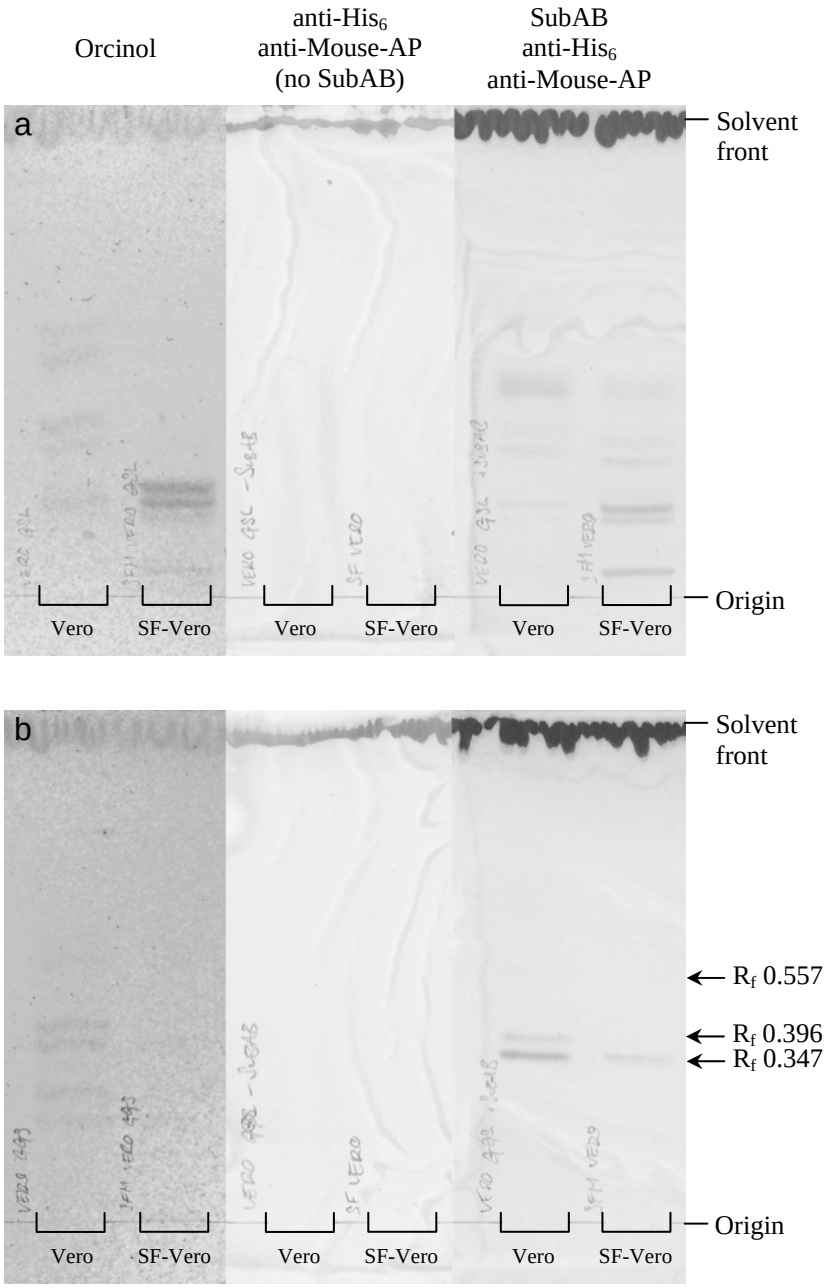

Figure 4.5: Glycolipid profiles of Vero cells in the presence and absence of FCS.

GSL (a) and GGS (b) membrane extracts from Vero cells grown with and without FCS were loaded in triplicate and separated by TLC. Chromatograms were either sprayed with orcinol reagent or sprayed with PIBM, overlaid with or without 1 $\mu g.ml^{-1}$ SubAB, probed with anti-His_6 and detected with anti-Mouse IgG-AP. Vero were extracted from Vero cells grown with FCS, SF-Vero was extracted from Vero cells grown in VP-SFM.

4.2.5 Toxin Inhibition with Receptor Analogues

Given that the data obtained from glycan array analysis (Section 4.2.3) indicated that SubAB possessed a high affinity for α_1-AGP and Neu5Gcα(2→3)Galβ, synthetic trisaccharides (designated Chen-1 to Chen-6) were obtained from Xi Chen (UC Davis, CA) with terminal Neu5Gc or Neu5Ac (Figure 4.6) in addition to commercial preparations of Neu5Gc monosaccharide and α_1-AGP derived from human and sheep plasma.

Chen-1

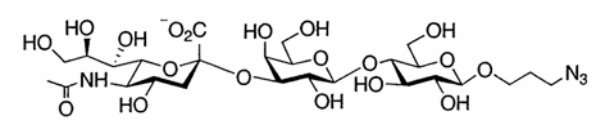

Neu5Acα(2→3)LacβProN$_3$

Chen-2

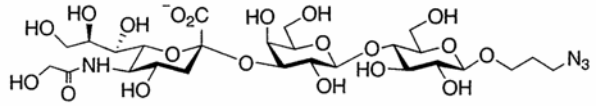

Neu5Gcα(2→3)LacβProN$_3$

Chen-3

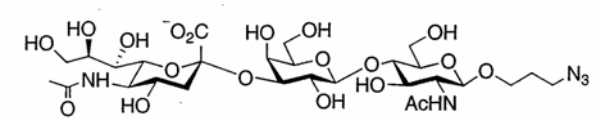

Neu5Acα(2→3)LacNAcβProN$_3$

Chen-4

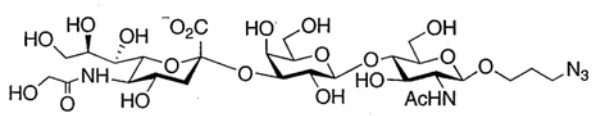

Neu5Gcα(2→3)LacNAcβProN$_3$

Chen-5

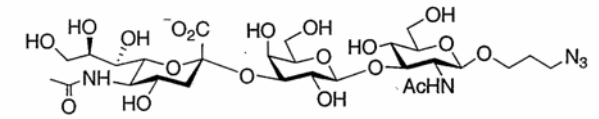

Neu5Acα(2→3)Galβ(1→3)GlcNAcβProN$_3$

Chen-6

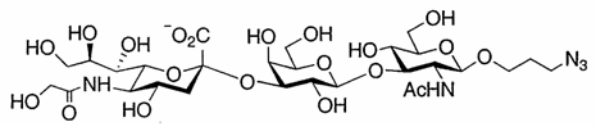

Neu5Gcα(2→3)Galβ(1→3)GlcNAcβProN$_3$

Figure 4.6: Synthetic oligosaccharide structures.

Conformational structures of the six trisaccharides synthesised by Xi Chen (UC Davis CA).

Serial dilutions of these sialylated compounds were incubated for 30 min with 0.1 μg.ml^{-1} SubAB, beginning with a 100:1 (receptor:toxin) mass ratio, applied to Vero cells and assessed for their ability to inhibit SubAB cytotoxicity after four days. The specific activity of SubAB was not diminished in the presence of Neu5Gc monosaccharide or with the synthetic trisaccharides, Chen-1 to Chen-6, regardless of the terminal sialic acid. Similarly, the inverse experiment, titrating SubAB against a constant 1 mg.ml^{-1} receptor analogue beginning with a 100:1 (receptor:toxin) mass ratio, indicated that the carbohydrates did not affect SubAB cytotoxicity. The inability for these free oligosaccharides to inhibit SubAB may be due to the lack of multivalent interactions with the receptor analogues. Indeed, it is known that polyvalent ligands are more effective than free oligosaccharides in inhibiting Ctx and Stx recognition of their cognate receptors and exploitation of the avidity conferred by multivalency is crucial in developing effective low-molecular weight inhibitors (Fan *et al.*, 2000; Mulvey *et al.*, 2001; Schengrund, 2003; Paton *et al.*, 2006b).

As humans do not normally express Neu5Gc (Muchmore *et al.*, 1998) and SubAB demonstrated a high affinity for the heavily sialylated protein α_1-AGP, the capacities for human and sheep α_1-AGP to inhibit SubAB-mediated cytotoxicity were compared. Although α_1-AGP derived from sheep plasma is presumably sialylated at least to some extent with Neu5Gc, whereas α_1-AGP from human plasma is not, no difference in their ability to inhibit SubAB cytotoxicity was observed. Furthermore, despite being heavily sialylated, neither form of α_1-AGP was able to diminish SubAB cytotoxicity and were unable to prevent toxin-mediated BiP cleavage when Vero cell lysates were subjected to a western blot and probed with anti-BiP as described in Section 2.6.3 (data not shown). Fluorescence microscopy of Vero cells exposed to SubAB-OG, which was pre-incubated with Neu5Gc or α_1-AGP derived from human or

sheep plasma, confirmed that the toxin was internalised despite more than a 100-fold mass excess of each of the receptor analogues (Figure 4.7). This suggests that although SubAB can bind Neu5Gc, it is a reversible interaction allowing SubAB to dissociate from the receptor analogue in solution and associate with its higher-affinity receptor on the target cell surface.

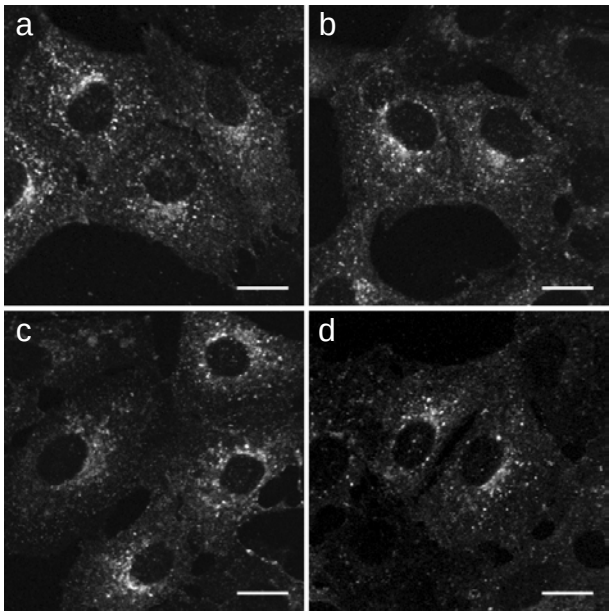

Figure 4.7: Affect of selected receptor analogues on SubAB-OG trafficking in Vero cells.

1 µg.ml^{-1} SubAB-OG was pre-incubated with 100 µg.ml^{-1} Neu5Gc (a), human-derived α_1-AGP (b), sheep-derived α_1-AGP (c) or media only (d) for 30 min, then applied to Vero cells for 60 min. Samples were viewed by laser confocal microscopy (60 × oil objective). Scale bars = 25 µm.

4.2.6 Putative Glycoprotein Receptor Affinity

Although Ctx and Stx typically recognise the oligosaccharide moiety of glycolipids (Merritt and Hol, 1995), SubAB exhibited a high avidity for α_1-AGP on the glycan array, the most heavily sialylated protein in serum (Kawasaki *et al.*, 1966; Hermentin *et al.*, 1992). It is therefore possible that SubAB recognises the carbohydrate moiety of other glycosylated surface proteins. Indeed, Yahiro *et al*. (2006) identified α2β1 integrin as a receptor for SubAB. α2β1 integrin is a heterodimeric glycoprotein (155 and 135 kDa, respectively) that binds the host cell to collagen in the extracellular matrix (Bellis, 2004; Gu and Taniguchi, 2004). However, this interaction was only implicated in SubB-mediated host cell vacuolation, and was not assessed for its role in SubA-mediated disruption of BiP.

In an attempt to verify the affinity of SubAB for glycoproteins, the experiments described by Yahiro *et al*. (2006) were duplicated by immunoprecipitating biotinylated Vero cell surface proteins bound by SubAB as described in Section 2.11. The biotinylated putative receptor proteins were separated by SDS-PAGE, blotted onto a PVDF filter and detected by ECL (Figure 4.8). When ECL detection was performed with streptavidin-HRP, a high background was generated, resulting in little difference between lysates treated with and without SubAB. The use of anti-biotin-HRP, however, was more specific and demonstrated that SubAB bound proteins of approximately 50, 90, 120 kDa and, to a lesser extent, a 135-kDa protein which is the same size as β1 integrin, which has been shown to be a sialylated surface glycoprotein (Bellis, 2004). While a SubAB-reactive protein of approximately 190 kDa was also detected, a 155-kDa species representing α2 integrin did not appear to bind SubAB.

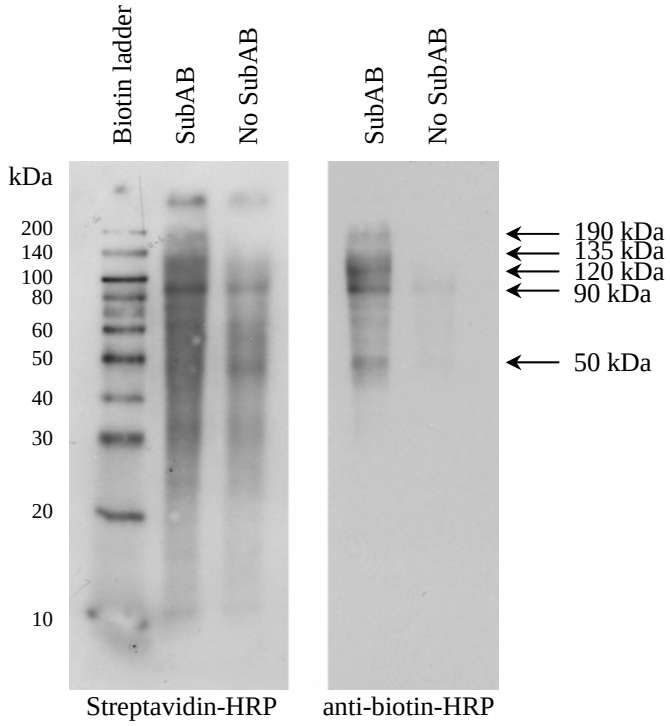

Figure 4.8: Immunoprecipitation of putative glycoproteins recognised by SubAB.

After biotinylating Vero cell suface proteins, cells were solubilised, incubated with and without SubAB and labelled with anti-His_6. Putative receptor proteins were collected with Protein G Sepharose FF, separated by SDS-PAGE and transferred onto PVDF. Membranes were probed with with either streptavidin-HRP or anti-biotin-HRP and detected by ECL.

4.3 Discussion

The pentameric B subunit of AB_5 toxins typically mediate binding to the eukaryotic cell surface via recognition of a specific carbohydrate moiety (Merritt and Hol, 1995). It was established in Chapter 3 that the subcellular transport route of SubAB-OG in Vero cells is similar, but not identical, to those of CtxB-AF594 and StxB-TR (Figure 3.6), suggesting that SubAB recognises a glycan receptor that is distinct from those of Ctx and Stx, which bind GM_1 and Gb_3, respectively (Lingwood *et al.*, 1987; Orlandi and Fishman, 1993). Previous studies have also demonstrated that SubAB-mediated cytotoxicity was not neutralised by *E. coli* expressing mimics of the glycan moieties of Gb_3, Gb_4 and lacto-*N*-neotetraosyl ceramide (Paton *et al.*, 2004). Furthermore, although 93.4% of SubAB was neutralised using a GM_2 RMC in the same study, this was significantly less than absorption of Stx with the Gb_3 RMC (> 98% neutralisation) (Paton *et al.*, 2000b). This indicates that the preferred target receptor for SubAB may not be GM_2 and potentially has a greater affinity for a structurally similar oligosaccharide.

As CtxB and StxB recognise the carbohydrate domains of glycolipids, the affinity of SubAB for glycolipid species extracted from Vero cells was analysed by a TLC toxin overlay assay, which has been used to demonstrate the glycolipid affinities of Ctx and Stx for GM_1 and Gb_3, respectively (Magnani *et al.*, 1980; Lingwood *et al.*, 2000). When compared to the intensity of the corresponding bands in the orcinol-sprayed plate, SubAB displayed a limited affinity for Vero cell GSL extracts, but exhibited strong binding for at least two GGS species extracted from Vero cells (Figure 4.1). None of the species, however, co-migrated with any of the commercially purified glycolipid standards. Curiously, SubAB clearly demonstrated an affinity for the commercial Gb_4 standard in a TLC toxin overlay assay (Figure 4.1a), contrary to

previous findings that the Gb_4 RMC did not significantly neutralise SubAB (Paton *et al.*, 2004), and that it did not bind to the LPS extract of the Gb_4 RMC in an LPS toxin overlay assay (Figure 4.3). Furthermore, SubAB did not recognise a species in the Vero cell neutral GSL extract that migrated in the vicinity of the commercially purified Gb_4 standard (Figure 4.1a) despite the expression of Gb_4 by Vero cells has been confirmed by Samuel *et al*. (1990). As the Gb_4 standard used in the chromatogram is purified from human erythrocytes, it is possible that the differences in the lipid chain length and saturation modulate not only its R_f value, but also the presentation of the carbohydrate domain when compared to that found in Vero cells. Although it would be ideal to use glycolipid standards isolated from Vero cells to assess toxin affinity, they were not commercially available at the time.

As the specificity of CtxB-POD for GM_1 was demonstrated in the context of a TLC toxin overlay assay (data not shown), the LPS toxin overlay assay developed in this study was validated by using this particular interaction as a positive control (Figure 4.2). SubAB-OG bound the oligosaccharide structures of the GM_2 and GM_3 RMCs, but not those of Gb_3 or Gb_4 RMCs in a toxin overlay assay using the chimeric LPS RMC extracts (Figure 4.3). Interestingly, no affinity of SubAB for the GM_2 or GM_3 standards was observed in the TLC toxin overlay assay demonstrating the chromatograms limited sensitivity. Nevertheless, the findings of this LPS toxin overlay correlate with previous studies showing that the GM_2 RMC neutralised a high proportion of SubAB-mediated cytotoxicity whereas the Gb_3 and Gb_4 RMCs did not (Paton *et al.*, 2004). Hence, this indicates that the LPS overlay is more sensitive than the TLC overlay assay and that the LPS extracts immobilised on the PVDF filter are a reliable representation of their native conformation in the RMC bacterial membrane.

The carbohydrate specificity of SubAB was also assessed against a diverse panel of 285 oligosaccharide structures spotted onto arrays that were incubated with SubAB-OG (Figure 4.4). From this, SubAB-OG exhibited only a mild affinity for the oligosaccharide components of GM_1, GM_2 and GM_3 on the printed array (glycans #201, #211 and #240, respectively) despite it binding the carbohydrate moieties of the GM_2 and GM_3 RMCs in an LPS toxin overlay assay. Considering that SubAB can bind to oligosaccharides terminating with Neu5Acα(2→3)Galβ(1→4) and that GM_3 is the only monosialo-GGS to display this terminal disaccharide (out of GM_1, GM_2 and GM_3) it is not surprising that the affinity of SubAB-OG for the GM_3 glycan structure was more than twice those for GM_1 and GM_2 on the array.

SubAB-OG preferentially bound glycans with either a terminal Neu5Gc or Neu5Gcα(2→3)Galβ disaccharide and, with a weaker affinity for similar structures terminating with Neu5Acα(2→3)Galβ, as mentioned above. As multivalent interactions may also be responsible for the avidity for some structures with a distal Neu5Acα(2→3) residue, SubAB-OG understandably exhibited a strong capacity to bind to the highly sialylated serum glycoprotein α1-AGP. Interestingly, when Neu5Ac is immobilised using the spacer arm Sp11 (#15), SubAB-OG binding has a CV of 29% whereas the monosaccharide sialic acids linked to Sp8, Neu5Gc (#264) and Neu5Ac (#14), were less consistent with CVs of 74% and 69%, respectively. This suggests that Sp11 may be a more flexible spacer arm than Sp8, allowing optimal presentation of sialic acid residues to interact with the SubB pentamer and accounting for a lower variability. A comparison of the Sp8 and Sp11 structures from CFG Core H revealed that Sp8 is essentially a short hydrocarbon chain ($–CH_2CH_2CH_2NH_2$) and Sp11 is more complex ($–OCH_2C_6H_4$-p-$NHCOCH_2NH$). To determine if the longer, more flexible Sp11 reduces variation between experiments, it would be ideal to compare SubAB-OG affinity for

Neu5Gc linked to Sp8 and Sp11 spacer arms. Unfortunately, version 2.1 of the array only contains Neu5Gcα-Sp8, but not Neu5Gcα-Sp11 and even the current version of the array (version 3.2) has yet to include Neu5Gcα-Sp11.

The results from the glycan array promoted the assessment of several sialylated carbohydrate structures for their ability to inhibit SubAB-mediated cytotoxicity on Vero cells. However, despite a 100-fold mass excess of the receptor analogues, all compounds (including α_1-AGP for which SubAB-OG exhibited the highest affinity) were unable to neutralise the toxin. Fluorescence microscopy revealed that Vero cells continue to internalise SubAB-OG in the presence of the receptor analogues indicating that monovalent interactions with free Neu5Gc monosaccharide are unable to protect cells from SubAB (Figure 4.7). Furthermore, despite the potential multivalent association with highly-sialylated α_1-AGP, SubAB was still taken up by host cells. This was possibly due to the oligosaccharides being presented on a relatively rigid protein surface, compared to a more fluid lipid bilayer, thereby preventing the sialic acid residues from being displayed in an optimal configuration. Accordingly, the inability of the receptor analogues to inhibit SubAB was most likely due to the toxin possessing a greater avidity for the target cell membrane. This highlights the significance of multivalent interactions and optimal positioning of carbohydrate receptors for efficient blockade of SubAB binding to the cell surface. Indeed, it has been shown that monovalent GM_1 oligosaccharide is less effective in blocking Ctx-GM_1 interactions than either GM_1 ganglioside or polyvalent GM_1 oligosaccharides conjugated to scaffolds including poly-L-lysine and termini of various dendrimers (Schengrund and Ringler, 1989; Thompson and Schengrund, 1997; Merritt *et al.*, 2002; Zhang *et al.*, 2002; Arosio *et al.*, 2004). The disruption of Stx-receptor interactions has been approached in a similar manner, in which globotriose has been chemically-linked to

silica beads, conjugated to scaffolds including dendrimers and acrylamide, or displayed on the surface of a bacterial RMC (Kitov *et al.*, 2000; Paton *et al.*, 2000b; Nishikawa *et al.*, 2002; Mulvey *et al.*, 2003; Watanabe *et al.*, 2004; Nishikawa *et al.*, 2005).

Although SubAB-OG bound to certain oligosaccharides containing a terminal Neu5Ac with a significantly lower affinity than those containing Neu5Gc, multivalent expression of Neu5Ac-containing receptors in a lipid bilayer may potentially facilitate stronger binding due to increased avidity, as is often observed in protein-glycan interactions (Evans and Roger MacKenzie, 1999; Fan *et al.*, 2000; Williams and Davies, 2001). As SubAB was found to recognise at least one GGS in FCS that was not expressed by Vero cells (Figure 4.5), it is also possible that SubAB uses this as an exogenous source of Neu5Gc or Neu5Gcα(2→3)Galβ disaccharide in order to gain entry to human cells. Indeed, human volunteers fed Neu5Gc revealed that, while most Neu5Gc was expelled in urine, small amounts can be incorporated into the synthesis of glycoproteins (Tangvoranuntakul *et al.*, 2003). Accordingly, ingested oligosaccharides with either a terminal Neu5Gc or Neu5Gcα(2→3)Galβ disaccharide may be incorporated into target cell membranes, therefore allowing SubAB to bind to human cells.

In addition to binding carbohydrates of glycolipids, the glycan array demonstrated the possibility of SubAB interacting with the glycoprotein α_1-AGP. It was also recently reported that the toxin can bind the glycoprotein α2β1 integrin isolated from Vero and HeLa cells (Yahiro *et al.*, 2006). While a 155-kDa band representing α2 integrin was not detected when duplicating the immunoprecipitation experiments in this study, it was confirmed that SubAB bound a 135-kDa protein that is the same size as β1 integrin (Figure 4.8), which is a sialylated surface protein (Bellis, 2004). Accordingly, the results of Yahiro *et al*. (2006) support the glycan array data obtained in the present

study, which reveal the toxins affinity for carbohydrates with terminal Neu5Gc and Neu5Ac residues. Furthermore, upon binding to the target cell surface, toxins can initiate cellular events including signal transduction and apoptosis, which are distinct from the direct toxic effects on host cell mechanisms (Popoff, 1998; Cherla *et al.*, 2003; Fujii *et al.*, 2003; Smith *et al.*, 2003). Indeed, binding of SubB alone to α2β1 integrin is reported to trigger vacuolation of the target cell, albeit at high doses (> 10 $\mu g.ml^{-1}$) (Yahiro *et al.*, 2006; Morinaga *et al.*, 2007). Studies are currently being undertaken to identify a surface receptor responsible for SubAB-mediated BiP cleavage.

The initial hypothesis that SubAB recognises an oligosaccharide domain from the acidic partition of the host cell glycolipid membrane extract is substantiated by the findings of this study. Sialic acids are major components of the mammalian cell surface and as surface bound sialic acids facilitate inter- and intra-cellular signalling, as well as host cell targeting by microbial toxins, the level of sialic acid hydroxylation is known to positively and negatively affect these interactions (Svennerholm, 1980; Muchmore *et al.*, 1998; Ono and Hakomori, 2004). Accordingly, there are potential functional consequences of this widespread structural change in humans affecting the surfaces of cells throughout the body.

One of the most common modifications of Neu5Ac is Neu5Gc; the terminal carbohydrate residue of the putative SubB receptor. Neu5Gc is synthesised by a cytidine monophospho-N-acetylneuraminic acid (CMP-Neu5Ac) hydroxylase that converts CMP-Neu5Ac to a CMP-Neu5Gc precursor in the cytosolic carbohydrate subunit pool (Shaw and Schauer, 1988; Muchmore *et al.*, 1989). Although a major sialic acid in mammalian tissues, including those of the four extant great apes (bonobo, chimpanzee, gorilla and orang-utan), human adults do not express significant levels of Neu5Gc, with the exception of foetal tissues and carcinomas (Ohashi *et al.*, 1983; Hirabayashi *et al.*,

1987; Devine *et al.*, 1991; Muchmore *et al.*, 1998; Malykh *et al.*, 2001). A comparison of human and chimpanzee CMP-Neu5Ac hydroxylase (*Cmah*) cDNA demonstrated that the Cmah enzyme is inactivated in humans by a 92-bp deletion that caused a frame-shift mutation allowing Neu5Ac surface expression to prevail (Chou *et al.*, 1998). Interestingly, Neu5Gc expression is selectively down-regulated in the brains of the great apes and the loss of *Cmah* is estimated to have occurred approximately 2.8 million years ago, after the divergence of the great apes and hominids, but shortly preceding human brain expansion (approximately 2.2 million years ago) (Chou *et al.*, 1998; Muchmore *et al.*, 1998; Chou *et al.*, 2002). Furthermore, *Cmah* knock-out adult mice exhibited symptoms including delayed wound healing and abnormal inner ear histology resulting in diminished hearing (Hedlund *et al.*, 2007).

The Hanganutziu-Deicher antigen has been shown to be a GGS containing Neu5Gc and when exposed to animal glycoproteins containing Neu5Gc, such as anti-venom IgG therapies, humans mount an immune response to this epitope and develop serum sickness (Higashi *et al.*, 1977; Merrick *et al.*, 1978). Accordingly, it is not surprising that oligosaccharides containing terminal Neu5Gc, as with Galα(1→3)Gal, have been implicated as xenoantigens and are responsible for the major clinical obstacle in xenotransplantation, namely hyperacute rejection (Galili *et al.*, 1988; Sandrin *et al.*, 1993; Zhu and Hurst, 2002).

Given the role of carbohydrate moieties in biological functions, aberrant glycosylation patterns may serve as markers for development, differentiation and disease states including cancer (Dennis *et al.*, 1999; Ono and Hakomori, 2004). Accordingly, SubAB may potentially be used to treat tumours as some human cancer cells exhibit increased surface expression of Neu5Gc (Ohashi *et al.*, 1983; Hirabayashi *et al.*, 1987; Devine *et al.*, 1991; Malykh *et al.*, 2001). They also express elevated levels

of BiP to counteract the ER stress caused by rapid cell division (Lee, 2007). As BiP is essential for cell survival and is also the intracellular substrate that is specifically cleaved by SubA (Paton *et al.*, 2006a), the mechanism of SubAB-mediated cytotoxicity may act in conjunction with its preferential binding to tumour cells that display Neu5Gc to specifically target cancer cells.

The results of this study comprise the first example of a bacterial protein toxin binding oligosaccharides that terminate with α2-3-linked Neu5Gc residues. Given that there is no known alternative pathway for synthesis of Neu5Gc in human cells and that human tissues can incorporate exogenous Neu5Gc into glycan synthesis (Tangvoranuntakul *et al.*, 2003; Hedlund *et al.*, 2007), it is possible that dietary Neu5Gc may confer human sensitivity to SubAB. Neu5Gc is not endogenously expressed by plants and bacteria, it is low or absent in poultry and fish, yet enriched in bovine milk and red meats including lamb, pork and beef. Accordingly, human tissues may incorporate dietary Neu5Gc by ingesting milk products and red meats. Ironically, dairy products and red meat are the richest sources of Neu5Gc and are also the foods most often contaminated with SubAB-producing STEC (Paton and Paton, 1998). Hence, by consuming these products, humans may ingest a bacterial pathogen and concurrently sensitise their cells to a major virulence factor.

Chapter 5

SubB Immunomodulation

5.1 Introduction

The majority of protein antigens are unable to elicit a strong immune response when administered alone and, accordingly, vaccines often exploit compounds such as Alum and Freund's adjuvants to increase the immunogenicity of the antigen (Cox *et al.*, 2006). In addition to mediating toxin binding and subcellular trafficking, the B subunits of AB_5 toxins also harbour substantial immunomodulatory properties. Despite conflicting reports in the literature, the B subunit of Ctx is known to be a potent modulator of the immune system with the potential to function as both a carrier protein for antigens that are directly linked to CtxB and as an adjuvant for those that are co-administered (Lycke and Holmgren, 1986; Holmgren *et al.*, 1993; Douce *et al.*, 1997; Rappuoli *et al.*, 1999; Park *et al.*, 2003). The immunomodulating properties of Ctx and CtxB stem from their ability to interact with professional APCs and enhance presentation of a co-administered antigen. It has been shown that Ctx increases macrophage cytokine secretion and B7.2 surface expression (Bromander *et al.*, 1991; Cong *et al.*, 1997; Cong *et al.*, 2001). It also promotes DC maturation and expression of co-stimulatory molecules and chemokine receptors to subsequently prime a mixed T_H1 and T_H2 immune response (Gagliardi *et al.*, 2000; Gagliardi *et al.*, 2002; Eriksson *et al.*, 2003).

Little is known of the capacity for CtxB to act as an adjuvant upon systemic (i.p.) delivery. Similar to Ctx however, CtxB interacts with APCs upregulating expression of CD40 and B7.2 on macrophages and DCs and primarily elicits a T_H2 type response against the co-administered antigen (George-Chandy *et al.*, 2001; Eriksson *et al.*, 2003). Park *et al.* (2003) demonstrated that CtxB enhances mucosal and systemic anti-BSA antibody titres upon i.p. immunisation with BSA. This was attributed, in part, to the increased expression of B7.2 on peritoneal macrophages. Similarly, Ctx and LT

enhanced both mucosal and systemic antibody responses upon transcutaneous immunisation by topical application to the skin of mice and humans (Glenn *et al.*, 1998b; Glenn *et al.*, 2000; Gockel *et al.*, 2000). Although an emerging field, recent studies have shown that non-toxic StxB and active-site mutant Stx can also behave as adjuvants, where mucosal administration enhances mucosal and serum antibody levels (Ohmura-Hoshino *et al.*, 2004) and subcutaneous delivery elicits a mixed T_H1 and T_H2 type response (Ohmura *et al.*, 2005).

Mice mount a rapid serum antibody response to SubAB when the toxin is expressed in the gastrointestinal tract by recombinant *E. coli* and this mediates recovery from severe toxin-induced weight loss (Paton *et al.*, 2004). These findings, and the known adjuvanticity of other AB_5 toxins (Ctx and Stx) and their respective B subunits, suggest that SubAB may also possess adjuvant properties. Although catalytically-inactivated $SubA_{A272}B$ has been shown to be an effective vaccine candidate against SubAB in mice (Talbot *et al.*, 2005), neither $SubA_{A272}B$ nor SubB have been examined previously for their ability to modulate the immune response to a co-administered antigen. For this reason, the ability for $SubA_{A272}B$ and SubB to augment the systemic antibody response to co-administered antigens was assessed in mice.

5.2 Results

5.2.1 Assessment of SubB as a Potential Immunomodulator

To establish if SubB has the capacity to modulate the immune response, the B subunit was assessed for its ability to enhance the antibody response to a co-administered antigen; the active site mutant $SubA_{A272}$. Furthermore, anti-$SubA_{A272}$ titres induced by co-administration with SubB were compared against those obtained using Alum adjuvant. Groups of five mice were injected three times i.p. with $SubA_{A272}$ antigen mixed with Alum and/or SubB as indicated (Figure 5.1). $SubA_{A272}$ doses in PBS were calculated with respect to 15 µg $SubA_{A272}B$ as either a mass (15 µg) or molar (142.9 pmol ≡ 5 µg) equivalent. To avoid any adjuvanticity and toxicity conferred by cross-contamination with trace amounts of SubA or SubAB, all subunits were affinity purified from recombinant bacterial hosts expressing either SubB or $SubA_{A272}$ only. Moreover, mice exposed to such preparations did not exhibit any symptoms of SubAB toxicity during the immunisation period. To determine the systemic immune response, murine sera were analysed for anti-$SubA_{A272}$ titres by ELISA (Section 2.19.3).

Immunisation of mice with either 5 or 15 µg $SubA_{A272}$ in PBS elicited a weak anti-$SubA_{A272}$ antibody response in most subjects resulting in geometric mean titres of 521 and 700, respectively. This demonstrates that the antigen in this study has an inherently low immunogenicity upon i.p. delivery in mice. However, when administered with Alum adjuvant, $SubA_{A272}$ induced a stronger immune response in all mice, with mean titres increasing more than three-fold to 1,876 and 2,552 for those treated with 5 and 15 µg $SubA_{A272}$, respectively. Mice immunised with 15 µg $SubA_{A272}B$ (equivalent to approximately 5 µg of $SubA_{A272}$ in complex with 10 µg SubB) produced a mean titre of 2,640, which was similar to those injected with either 5 µg or 15 µg $SubA_{A272}$ complexed with Alum ($P > 0.05$, Student's *t*-test). However, the titres induced by

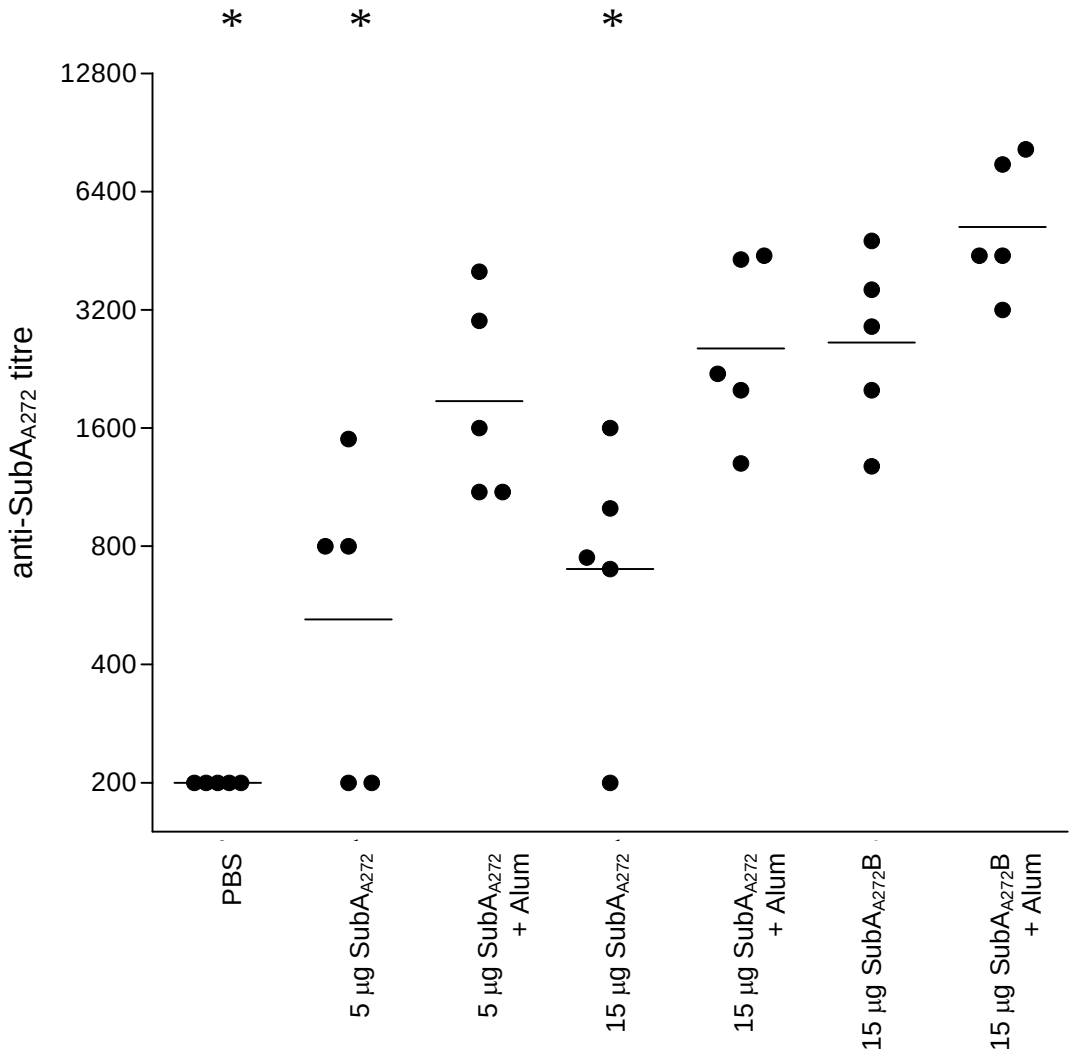

Figure 5.1: Adjuvanticity of SubB with SubA$_{A272}$.

Groups of five mice were injected with 5 or 15 µg SubA$_{A272}$ antigen alone or complexed with Alum or SubB, as indicated. Mice were immunised i.p. three times every two weeks and sera were collected two weeks after the final injection. Sera were tested for anti-SubA$_{A272}$ titres by ELISA, as described in Section 2.19.3. Titres are defined as the reciprocal of the serum dilution resulting in an A_{405} reading of 0.2 above background. Significance was determined by a Student's *t*-Test on $\log_2$(titre). *, $P < 0.05$ relative to 15 µg SubA$_{A272}$B.

$SubA_{A272}$ in complex with either SubB or Alum were significantly higher than those obtained in mice that received $SubA_{A272}$ only ($P < 0.05$). Anti-$SubA_{A272}$ titres were further increased to a mean of 5,202 when mice received 15 µg $SubA_{A272}B$ with Alum, but this did not reach statistical significance relative to titres elicited by $SubA_{A272}$ with Alum or $SubA_{A272}B$ alone. This demonstrates that SubB has the capacity to enhance the immunogenicity of the antigen $SubA_{A272}$ upon i.p. administration in mice. The immune response was increased to a level that is comparable to that elicited by Alum, indicating that SubB may potentially be employed as an adjuvant.

5.2.2 Relative Efficacy of SubB as an Adjuvant

While SubB was shown to enhance the immunogenicity of $SubA_{A272}$, comparable to Alum, SubB has a natural affinity for $SubA_{A272}$ which may have contributed significantly to the observed adjuvanticity. Furthermore, its efficacy had yet to be compared to CtxB, which, in addition to facilitating Ctx recognition of the target cell surface, is a potent mucosal adjuvant (Holmgren and Czerkinsky, 2005). CtxB has also been shown to enhance the systemic antibody response to BSA in mice upon i.p. immunisation (Park *et al.*, 2003). Accordingly, SubB and $SubA_{A272}B$ were assessed for their ability to enhance the host immune response against OVA (an antigen to which neither SubB nor CtxB are natively coupled) and compared to the adjuvanticity of Alum and CtxB (Figure 5.2). OVA admixed with Alum, CtxB, SubB or $SubA_{A272}B$ as indicated was administered i.p. three times to groups of five mice, and sera were analysed for anti-OVA titres by ELISA (Section 2.19.3). Mice immunised with 15 µg OVA in PBS produced a mean titre of 1,125. Mice had a significantly stronger response to OVA complexed with Alum (mean titre of 10,966 ($P < 0.005$)) and when co-administered with CtxB, similar systemic anti-OVA titres were obtained (a mean of

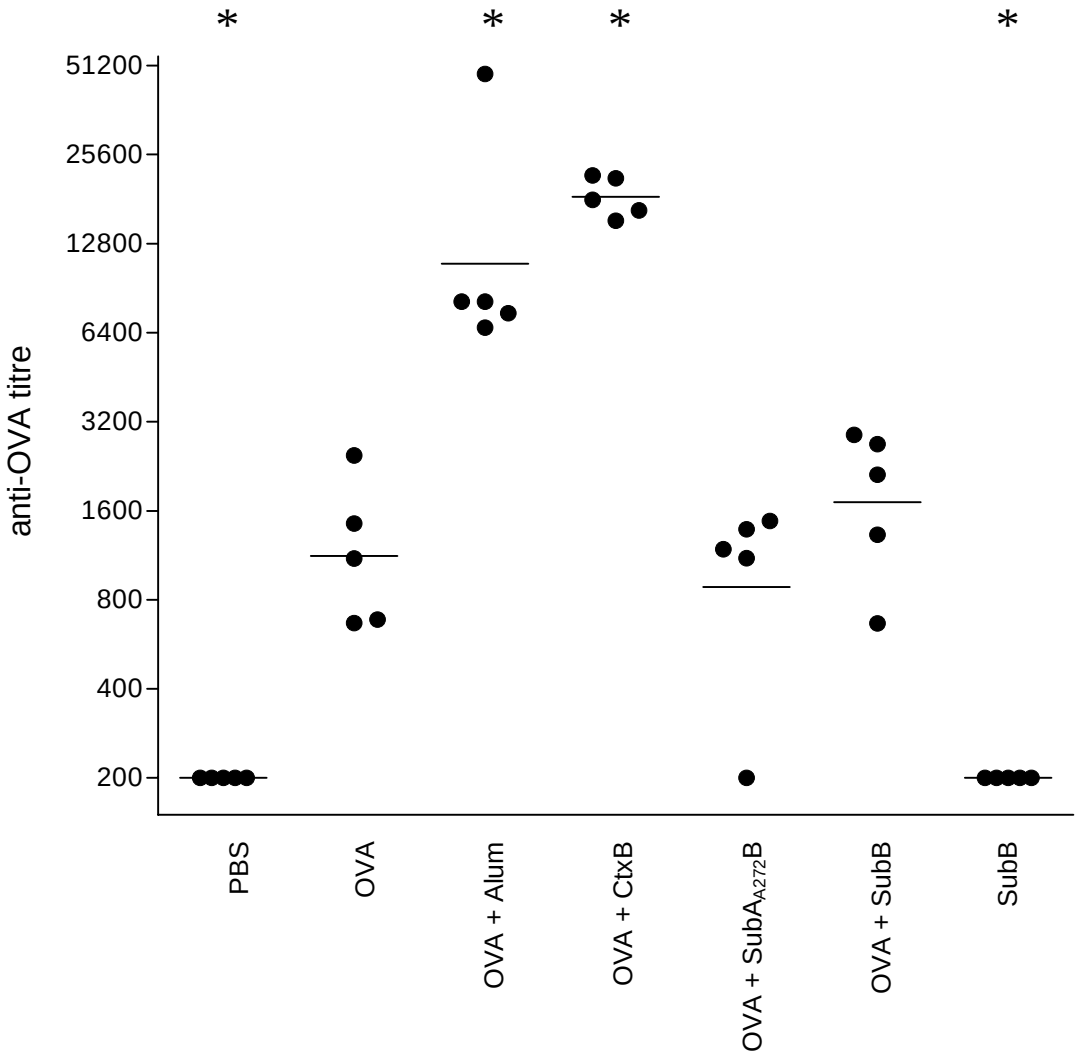

Figure 5.2: Adjuvanticity of SubB with OVA.

Groups of five mice were injected with 15 µg OVA alone or complexed with Alum, CtxB, $SubA_{A272}B$ or SubB. Mice were immunised i.p. three times every two weeks and sera were collected two weeks after the final injection. Sera were tested for anti-OVA titres by ELISA, as described in Section 2.19.3. Titres are defined as the reciprocal of the serum dilution resulting in an A_{405} reading of 0.2 above background. Significance was determined by a Student's *t*-test on $\log_2$(titre). *, $P < 0.05$ relative to OVA + SubB.

18,414 ($P < 0.000005$)). Groups of mice were also immunised with OVA mixed with either SubB or $SubA_{A272}B$ to assess their potential adjuvant activity, and yielded mean anti-OVA titres of only 1,709 and 884, respectively. These titres were not significantly different from each another, nor were these titres different to those elicited by OVA alone indicating that $SubA_{A272}B$ and SubB were incapable of enhancing the host immune response to co-administered OVA. Hence, both $SubA_{A272}B$ and SubB are clearly not as effective as Alum or CtxB in enhancing the systemic immune response to OVA when administered via the i.p. route.

5.3 Discussion

The holotoxins and respective B subunits of Ctx and Stx have been shown to be potent adjuvants when administered via the mucosal and, more recently, i.p. routes (Holmgren *et al.*, 2003; Park *et al.*, 2003; Ohmura-Hoshino *et al.*, 2004; Ohmura *et al.*, 2005). This raised the possibility of SubB also enhancing the systemic antibody response to a co-administered antigen delivered via the i.p. route in mice. The presence of SubB significantly increased serum anti-$SubA_{A272}$ antibody levels upon its co-administration with $SubA_{A272}$ compared to $SubA_{A272}$ alone and elicited titres similar to those using Alum. It was previously demonstrated that mice immunised with 10 μg $SubA_{A272}B$ complexed with Alum adjuvant exhibited strong systemic anti-$SubA_{A272}$ antibody responses with a geometric mean titre between 3,200 and 6,400 with PBS controls yielding a basal titre of less than 200 (Talbot *et al.*, 2005). In the current study, 15 μg $SubA_{A272}B$ elicited similar titres when compared to a basal level of less than 200 in the same host. Talbot *et al*. (2005) also found that anti-$SubA_{A272}B$ sera cross-reacted with SubAB, and conferred protection against active holotoxin. Mice exhibiting high anti-$SubA_{A272}$ titres survived i.p. challenge with 5 μg purified SubAB (more than 25 times the lethal dose (Paton *et al.*, 2004)) and were protected from significant weight-loss induced by oral challenge with an *E. coli* DH5α clone expressing SubAB.

Although not significantly different, the mean titre from mice treated with $SubA_{A272}B$ complexed with Alum was slightly higher than those with $SubA_{A272}B$ indicating that SubB and Alum may work in synergy to modulate the systemic immune response. The efficacy of SubB to modulate the systemic immune response against $SubA_{A272}$ may have been promoted by the spontaneous formation of the enzymatically-inactive holotoxin. Therefore, the ability for SubB to enhance the immune response to

$SubA_{A272}$ may not be a result of its capacity as an adjuvant, but rather, its function as a carrier protein for the antigen.

To address the possibility of SubB behaving as a carrier protein, the structurally-unrelated protein OVA was used as an antigen in place of $SubA_{A272}$. Furthermore, the ability of SubB to augment anti-OVA antibody titres was compared to those of previously-characterised adjuvants, Alum and CtxB. While the use of Alum adjuvant is relatively well-documented, there are limited reports concerning the adjuvanticity of CtxB, and even fewer regarding its effects on systemic immunity. Initially, the absence of ADP-ribosylase activity was shown to curb the adjuvanticity of CtxB and the disparity between these reports in the literature was primarily attributed to contamination with CtxA or holotoxin (Lycke and Holmgren, 1986; Holmgren *et al.*, 1993). CtxB was believed to function as a carrier protein capable of enhancing the host immune response to unrelated antigens that were directly linked to the non-toxic subunit (McKenzie and Halsey, 1984; Sun *et al.*, 1994). However, more recent reports showed that CtxB can also modulate host immune responses against unrelated antigens without chemical or genetic coupling (Russell *et al.*, 1996; Tochikubo *et al.*, 1998; Park *et al.*, 2003). Indeed, this study demonstrates that, like Alum, recombinant CtxB that is free of holotoxin contaminants can significantly enhance the systemic antibody response to OVA antigen simply by co-administration via the i.p. route. Hence, these findings provide further evidence of the adjuvanticity of CtxB and specifically, its ability to enhance the systemic immune response.

Like CtxB, StxB is also an effective adjuvant upon i.n. immunisation when co-administered with OVA, obtaining both mucosal and systemic immune responses in mice (Ohmura-Hoshino *et al.*, 2004). It is therefore reasonable to expect that other AB_5 toxins and their B subunits, including the active site-mutant $SubA_{A272}B$ and SubB,

might possess similar adjuvant properties. $SubA_{A272}B$ and SubB, however, were not as effective as either Alum or CtxB when mixed with OVA, yielding titres that were not significantly different to those observed in mice treated with OVA alone. The non-toxic LT mutant, LT-K63 co-administered with keyhole limpet haemocyanin was shown to be a more effective adjuvant when delivered orally rather than intranasally (Douce *et al.*, 1999). It is therefore possible that i.p. administration of SubB and $SubA_{A272}B$ affected the adjuvant properties of either molecule and that a different delivery route may have proved more successful.

The adjuvant activity of SubB may also be partly determined by the antigen itself as SubB exhibited strong immunomodulatory effects when using $SubA_{A272}$ as an antigen, but not OVA. Indeed, the adjuvant activities of both Cry1Ac protoxin and Ctx have been shown to vary depending on the co-administered antigen (Esquivel-Perez and Moreno-Fierros, 2005). However, unlike OVA, $SubA_{A272}$ can natively couple to SubB suggesting that the immunomodulatory effect of SubB on anti-$SubA_{A272}$ titres was caused by the spontaneous formation of the inactive holotoxin. Hence, unlike Alum, CtxB and StxB, SubB did not possess any significant adjuvant properties when co-administered with OVA via the i.p. route. Its adjuvanticity, however, may potentially be realised with other antigens that may be considered for future studies. Interestingly, when co-administered with $SubA_{A272}$, SubB was revealed to be equally as effective as Alum adjuvant yielding titres which have been previously shown to protect mice upon challenge with a lethal dose of SubAB. It is therefore highly likely that SubB behaves as a carrier protein, as opposed to an adjuvant, for antigens with which it can form sufficient hydrogen bonds, including $SubA_{A272}$.

Chapter 6
Final Discussion

6.1 Final Discussion

Pathogenic bacteria can elaborate a range of toxins to damage their hosts and these are frequently key virulence factors of the micro-organism that produces them. One such family is the AB_5 protein toxins, which, until recently, were exemplified by three classes: Ctx (and related LT), Stx and Ptx (Fan *et al.*, 2000). The pathology produced by infection with STEC, including life-threatening HUS and gastrointestinal symptoms, is primarily attributed to its key virulence factor Stx, which has RNA *N*-glycosidase activity (Nataro and Kaper, 1998; Paton and Paton, 1998). A fourth AB_5 toxin family was shown to be produced by particular STEC strains in addition to Stx; it was designated subtilase cytotoxin (SubAB) because it's a subunit enzymatic site is characteristic of the subtilase family of serine proteases and crucial for the cytotoxicity of SubAB (Siezen and Leunissen, 1997; Paton *et al.*, 2004). Paton *et al*. (2006a) revealed that the extreme toxicity of SubAB for Vero cells is due to the highly-specific cleavage of BiP or GRP78 (a master regulator of ER stress signalling (Hendershot, 2004)) that is mediated by SubA. The loss of BiP function has inexorably detrimental consequences for the targeted cell, causing cell death by a previously-uncharacterised mechanism (Hamman *et al.*, 1998; Kim and Arvan, 1998; Rao *et al.*, 2004; Lee, 2005). As no cytotoxin has previously been shown to target components of the ER, SubAB is the prototype of a novel class of bacterial serine protease cytotoxins.

Although the mode of action of SubA and its intracellular target have been identified, SubB is relatively uncharacterised. The B subunit of each of the three previously-characterised AB_5 toxins facilitate toxin binding to the target cell by recognising distinct oligosaccharide receptors expressed on the host cell surface. Additionally, they direct the subcellular trafficking of the catalytic A subunit to its intracellular substrate and, for CtxB, LT-B and StxB, are potent adjuvants (Holmgren *et*

al., 2003; Ohmura-Hoshino *et al.*, 2004). While the mechanism of SubAB-mediated cytotoxicity has been elucidated, its intracellular transport route from the cell surface to its ER substrate BiP and a corresponding functional host cell surface receptor were not determined prior to this study. Furthermore, although $SubA_{A272}B$ has been shown to be a potent immunogen that protects mice from challenge with a lethal dose of SubAB (Talbot *et al.*, 2005), the adjuvanticity of SubB had not been investigated. This study, therefore, provides an understanding of SubB with respect to its role in cytotoxicity and immunomodulation.

Analysis of the subcellular trafficking pathway of SubAB in Vero cells was undertaken in Chapter 3. Fluorescence confocal microscopy revealed that uptake of SubAB by Vero cells occurred within 5 min of exogenous addition of the toxin, co-localising with its ER-resident substrate BiP in less than 30 min (Section 3.2.5). These kinetics correlated with previous reports that SubAB-mediated BiP cleavage was evident in Vero cells within 20 min (Paton *et al.*, 2006a). Inhibition studies presented in Section 3.2.6 examined the pathway via which SubAB is internalised and transported within the cell. Specifically, inhibition of clathrin-dependent (cholesterol-independent) endocytosis with PAO protected cells from SubAB-OG internalisation and cytotoxicity (measured by BiP cleavage in Section 3.2.7), whereas cholesterol depletion using methyl-β-cyclodextrin (MβCD) and/or filipin did not prevent SubAB cytotoxicity. This was also demonstrated in HCT-8, HeLa and N2A cells despite the negligible uptake of SubAB-OG observed in these cell lines by confocal fluorescence microscopy. Fluorescence co-localisation revealed that, like CtxB and StxB, SubAB-OG was actively transported via a retrograde pathway to the TGN, Golgi and ER in Vero cells. Furthermore, individual Vero cells exposed to SubAB-OG and co-incubated with either CtxB-AF594 or StxB-TR preferentially internalised one or both toxins (Section 3.2.4).

These experiments demonstrated that the trafficking route of SubAB in Vero cells is similar, but not identical, to those of CtxB and StxB, and that SubAB is internalised exclusively via clathrin-dependent endocytosis, whereas CtxB and StxB engaged both clathrin- and cholesterol-dependent routes. The reason why SubAB is incapable of exploiting multiple endocytic pathways is still to be determined, but may be influenced by its surface receptor associating with selected membrane microdomains.

Mammalian cells display a vast array of oligosaccharide moieties in the context of surface glycoproteins and glycolipids and recognition of these carbohydrate receptors by bacterial AB_5 protein toxins contributes significantly to toxin trafficking and the pathogenesis of disease (Merritt and Hol, 1995; Karlsson, 1998). Accordingly, the differential toxin internalisation observed in individual cells exposed to SubAB-OG and either CtxB-AF594 or StxB-TR indicated that SubAB recognised a target cell receptor that is distinct from those bound by CtxB and StxB. Previous studies demonstrated SubAB affinity for acidic oligosaccharides as the toxin was partially neutralised using a bacterial GM_2 RMC (Paton *et al.*, 2004) and that SubB, but not SubA, bound to the heavily-sialylated glycoprotein α2β1 integrin (Yahiro *et al.*, 2006). Identification of the cognate glycan receptor of SubAB was achieved by several approaches which, collectively, support the hypothesis that the toxin recognises an acidic oligosaccharide. Analysis of Vero cell glycolipid extracts in TLC toxin overlay assays revealed that SubAB possessed a greater affinity for acidic species (R_f = 0.347, 0.396 and 0.557) in the GGS fraction than for neutral species in the GSL portion. To ensure that chimeric LPS from bacterial RMCs were displayed in a similar context to the GGS species on TLC plates, a bacterial RMC toxin overlay was developed in Section 4.2.2, which included LPS extracts from RMCs that had not been assessed by Paton *et al.* (2004). The toxin overlay performed with SubAB-OG revealed an affinity for the glycan

structures of LPS from GM_2 and GM_3 RMCs which correlates with previous findings that a GM_2 RMC can neutralise SubAB and concurrently demonstrates that the assay is a valid representation of the RMC in the bacterial membrane. Additionally, glycan array analysis demonstrated that SubB possessed a unique affinity for oligosaccharides with either a distal Neu5Gc or Neu5Gcα(2→3)Galβ disaccharide and a weaker affinity for similar glycans terminating with Neu5Acα(2→3)Galβ. Neu5Gc is widely expressed by mammals with the exception of humans; however, exogenous Neu5Gc might be incorporated into human cells by ingesting foods such as dairy products and red meat (Tangvoranuntakul *et al.*, 2003). Curiously, while dairy products and red meat are the richest sources of Neu5Gc, they are also the foods most often contaminated with SubAB-producing STEC (Paton and Paton, 1998). Hence, by ingesting these products, humans may be exposed to a bacterial pathogen while concurrently sensitising their cells to a major virulence factor of the pathogen.

Monovalent oligosaccharides terminating with either Neu5Gc or Neu5Gcα(2→3)Galβ and highly-sialylated serum protein α_1-AGP were unable to prevent Vero cells from internalising SubAB-OG (Section 4.2.5). Furthermore, the receptor analogues did not prevent SubAB-mediated cytotoxicity nor BiP cleavage, suggesting that SubAB possessed a higher affinity for the host cell receptors than the receptor analogues. Therefore, SubAB may overcome the low inherent affinity of carbohydrate-protein interactions by engaging multiple host receptors (at least one per SubB monomer) that are presented in a fluid lipid bilayer. Indeed, such low-affinity associations have been harnessed by multivalency in designing effective, low-molecular weight carbohydrate ligand inhibitors of CtxB (Merritt *et al.*, 2002) and StxB (Kitov *et al.*, 2000) and highlights the importance of optimal spatial arrangement of receptors and the resulting avidity for SubAB to bind to the target cell. Although the terminal

oligosaccharide of the SubB receptor has been identified, further studies are required to determine the complete functional receptor expressed by target cells.

The elucidation of the distal Neu5Gcα(2→3)Galβ disaccharide as the receptor recognised by SubB confirms that its receptor was distinct from those of CtxB (GM_1) and StxB (Gb_3 and Gb_4) and partly explains the differential uptake of SubAB-OG, CtxB-AF594 and StxB-TR by individual Vero cells observed in Section 3.2.4. This phenomenon was also shown to be a function of the cell cycle, in which, SubAB-OG was internalised by Vero cells traversing G1 phase and cells in early S phase, whereas cells migrating through the remainder of the cycle exhibited minimal uptake (Section 3.2.8). Furthermore, CtxB-AF594 was preferentially internalised by cells in S through M phases and by a majority of cells in G1, whereas StxB-TR uptake occurred in cells migrating through G1. Pudymaitis and Lingwood (1992) also showed that total Gb_3 composition did not vary during the cell cycle and that Stx internalisation may be influenced by transport of Gb_3 to the cell surface. Conversely, Majoul *et al*. (2002) demonstrated that toxin uptake was determined by differential expression of the glycolipid receptor, rather than receptor cycling. Although the mechanism of cell cycle-dependent SubAB internalisation (e.g. receptor cycling or receptor expression) has yet to be clarified, it is anticipated that rapid cell division (such as that of cancer cells or during tissue repair) will increase susceptibility to SubAB.

While B subunits of AB_5 toxins mediate target cell binding and subcellular trafficking, they can also potentiate the immune response to co-administered antigen. Given the adjuvanticity of CtxB and StxB (Holmgren *et al.*, 2003; Ohmura-Hoshino *et al.*, 2004), the systemic immunomodulatory properties of SubB were assessed in Chapter 5. SubB significantly increased the immune response against $SubA_{A272}$ in mice when delivered via the i.p. route and achieved titres that were comparable to those

obtained using Alum adjuvant (Section 5.2.1). Furthermore, even higher anti-$SubA_{A272}$ titres were observed when employing Alum and SubB simultaneously, although this was not significantly higher than when using either compound individually. In contrast, SubB did not enhance the immune response to structurally-unrelated OVA antigen whereas Alum and CtxB did (Section 5.2.2). This indicated that SubB may function as a systemic carrier protein for antigens with which it can form significant hydrogen bonds, such as $SubA_{A272}$. This study also demonstrated that CtxB can function as a systemic adjuvant upon i.p. administration and provides further evidence to support the findings of Park *et al.* (2003). However, as with other adjuvants derived from AB_5 toxins, SubB adjuvanticity might be realised if an antigen other than OVA or a different immunisation route (e.g. mucosal) were used and should be considered for future studies (Douce *et al.*, 1999; Esquivel-Perez and Moreno-Fierros, 2005). SubB may therefore be a valuable tool in systemic immunomodulation as a carrier protein and/or an adjuvant.

This study provides a greater understanding of a novel AB_5 toxin and major STEC pathogenesis factor. Treatment of STEC disease with antibiotics is contraindicated and treatment is largely focused on supportive medical care (Nataro and Kaper, 1998; Paton and Paton, 1998). However, several promising approaches to managing STEC disease disrupt Stx binding to the host cell membrane, rather than targeting the pathogen itself (Kitov *et al.*, 2000; Paton *et al.*, 2000b; Mulvey *et al.*, 2003). While the enteric pathogenicity of STEC signifies the benefit of a bacterial RMC to neutralise SubAB in the digestive tract, the need for receptor analogues to limit SubAB in the circulation are indicated by the HUS-like symptoms previously observed in toxin-treated mice (Wang *et al.*, 2007). Accordingly, the elucidation of the terminal disaccharide of the SubB receptor allows the development of carbohydrate therapeutics

to abrogate this fundamental step of SubAB cytotoxicity and subsequently limit the systemic complications of severe STEC disease.

The discovery of STEC strains that elaborate SubAB raises the issue of the effects that both SubAB and Stx may have upon targeting the same cell. SubAB-mediated cleavage of BiP may diminish Stx cytotoxicity as Stx interacts with BiP for its retrotranslocation to the cytosol (Yu and Haslam, 2005; Falguieres and Johannes, 2006). Conversely, as BiP seals the Sec61 translocon pore of the ER membrane (Hamman *et al.*, 1998), its degradation by SubAB may deregulate Stx retrotranslocation and expedite Stx-mediated cell death. SubAB has the potential to substantially augment the severity of clinical manifestations possibly acting in synergism with Stx, or by causing disease in its own right and additional studies are needed to determine its complete role in STEC disease.

STEC are the cause of substantial morbidity and mortality, placing a significant burden on health care services worldwide. Although the precise contribution of SubAB to human disease is still uncertain, this study has provided important insights into the biological properties of a potentially significant virulence factor.

APPENDIX A

Glycan Array

A.1 Glycan Array Data by Glycan Number

A complete list of glycans for which the affinity of SubAB-OG was tested is presented in Table A.1; data are sorted by glycan number. The printed array (version 2.1) consisted of 285 glycans in replicates of six with maxima and mimima removed from each set (n = 4). Data were provided by David Smith (CFG Core H).

Table A.1: Glycan affinity of SubAB-OG (100 µg.ml^{-1}) by glycan number.

#	Glycan Name	Mean RFU (n=4)*	STDEV	SEM	% CV
1	α_1-AGP	41519	1823	911	4
2	AGP-A	36382	800	400	2
3	AGP-βl	9830	1607	804	16
4	Ceruloplasmine	3028	764	382	25
5	Fibrinogen	272	144	72	53
6	Transferrin	3527	209	104	6
7	α-D-Gal–Sp8	428	80	40	19
8	α-D-Glc–Sp8	195	129	64	66
9	α-D-Man–Sp8	357	369	23	104
10	α-GalNAc–Sp8	466	164	82	35
11	α-L-Fuc–Sp8	178	123	62	69
12	α-L-Fuc–Sp9	340	177	88	52
13	α-L-Rhα–Sp8	394	184	92	47
14	α-Neu5Ac–Sp8	1260	823	412	65
15	α-Neu5Ac–Sp11	4492	1293	647	29
16	β-Neu5Ac-Sp8	160	74	37	46
17	β-D-Gal–Sp8	557	354	177	64
18	β-D-Glc–Sp8	289	97	48	33
19	β-D-Man–Sp8	71	29	15	41
20	β-GalNAc–Sp8	429	183	92	43
21	β-GlcNAc–Sp0	290	147	74	51
22	β-GlcNAc–Sp8	268	161	80	60
23	β-GlcN(Gc)-Sp8	176	119	60	68
24	(Galβ1-4GlcNAcβ)$_2$-3,6-GalNAcα–Sp8	182	106	53	58
25	GlcNAcβ1-3(GlcNAcβ1-4)(GlcNAcβ1-6)GlcNAc-Sp8	355	200	100	56

#	Glycan Name	Mean RFU (n=4)*	STDEV	SEM	% CV
26	[3OSO3][6OSO3]Galβ1-4[6OSO3]GlcNAcβ-Sp0	464	121	61	26
27	[3OSO3][6OSO3]Galβ1-4GlcNAcβ-Sp0	600	197	98	33
28	[3OSO3]Galβ1-4Glcβ-Sp8	170	93	46	55
29	[3OSO3]Galβ1-4(6OSO3)Glcβ–Sp0	409	72	36	18
30	[3OSO3]Galβ1-4(6OSO3)Glcβ–Sp8	586	207	104	35
31	[3OSO3]Galβ1-3(Fucα1-4)GlcNAcβ–Sp8	249	167	84	67
32	[3OSO3]Galβ1-3GalNAcα–Sp8	467	78	39	17
33	[3OSO3]Galβ1-3GlcNAcβ–Sp8	541	111	55	21
34	[3OSO3]Galβ1-4(Fucα1-3)GlcNAcβ–Sp8	420	158	79	38
35	[3OSO3]Galβ1-4[6OSO3]GlcNAcβ-Sp8	685	148	74	22
36	[3OSO3]Galβ1-4GlcNAcβ–Sp0	1076	946	473	88
37	[3OSO3]Galβ1-4GlcNAcβ-Sp8	457	184	92	40
38	[3OSO3]Galβ–Sp8	371	83	41	22
39	[4OSO3][6OSO3]Galβ1-4GlcNAcβ-Sp0	395	129	65	33
40	[4OSO3]Galβ1-4GlcNAcβ-Sp8	592	207	104	35
41	6-H_2PO_3Manα–Sp8	156	37	18	23
42	[6OSO3]Galβ1-4Glcβ–Sp0	395	52	26	13
43	[6OSO3]Galβ1-4Glcβ–Sp8	582	161	81	28
44	[6OSO3]Galβ1-4GlcNAcβ–Sp8	554	76	38	14
45	[6OSO3]Galβ1-4[6OSO3]Glcβ-Sp8	385	298	149	77
46	NeuAcα2-3[6OSO3]Galβ1-4GlcNAcβ–Sp8	672	270	135	40
47	[6OSO3]GlcNAcβ–Sp8	386	169	85	44
48	9-O-AcNeu5NAcα-Sp8	902	363	182	40
49	9-O-AcNeu5NAcα2-6Galβ1-4GlcNAcβ-Sp8	562	236	118	42
50	Manα1-3(Manα1-6)Manβ1-4GlcNAcβ1-4GlcNAcβ-Gly	139	53	26	38
51	GlcNAcβ1-2Manα1-3(GlcNAcβ1-2Manα1-6)Manβ1-4GlcNAcβ1-4GlcNAcβ-Gly	250	90	45	36
52	Galβ1-4GlcNAcβ1-2Manα1-3(Galβ1-4GlcNAcβ1-2Manα1-6)Manβ1-4GlcNAcβ1-4GlcNAcβ-Gly	333	219	109	66
53	Neu5Acα2-6Galβ1-4GlcNAcβ1-2Manα1-3(Neu5Acα2-6Galβ1-4GlcNAcβ1-2Manα1-6)Manβ1-4GlcNAcβ1-4GlcNAcβ-Gly	597	134	67	22
54	Neu5Acα2-6Galβ1-4GlcNAcβ1-2Manα1-3(Neu5Acα2-6Galβ1-4GlcNAcβ1-2Manα1-6)Manβ1-4GlcNAcβ1-4GlcNAcβ-Sp8	774	295	147	38
55	Fucα1-2Galβ1-3GalNAcβ1-3Galα-Sp9	375	316	158	84
56	Fucα1-2Galβ1-3GalNAcβ1-3Galα1-4Galβ1-4Glcβ-Sp9	319	85	43	27
57	Fucα1-2Galβ1-3(Fucα1-4)GlcNAcβ–Sp8	243	81	41	33
58	Fucα1-2Galβ1-3GalNAcα–Sp8	394	118	59	30

#	Glycan Name	Mean RFU (n=4)*	STDEV	SEM	% CV
59	Fucα1-2Galβ1-3GalNAcβ1-4(Neu5Acα2-3)Galβ1-4Glcβ-Sp0	462	144	72	31
60	Fucα1-2Galβ1-3GalNAcβ1-4(Neu5Acα2-3)Galβ1-4Glcβ-Sp9	438	145	72	33
61	Fucα1-2Galβ1-3GlcNAcβ1-3Galβ1-4Glcβ–Sp10	178	89	44	50
62	Fucα1-2Galβ1-3GlcNAcβ1-3Galβ1-4Glcβ–Sp8	465	105	52	23
63	Fucα1-2Galβ1-3GlcNAcβ–Sp0	569	104	52	18
64	Fucα1-2Galβ1-3GlcNAcβ–Sp8	352	100	50	28
65	Fucα1-2Galβ1-4(Fucα1-3)GlcNAcβ1-3Galβ1-4(Fucα1-3)GlcNAcβ-Sp0	448	119	60	27
66	Fucα1-2Galβ1-4(Fucα1-3)GlcNAcβ1-3Galβ1-4(Fucα1-3)GlcNAcβ1-3Galβ1-4(Fucα1-3)GlcNAcβ-Sp0	410	57	28	14
67	Fucα1-2Galβ1-4(Fucα1-3)GlcNAcβ–Sp0	488	161	80	33
68	Fucα1-2Galβ1-4(Fucα1-3)GlcNAcβ–Sp8	159	110	55	69
69	Fucα1-2Galβ1-4GlcNAcβ1-3Galβ1-4GlcNAc–Sp0	687	334	167	49
70	Fucα1-2Galβ1-4GlcNAcβ1-3Galβ1-4GlcNAcβ1-3Galβ1-4GlcNAcβ-Sp0	1267	82	41	6
71	Fucα1-2Galβ1-4GlcNAcβ–Sp0	481	129	65	27
72	Fucα1-2Galβ1-4GlcNAcβ–Sp8	429	65	32	15
73	Fucα1-2Galβ1-4Glcβ–Sp0	488	273	137	56
74	Fucα1-2Galβ–Sp8	350	96	48	27
75	Fucα1-3GlcNAcβ-Sp8	317	127	63	40
76	Fucα1-3GlcNAcβ-Sp8	311	126	63	40
77	Fucα1-4GlcNAcβ–Sp8	172	65	33	38
78	Fucβ1-3GlcNAcβ-Sp8	262	187	94	72
79	GalNAcα1-3(Fucα1-2)Galβ1-3GlcNAcβ-Sp0	495	160	80	32
80	GalNAcα1-3(Fucα1-2)Galβ1-4(Fucα1-3)GlcNAcβ-Sp0	372	149	74	40
81	GalNAcα1-3(Fucα1-2)Galβ1-4GlcNAcβ-Sp0	352	21	11	6
82	GalNAcα1-3(Fucα1-2)Galβ1-4GlcNAcβ–Sp8	398	77	38	19
83	GalNAcα1-3(Fucα1-2)Galβ1-4Glcβ-Sp0	337	64	32	19
84	GalNAcα1-3(Fucα1-2)Galβ–Sp8	366	56	28	15
85	GalNAcα1-3GalNAcβ–Sp8	405	218	109	54
86	GalNAcα1-3Galβ–Sp8	326	94	47	29
87	GalNAcα1-4(Fucα1-2)Galβ1-4GlcNAcβ-Sp8	223	129	65	58
88	GalNAcβ1-3GalNAca–Sp8	319	96	48	30
89	GalNAcβ1-3(Fucα1-2)Galβ-Sp8	230	145	73	63
90	GalNAcβ1-3Galα1-4Galβ1-4GlcNAcβ-Sp0	356	170	85	48
91	GalNAcβ1-4(Fucα1-3)GlcNAcβ-Sp0	260	109	54	42
92	GalNAcβ1-4GlcNAcβ–Sp0	586	337	169	58

#	Glycan Name	Mean RFU (n=4)*	STDEV	SEM	% CV
93	GalNAcβ1-4GlcNAcβ–Sp8	335	266	133	79
94	Galα1-2Galβ–Sp8	323	238	119	74
95	Galα1-3(Fucα1-2)Galβ1-3GlcNAcβ-Sp0	303	112	56	37
96	Galα1-3(Fucα1-2)Galβ1-4(Fucα1-3)GlcNAcβ-Sp0	418	252	126	60
97	Galα1-3(Fucα1-2)Galβ1-4GlcNAc-Sp0	186	80	40	43
98	Galα1-3(Fucα1-2)Galβ1-4Glcβ-Sp0	226	104	52	46
99	Galα1-3(Fucα1-2)Galβ–Sp8	250	208	104	83
100	Galα1-3(Galα1-4)Galβ1-4GlcNAcβ-Sp8	299	141	71	47
101	Galα1-3GalNAcα-Sp8	275	96	48	35
102	Galα1-3GalNAcβ–Sp8	191	42	21	22
103	Galα1-3Galβ1-4(Fucα1-3)GlcNAcβ–Sp8	374	67	33	18
104	Galα1-3Galβ1-3GlcNAcβ-Sp0	278	65	33	24
105	Galα1-3Galβ1-4GlcNAcβ–Sp8	439	102	51	23
106	Galα1-3Galβ1-4Glcβ–Sp0	344	219	109	64
107	Galα1-3Galβ–Sp8	364	149	75	41
108	Galα1-4(Fucα1-2)Galβ1-4GlcNAcβ-Sp8	206	67	33	33
109	Galα1-4Galβ1-4GlcNAcβ–Sp0	394	45	23	12
110	Galα1-4Galβ1-4GlcNAcβ–Sp8	251	35	18	14
111	Galα1-4Galβ1-4Glcβ–Sp0	350	88	44	25
112	Galα1-4GlcNAcβ–Sp8	499	93	46	19
113	Galα1-6Glcβ-Sp8	384	116	58	30
114	Galβ1-2Galβ–Sp8	344	115	58	33
115	Galβ1-3(Fucα1-4)GlcNAcβ1-3Galβ1-4(Fucα1-3)GlcNAcβ-Sp0	334	121	61	36
116	Galβ1-3(Fucα1-4)GlcNAcβ1-3Galβ1-4GlcNAcβ-Sp0	356	87	43	24
117	Galβ1-3(Fucα1-4)GlcNAc–Sp0	262	63	31	24
118	Galβ1-3(Fucα1-4)GlcNAc–Sp8	292	21	11	7
119	Galβ1-3(Fucα1-4)GlcNAcβ–Sp8	125	110	55	88
120	Galβ1-3(Galβ1-4GlcNAcβ1-6)GalNAcα-Sp8	352	219	110	62
121	Galβ1-3(GlcNAcβ1-6)GalNAcα-Sp8	315	107	54	34
122	Galβ1-3(Neu5Acα2-6)GalNAcα-Sp8	394	165	83	42
123	Galβ1-3(Neu5Acβ2-6)GalNAcα-Sp8	479	460	230	96
124	Galβ1-3(Neu5Acα2-6)GlcNAcβ1-4Galβ1-4Glcβ-Sp10	1115	361	180	32
125	Galβ1-3GalNAcα-Sp8	229	118	59	52
126	Galβ1-3GalNAcβ–Sp8	205	49	25	24
127	Galβ1-3GalNAcβ1-3Galα1-4Galβ1-4Glcβ-Sp0	312	59	30	19

#	Glycan Name	Mean RFU (n=4)*	STDEV	SEM	% CV
128	Galβ1-3GalNAcβ1-4(Neu5Acα2-3)Galβ1-4Glcβ-Sp0	341	48	24	14
129	Galβ1-3GalNAcβ1-4Galβ1-4Glcβ–Sp8	305	78	39	25
130	Galβ1-3Galβ–Sp8	331	26	13	8
131	Galβ1-3GlcNAcβ1-3Galβ1-4GlcNAcβ-Sp0	117	110	55	94
132	Galβ1-3GlcNAcβ1-3Galβ1-4Glcβ–Sp10	317	87	43	27
133	Galβ1-3GlcNAcβ–Sp0	408	148	74	36
134	Galβ1-3GlcNAcβ–Sp8	202	72	36	36
135	Galβ1-4(Fucα1-3)GlcNAcβ–Sp0	170	110	55	65
136	Galβ1-4(Fucα1-3)GlcNAcβ–Sp8	376	161	81	43
137	Galβ1-4(Fucα1-3)GlcNAcβ1-4Galβ1-4(Fucα1-3)GlcNAcβ-Sp0	300	71	36	24
138	Galβ1-4(Fucα1-3)GlcNAcβ1-4Galβ1-4(Fucα1-3)GlcNAcβ1-4Galβ1-4(Fucα1-3)GlcNAcβ–Sp0	254	86	43	34
139	Galβ1-4[6OSO3]Glcβ–Sp0	158	102	51	65
140	Galβ1-4[6OSO3]Glcβ–Sp8	270	53	27	20
141	Galβ1-4GalNAcα1-3(Fucα1-2)Galβ1-4GlcNAcβ-Sp8	212	110	55	52
142	Galβ1-4GalNAcβ1-3(Fucα1-2)Galβ1-4GlcNAcβ-Sp8	195	35	17	18
143	Galβ1-4GlcNAcβ1-3(Galβ1-4GlcNAcβ1-6)GalNAcα-Sp8	186	100	50	54
144	Galβ1-4GlcNAcβ1-3GalNAcα–Sp8	248	117	59	47
145	Galβ1-4GlcNAcβ1-3Galβ1-4(Fucα1-3)GlcNAcβ1-3Galβ1-4(Fucα1-3)GlcNAcβ-Sp0	285	76	38	27
146	Galβ1-4GlcNAcβ1-3Galβ1-4GlcNAcβ1-3Galβ1-4GlcNAcβ–Sp0	337	140	70	41
147	Galβ1-4GlcNAcβ1-3Galβ1-4GlcNAcβ–Sp0	256	52	26	20
148	Galβ1-4GlcNAcβ1-3Galβ1-4Glcβ–Sp0	244	105	53	43
149	Galβ1-4GlcNAcβ1-3Galβ1-4Glcβ–Sp8	241	156	78	65
150	Galβ1-4GlcNAcβ1-6(Galβ1-3)GalNAcα–Sp8	113	40	20	35
151	Galβ1-4GlcNAcβ1-6GalNAcα–Sp8	362	19	9	5
152	Galβ1-4GlcNAcβ–Sp0	367	249	124	68
153	Galβ1-4GlcNAcβ–Sp8	323	75	38	23
154	Galβ1-4Glcβ–Sp0	255	126	63	49
155	Galβ1-4Glcβ–Sp8	231	60	30	26
156	GlcNAcα1-3Galβ1-4GlcNAcβ-Sp8	270	146	73	54
157	GlcNAcα1-6Galβ1-4GlcNAcβ-Sp8	260	112	56	43
158	GlcNAcβ1-2Galβ1-3GalNAcα–Sp8	196	53	27	27
159	GlcNAcβ1-3(GlcNAcβ1-6)GalNAcα–Sp8	287	82	41	29
160	GlcNAcβ1-3(GlcNAcβ1-6)Galβ1-4GlcNAcβ–Sp8	128	118	59	92
161	GlcNAcβ1-3GalNAcα–Sp8	214	72	36	34

#	Glycan Name	Mean RFU (n=4)*	STDEV	SEM	% CV
162	GlcNAcβ1-3Galβ-Sp8	174	105	53	60
163	GlcNAcβ1-3Galβ1-3GalNAcα-Sp8	209	46	23	22
164	GlcNAcβ1-3Galβ1-4GlcNAcβ–Sp0	276	140	70	51
165	GlcNAcβ1-3Galβ1-4GlcNAcβ-Sp8	157	30	15	19
166	GlcNAcβ1-3Galβ1-4GlcNAcβ1-3Galβ1-4GlcNAcβ-Sp0	280	133	66	47
167	GlcNAcβ1-3Galβ1-4Glcβ–Sp0	148	49	24	33
168	GlcNAcβ1-4MDPLys	121	86	43	71
169	GlcNAcβ1-4(GlcNAcβ1-6)GalNAcα-Sp8	174	164	82	94
170	GlcNAcβ1-4Galβ1-4GlcNAcβ-Sp8	488	159	79	33
171	(GlcNAcβ1-4)6β-Sp8	185	90	45	48
172	(GlcNAcβ1-4)5β-Sp8	307	113	57	37
173	GlcNAcβ1-4GlcNAcβ1-4GlcNAcβ–Sp8	274	97	49	36
174	GlcNAcβ1-6(Galβ1-3)GalNAcα–Sp8	227	135	68	60
175	GlcNAcβ1-6GalNAcα–Sp8	302	178	89	59
176	GlcNAcβ1-6Galβ1-4GlcNAcβ-Sp8	219	224	112	102
177	Glcα1-4Glcβ–Sp8	241	144	72	60
178	Glcα1-4Glcα–Sp8	125	70	35	56
179	Glcα1-6Glcα1-6Glcβ-Sp8	191	104	52	54
180	Glcβ1-4Glcβ-Sp8	324	235	117	72
181	Glcβ1-6Glcβ-Sp8	188	79	39	42
182	Sorbitol-Sp8	166	79	39	47
183	GlcAα-Sp8	174	198	99	113
184	GlcAβ-Sp8	326	108	54	33
185	GlcAβ1-3Galβ-Sp8	255	173	86	68
186	GlcAβ1-6Galβ-Sp8	277	137	68	49
187	KDNα2-3Galβ1-3GlcNAcβ–Sp0	277	68	34	25
188	KDNα2-3Galβ1-4GlcNAcβ–Sp0	415	135	68	33
189	Manα1-2Manα1-2Manα1-3Manα-Sp9	372	112	56	30
190	Manα1-2Manα1-3(Manα1-2Manα1-6)Manα-Sp9	234	129	65	55
191	Manα1-2Manα1-3Manα-Sp9	536	242	121	45
192	Manα1-6(Manα1-2Manα1-3)Manα1-6(Manα2Manα1-3)Manβ1-4GlcNAcβ1-4GlcNAcβ-N	324	143	71	44
193	Manα1-2Manα1-6(Manα1-3)Manα1-6(Manα2Manα2Manα1-3)Manβ1-4GlcNAcβ1-4GlcNAcβ-N	216	89	44	41
194	Manα1-2Manα1-2Manα1-3(Manα1-2Manα1-3(Manα1-2Manα1-6)Manα1-6)Manβ1-4GlcNAcβ1-4GlcNAcβ-N	218	113	57	52

#	Glycan Name	Mean RFU (n=4)*	STDEV	SEM	% CV
195	Manα1-3(Manα1-6)Manα–Sp9	455	56	28	12
196	Manα1-3(Manα1-2Manα1-2Manα1-6)Manα-Sp9	256	131	65	51
197	Manα1-6(Manα1-3)Manα1-6(Manα2Manα1-3)Manβ1-4GlcNAcβ1-4GlcNAcβ-N	338	83	41	24
198	Manα1-6(Manα1-3)Manα1-6(Manα1-3)Manβ1-4GlcNAcβ1-4 GlcNAcβ-N	237	181	91	77
199	Man5_9mix N	219	79	40	36
200	Manβ1-4GlcNAcβ-Sp0	130	82	41	63
201	Neu5Acα2-3(Galβ1-3GalNAcβ1-4)Galβ1-4Glcβ-Sp0	373	134	67	36
202	Neu5Acα2-3Galβ1-3GalNAcα-Sp8	1610	711	355	44
203	NeuAcα2-8NeuAcα2-8NeuAcα2-8NeuAcα2-3(GalNAcβ1-4)Galβ1-4Glcβ-Sp0	188	116	58	62
204	Neu5Acα2-8Neu5Acα2-8Neu5Acα2-3(GalNAcβ1-4)Galβ1-4Glcβ-Sp0	271	212	106	78
205	Neu5Acα2-8Neu5Acα2-8Neu5Acα2-3Galβ1-4Glcβ–Sp0	277	171	85	62
206	Neu5Acα2-8Neu5Acα2-3(GalNAcβ1-4)Galβ1-4Glcβ–Sp0	107	58	29	55
207	Neu5Acα2-8Neu5Acα2-8Neu5Acα-Sp8	334	135	68	40
208	Neu5Acα2-3(6-O-Su)Galβ1-4(Fucα1-3)GlcNAcβ–Sp8	213	83	41	39
209	Neu5Acα2-3(GalNAcβ1-4)Galβ1-4GlcNAcβ-Sp0	414	92	46	22
210	Neu5Acα2-3(GalNAcβ1-4)Galβ1-4GlcNAcβ-Sp8	935	347	174	37
211	Neu5Acα2-3(GalNAcβ1-4)Galβ1-4Glcβ–Sp0	360	192	96	53
212	NeuAcα2-3(NeuAcα2-3Galβ1-3GalNAcβ1-4)Galβ1-4Glcβ-Sp0	760	315	157	41
213	Neu5Acα2-3(Neu5Acα2-6)GalNAcα–Sp8	477	299	149	63
214	Neu5Acα2-3GalNAcα–Sp8	112	24	12	22
215	Neu5Acα2-3GalNAcβ1-4GlcNAcβ-Sp0	222	77	38	35
216	Neu5Acα2-3Galβ1-3(6OSO3)GlcNAc-Sp8	140	98	49	70
217	Neu5Acα2-3Galβ1-3(Fucα1-4)GlcNAcβ–Sp8	228	65	33	29
218	NeuAcα2-3Galβ1-3(Fucα1-4)GlcNAcβ1-3Galβ1-4(Fucα1-3)GlcNAcβ Sp0	429	21	10	5
219	Neu5Acα2-3Galβ1-3(Neu5Acα2-3Galβ1-4)GlcNAcβ-Sp8	1577	1037	519	66
220	Neu5Acα2-3Galβ1-3[6OSO3]GalNAcα-Sp8	1022	445	222	44
221	Neu5Acα2-3Galβ1-3(Neu5Acα2-6)GalNAcα–Sp8	483	429	215	89
222	Neu5Acα2-3Galβ-Sp8	711	481	240	68
223	NeuAcα2-3Galβ1-3GalNAcβ1-3Galα1-4Galβ1-4Glcβ-Sp0	1791	1121	560	63
224	NeuAcα2-3Galβ1-3GlcNAcβ1-3Galβ1-4GlcNAcβ-Sp0	1802	353	176	20
225	Neu5Acα2-3Galβ1-3GlcNAcβ–Sp0	879	609	305	69
226	Neu5Acα2-3Galβ1-3GlcNAcβ–Sp8	1200	730	365	61
227	Neu5Acα2-3Galβ1-4[6OSO3]GlcNAcβ-Sp8	4992	365	183	7
228	Neu5Acα2-3Galβ1-4(Fucα1-3)(6OSO3) GlcNAcβ –Sp8	537	492	246	92

#	Glycan Name	Mean RFU (n=4)*	STDEV	SEM	% CV
229	Neu5Acα2-3Galβ1-4(Fucα1-3)GlcNAcβ1-3Galβ1-4(Fucα1-3)GlcNAcβ1-3Galβ1-4(Fucα1-3) GlcNAcβ–Sp0	133	104	52	78
230	Neu5Acα2-3Galβ1-4(Fucα1-3)GlcNAcβ–Sp0	299	136	68	45
231	Neu5Acα2-3Galβ1-4(Fucα1-3)GlcNAcβ–Sp8	417	138	69	33
232	Neu5Acα2-3Galβ1-4(Fucα1-3)GlcNAcβ1-3Galβ-Sp8	302	189	95	63
233	Neu5Acα2-3Galβ1-4(Fucα1-3)GlcNAcβ1-3Galβ1-4GlcNAcβ-Sp8	337	214	107	64
234	Neu5Acα2-3Galβ1-4GlcNAcβ1-3Galβ1-4(Fucα1-3)GlcNAc-Sp0	291	187	94	64
235	Neu5Acα2-3Galβ1-4GlcNAcβ1-3Galβ1-4GlcNAcβ1-3Galβ1-4GlcNAcβ–Sp0	5118	1064	532	21
236	Neu5Acα2-3Galβ1-4GlcNAcβ–Sp0	539	718	359	133
237	Neu5Acα2-3Galβ1-4GlcNAcβ–Sp8	1883	1883	941	100
238	Neu5Acα2-3Galβ1-4GlcNAcβ1-3Galβ1-4GlcNAcβ-Sp0	3552	440	220	12
239	Neu5Acα2-3Galβ1-4Glcβ–Sp0	211	187	94	89
240	Neu5Acα2-3Galβ1-4Glcβ–Sp8	960	700	350	73
241	Neu5Acα2-6(Galβ1-3)GalNAcα–Sp8	300	75	38	25
242	Neu5Acα2-6GalNAcα–Sp8	365	117	59	32
243	Neu5Acα2-6GalNAcβ1-4GlcNAcβ-Sp0	218	273	136	125
244	Neu5Acα2-6Galβ1-4[6OSO3]GlcNAcβ-Sp8	213	70	35	33
245	Neu5Acα2-6Galβ1-4GlcNAcβ–Sp0	173	129	65	75
246	Neu5Acα2-6Galβ1-4GlcNAcβ–Sp8	537	146	73	27
247	Neu5Acα2-6Galβ1-4GlcNAcβ1-3Galβ1-4(Fucα1-3)GlcNAcβ1-3Galβ1-4(Fucα1-3)GlcNAcβ-Sp0	336	131	65	39
248	Neu5Acα2-6Galβ1-4GlcNAcβ1-3Galβ1-4GlcNAcβ-Sp0	507	262	131	52
249	Neu5Acα2-6Galβ1-4Glcβ–Sp0	716	440	220	61
250	Neu5Acα2-6Galβ1-4Glcβ–Sp8	421	275	138	65
251	Neu5Acα2-6Galβ–Sp8	385	267	134	69
252	Neu5Acα2-8Neu5Acα-Sp8	301	213	106	71
253	Neu5Acα2-8Neu5Acα2-3Galβ1-4Glcβ–Sp0	194	72	36	37
254	Neu5Acβ2-6GalNAcα–Sp8	179	138	69	77
255	Neu5Acβ2-6Galβ1-4GlcNAcβ-Sp8	388	326	163	84
256	Neu5Acβ2-6(Galβ1-3)GalNAcα–Sp8	239	98	49	41
257	Neu5Gcα2-3Galβ1-3(Fucα1-4)GlcNAcβ-Sp0	465	348	174	75
258	Neu5Gcα2-3Galβ1-3GlcNAcβ-Sp0	30045	3164	1582	11
259	Neu5Gcα2-3Galβ1-4(Fucα1-3)GlcNAcβ-Sp0	559	311	156	56
260	Neu5Gcα2-3Galβ1-4GlcNAcβ–Sp0	41467	15476	7738	37
261	Neu5Gcα2-3Galβ1-4Glcβ–Sp0	31202	1458	729	5

#	Glycan Name	Mean RFU (n=4)*	STDEV	SEM	% CV
262	Neu5Gcα2-6GalNAcα–Sp0	2505	782	391	31
263	Neu5Gcα2-6Galβ1-4GlcNAcβ–Sp0	1484	1460	730	98
264	Neu5Gcα–Sp8	11973	8821	4411	74
265	[3OSO3]Galβ1-4(Fucα1-3)(6OSO3)Glc-Sp0	410	302	151	74
266	[3OSO3]Galβ1-4(Fucα1-3)Glc-Sp0	235	87	43	37
267	[3OSO3]Galβ1-4[Fucα1-3][6OSO3]GlcNAc-Sp8	328	172	86	52
268	[3OSO3]Galβ1-4[Fucα1-3]GlcNAc-Sp0	155	47	24	31
269	Fucα1-2[6OSO3]Galβ1-4GlcNAc-Sp0	104	38	19	37
270	Fucα1-2Galβ1-4[6OSO3]GlcNAc-Sp8	245	155	78	63
271	Fucα1-2[6OSO3]Galβ1-4[6OSO3]Glc-Sp0	136	67	34	49
272	Fucα1-2-(6OSO3)-Galβ1-4Glc-Sp0	170	32	16	19
273	Fucα1-2-Galβ1-4[6OSO3]Glc-Sp0	154	124	62	80
274	Galβ1-3(Fucα1-4)GlcNAcβ1-3Galβ1-3(Fucα1-4)GlcNAcβ-Sp0	158	66	33	42
275	Galβ1-3-(Galβ1-4GlcNacβ1-6)GalNAc-T	76	39	20	52
276	Galβ1-3(GlcNacβ1-6)GalNAc-T	185	101	50	54
277	Galβ1-3-(Neu5Aα2-3Galβ1-4GlcNacβ1-6)GalNAc-T	330	306	153	93
278	Galβ1-3GalNAc-T	375	355	178	95
279	Galβ1-3GlcNAcβ1-3Galβ1-3GlcNAcβ-Sp0	53	19	9	35
280	Galβ1-4[Fucα1-3][6OSO3]GlcNAc-Sp0	180	115	57	64
281	Galβ1-4[Fucα1-3][6OSO3]Glc-Sp0	149	79	39	53
282	Galβ1-4(Fucα1-3)GlcNAcβ1-3Galβ1-3(Fucα1-4)GlcNAcβ-Sp0	234	84	42	36
283	Galβ1-4GlcNAcβ1-3Galβ1-3GlcNAcβ-Sp0	138	102	51	74
284	Neu5Acα2-3Galβ1-3GlcNAcβ1-3Galβ1-3GlcNAcβ-Sp0	333	304	152	91
285	Neu5Acα2-3Galβ1-4GlcNAcβ1-3Galβ1-3GlcNAcβ-Sp0	752	96	48	13

* Although six spots are tested for each glycan, data are mean fluorescence for four spots, after discarding the two spots with the highest and lowest values. Sp#: spacer. Spacer structures can be found at http://www.functionalglycomics.org/. STDEV: standard deviation. SEM: standard error about the mean. CV: coefficient of variation.

A.2 Glycan Array Data by SubAB Affinity

A complete list of glycans for which the affinity of SubAB-OG was tested is presented in Table A.2; data are sorted by mean RFU. The printed array (version 2.1) consisted of 285 glycans in replicates of six with maxima and mimima removed from each set (n = 4). Data were provided by David Smith (CFG Core H).

Table A.2: Glycan affinity of SubAB-OG (100 µg.ml^{-1}) by mean RFU.

#	Glycan Name	Mean RFU (n=4)*	STDEV	SEM	% CV
1	α_1-AGP	41519	1823	911	4
260	Neu5Gcα2-3Galβ1-4GlcNAcβ–Sp0	41467	15476	7738	37
2	AGP-A	36382	800	400	2
261	Neu5Gcα2-3Galβ1-4Glcβ–Sp0	31202	1458	729	5
258	Neu5Gcα2-3Galβ1-3GlcNAcβ-Sp0	30045	3164	1582	11
264	Neu5Gcα–Sp8	11973	8821	4411	74
3	AGP-βl	9830	1607	804	16
235	Neu5Acα2-3Galβ1-4GlcNAcβ1-3Galβ1-4GlcNAcβ1-3Galβ1-4GlcNAcβ–Sp0	5118	1064	532	21
227	Neu5Acα2-3Galβ1-4[6OSO3]GlcNAcβ-Sp8	4992	365	183	7
15	α-Neu5Ac–Sp11	4492	1293	647	29
238	Neu5Acα2-3Galβ1-4GlcNAcβ1-3Galβ1-4GlcNAcβ-Sp0	3552	440	220	12
6	Transferrin	3527	209	104	6
4	Ceruloplasmine	3028	764	382	25
262	Neu5Gcα2-6GalNAcα–Sp0	2505	782	391	31
237	Neu5Acα2-3Galβ1-4GlcNAcβ–Sp8	1883	1883	941	100
224	NeuAcα2-3Galβ1-3GlcNAcβ1-3Galβ1-4GlcNAcβ-Sp0	1802	353	176	20
223	NeuAcα2-3Galβ1-3GalNAcβ1-3Galα1-4Galβ1-4Glcβ-Sp0	1791	1121	560	63
202	Neu5Acα2-3Galβ1-3GalNAcα-Sp8	1610	711	355	44
219	Neu5Acα2-3Galβ1-3(Neu5Acα2-3Galβ1-4)GlcNAcβ-Sp8	1577	1037	519	66
263	Neu5Gcα2-6Galβ1-4GlcNAcβ–Sp0	1484	1460	730	98
70	Fucα1-2Galβ1-4GlcNAcβ1-3Galβ1-4GlcNAcβ1-3Galβ1-4GlcNAcβ-Sp0	1267	82	41	6
14	α-Neu5Ac–Sp8	1260	823	412	65
226	Neu5Acα2-3Galβ1-3GlcNAcβ–Sp8	1200	730	365	61
124	Galβ1-3(Neu5Acα2-6)GlcNAcβ1-4Galβ1-4Glcβ-Sp10	1115	361	180	32
36	[3OSO3]Galβ1-4GlcNAcβ–Sp0	1076	946	473	88

#	Glycan Name	Mean RFU (n=4)*	STDEV	SEM	% CV
220	Neu5Acα2-3Galβ1-3[6OSO3]GalNAcα-Sp8	1022	445	222	44
240	Neu5Acα2-3Galβ1-4Glcβ–Sp8	960	700	350	73
210	Neu5Acα2-3(GalNAcβ1-4)Galβ1-4GlcNAcβ-Sp8	935	347	174	37
48	9-O-AcNeu5NAcα-Sp8	902	363	182	40
225	Neu5Acα2-3Galβ1-3GlcNAcβ–Sp0	879	609	305	69
54	Neu5Acα2-6Galβ1-4GlcNAcβ1-2Manα1-3(Neu5Acα2-6Galβ1-4GlcNAcβ1-2Manα1-6)Manβ1-4GlcNAcβ1-4GlcNAcβ-Sp8	774	295	147	38
212	NeuAcα2-3(NeuAcα2-3Galβ1-3GalNAcβ1-4)Galβ1-4Glcβ-Sp0	760	315	157	41
285	Neu5Acα2-3Galβ1-4GlcNAcβ1-3Galβ1-3GlcNAcβ-Sp0	752	96	48	13
249	Neu5Acα2-6Galβ1-4Glcβ–Sp0	716	440	220	61
222	Neu5Acα2-3Galβ-Sp8	711	481	240	68
69	Fucα1-2Galβ1-4GlcNAcβ1-3Galβ1-4GlcNAc–Sp0	687	334	167	49
35	[3OSO3]Galβ1-4[6OSO3]GlcNAcβ-Sp8	685	148	74	22
46	NeuAcα2-3[6OSO3]Galβ1-4GlcNAcβ–Sp8	672	270	135	40
27	[3OSO3][6OSO3]Galβ1-4GlcNAcβ-Sp0	600	197	98	33
53	Neu5Acα2-6Galβ1-4GlcNAcβ1-2Manα1-3(Neu5Acα2-6Galβ1-4GlcNAcβ1-2Manα1-6)Manβ1-4GlcNAcβ1-4GlcNAcβ-Gly	597	134	67	22
40	[4OSO3]Galβ1-4GlcNAcβ-Sp8	592	207	104	35
92	GalNAcβ1-4GlcNAcβ–Sp0	586	337	169	58
30	[3OSO3]Galβ1-4(6OSO3)Glcβ–Sp8	586	207	104	35
43	[6OSO3]Galβ1-4Glcβ–Sp8	582	161	81	28
63	Fucα1-2Galβ1-3GlcNAcβ–Sp0	569	104	52	18
49	9-O-AcNeu5NAcα2-6Galβ1-4GlcNAcβ-Sp8	562	236	118	42
259	Neu5Gcα2-3Galβ1-4(Fucα1-3)GlcNAcβ-Sp0	559	311	156	56
17	β-D-Gal–Sp8	557	354	177	64
44	[6OSO3]Galβ1-4GlcNAcβ–Sp8	554	76	38	14
33	[3OSO3]Galβ1-3GlcNAcβ–Sp8	541	111	55	21
236	Neu5Acα2-3Galβ1-4GlcNAcβ–Sp0	539	718	359	133
228	Neu5Acα2-3Galβ1-4(Fucα1-3)(6OSO3) GlcNAcβ –Sp8	537	492	246	92
246	Neu5Acα2-6Galβ1-4GlcNAcβ–Sp8	537	146	73	27
191	Manα1-2Manα1-3Manα-Sp9	536	242	121	45
248	Neu5Acα2-6Galβ1-4GlcNAcβ1-3Galβ1-4GlcNAcβ-Sp0	507	262	131	52
112	Galα1-4GlcNAcβ–Sp8	499	93	46	19
79	GalNAcα1-3(Fucα1-2)Galβ1-3GlcNAcβ-Sp0	495	160	80	32
67	Fucα1-2Galβ1-4(Fucα1-3)GlcNAcβ–Sp0	488	161	80	33
73	Fucα1-2Galβ1-4Glcβ–Sp0	488	273	137	56

#	Glycan Name	Mean RFU (n=4)*	STDEV	SEM	% CV
170	GlcNAcβ1-4Galβ1-4GlcNAcβ-Sp8	488	159	79	33
221	Neu5Acα2-3Galβ1-3(Neu5Acα2-6)GalNAcα–Sp8	483	429	215	89
71	Fucα1-2Galβ1-4GlcNAcβ–Sp0	481	129	65	27
123	Galβ1-3(Neu5Acβ2-6)GalNAcα-Sp8	479	460	230	96
213	Neu5Acα2-3(Neu5Acα2-6)GalNAcα–Sp8	477	299	149	63
32	[3OSO3]Galβ1-3GalNAcα–Sp8	467	78	39	17
10	α-GalNAc–Sp8	466	164	82	35
257	Neu5Gcα2-3Galβ1-3(Fucα1-4)GlcNAcβ-Sp0	465	348	174	75
62	Fucα1-2Galβ1-3GlcNAcβ1-3Galβ1-4Glcβ–Sp8	465	105	52	23
26	[3OSO3][6OSO3]Galβ1-4[6OSO3]GlcNAcβ-Sp0	464	121	61	26
59	Fucα1-2Galβ1-3GalNAcβ1-4(Neu5Acα2-3)Galβ1-4Glcβ-Sp0	462	144	72	31
37	[3OSO3]Galβ1-4GlcNAcβ-Sp8	457	184	92	40
195	Manα1-3(Manα1-6)Manα–Sp9	455	56	28	12
65	Fucα1-2Galβ1-4(Fucα1-3)GlcNAcβ1-3Galβ1-4(Fucα1-3)GlcNAcβ-Sp0	448	119	60	27
105	Galα1-3Galβ1-4GlcNAcβ–Sp8	439	102	51	23
60	Fucα1-2Galβ1-3GalNAcβ1-4(Neu5Acα2-3)Galβ1-4Glcβ-Sp9	438	145	72	33
218	NeuAcα2-3Galβ1-3(Fucα1-4)GlcNAcβ1-3Galβ1-4(Fucα1-3)GlcNAcβ Sp0	429	21	10	5
72	Fucα1-2Galβ1-4GlcNAcβ–Sp8	429	65	32	15
20	β-GalNAc–Sp8	429	183	92	43
7	α-D-Gal–Sp8	428	80	40	19
250	Neu5Acα2-6Galβ1-4Glcβ–Sp8	421	275	138	65
34	[3OSO3]Galβ1-4(Fucα1-3)GlcNAcβ–Sp8	420	158	79	38
96	Galα1-3(Fucα1-2)Galβ1-4(Fucα1-3)GlcNAcβ-Sp0	418	252	126	60
231	Neu5Acα2-3Galβ1-4(Fucα1-3)GlcNAcβ–Sp8	417	138	69	33
188	KDNα2-3Galβ1-4GlcNAcβ–Sp0	415	135	68	33
209	Neu5Acα2-3(GalNAcβ1-4)Galβ1-4GlcNAcβ-Sp0	414	92	46	22
66	Fucα1-2Galβ1-4(Fucα1-3)GlcNAcβ1-3Galβ1-4(Fucα1-3)GlcNAcβ1-3Galβ1-4(Fucα1-3)GlcNAcβ-Sp0	410	57	28	14
265	[3OSO3]Galβ1-4(Fucα1-3)(6OSO3)Glc-Sp0	410	302	151	74
29	[3OSO3]Galβ1-4(6OSO3)Glcβ–Sp0	409	72	36	18
133	Galβ1-3GlcNAcβ–Sp0	408	148	74	36
85	GalNAcα1-3GalNAcβ–Sp8	405	218	109	54
82	GalNAcα1-3(Fucα1-2)Galβ1-4GlcNAcβ–Sp8	398	77	38	19
39	[4OSO3][6OSO3]Galβ1-4GlcNAcβ-Sp0	395	129	65	33
42	[6OSO3]Galβ1-4Glcβ–Sp0	395	52	26	13

#	Glycan Name	Mean RFU (n=4)*	STDEV	SEM	% CV
58	Fucα1-2Galβ1-3GalNAcα–Sp8	394	118	59	30
122	Galβ1-3(Neu5Acα2-6)GalNAcα-Sp8	394	165	83	42
13	α-L-Rhα–Sp8	394	184	92	47
109	Galα1-4Galβ1-4GlcNAcβ–Sp0	394	45	23	12
255	Neu5Acβ2-6Galβ1-4GlcNAcβ-Sp8	388	326	163	84
47	[6OSO3]GlcNAcβ–Sp8	386	169	85	44
45	[6OSO3]Galβ1-4[6OSO3]Glcβ-Sp8	385	298	149	77
251	Neu5Acα2-6Galβ–Sp8	385	267	134	69
113	Galα1-6Glcβ-Sp8	384	116	58	30
136	Galβ1-4(Fucα1-3)GlcNAcβ–Sp8	376	161	81	43
278	Galβ1-3GalNAc-T	375	355	178	95
55	Fucα1-2Galβ1-3GalNAcβ1-3Galα-Sp9	375	316	158	84
103	Galα1-3Galβ1-4(Fucα1-3)GlcNAcβ–Sp8	374	67	33	18
201	Neu5Acα2-3(Galβ1-3GalNAcβ1-4)Galβ1-4Glcβ-Sp0	373	134	67	36
80	GalNAcα1-3(Fucα1-2)Galβ1-4(Fucα1-3)GlcNAcβ-Sp0	372	149	74	40
189	Manα1-2Manα1-2Manα1-3Manα-Sp9	372	112	56	30
38	[3OSO3]Galβ–Sp8	371	83	41	22
152	Galβ1-4GlcNAcβ–Sp0	367	249	124	68
84	GalNAcα1-3(Fucα1-2)Galβ–Sp8	366	56	28	15
242	Neu5Acα2-6GalNAcα–Sp8	365	117	59	32
107	Galα1-3Galβ–Sp8	364	149	75	41
151	Galβ1-4GlcNAcβ1-6GalNAcα–Sp8	362	19	9	5
211	Neu5Acα2-3(GalNAcβ1-4)Galβ1-4Glcβ–Sp0	360	192	96	53
9	α-D-Man–Sp8	357	369	23	104
90	GalNAcβ1-3Galα1-4Galβ1-4GlcNAcβ-Sp0	356	170	85	48
116	Galβ1-3(Fucα1-4)GlcNAcβ1-3Galβ1-4GlcNAcβ-Sp0	356	87	43	24
25	GlcNAcβ1-3(GlcNAcβ1-4)(GlcNAcβ1-6)GlcNAc-Sp8	355	200	100	56
64	Fucα1-2Galβ1-3GlcNAcβ–Sp8	352	100	50	28
81	GalNAcα1-3(Fucα1-2)Galβ1-4GlcNAcβ-Sp0	352	21	11	6
120	Galβ1-3(Galβ1-4GlcNAcβ1-6)GalNAcα-Sp8	352	219	110	62
74	Fucα1-2Galβ–Sp8	350	96	48	27
111	Galα1-4Galβ1-4Glcβ–Sp0	350	88	44	25
114	Galβ1-2Galβ–Sp8	344	115	58	33
106	Galα1-3Galβ1-4Glcβ–Sp0	344	219	109	64
128	Galβ1-3GalNAcβ1-4(Neu5Acα2-3)Galβ1-4Glcβ-Sp0	341	48	24	14

#	Glycan Name	Mean RFU (n=4)*	STDEV	SEM	% CV
12	α-L-Fuc–Sp9	340	177	88	52
197	Manα1-6(Manα1-3)Manα1-6(Manα2Manα1-3)Manβ1-4GlcNAcβ1-4GlcNAcβ-N	338	83	41	24
233	Neu5Acα2-3Galβ1-4(Fucα1-3)GlcNAcβ1-3Galβ1-4GlcNAcβ-Sp8	337	214	107	64
146	Galβ1-4GlcNAcβ1-3Galβ1-4GlcNAcβ1-3Galβ1-4GlcNAcβ–Sp0	337	140	70	41
83	GalNAcα1-3(Fucα1-2)Galβ1-4Glcβ-Sp0	337	64	32	19
247	Neu5Acα2-6Galβ1-4GlcNAcβ1-3Galβ1-4(Fucα1-3)GlcNAcβ1-3Galβ1-4(Fucα1-3)GlcNAcβ-Sp0	336	131	65	39
93	GalNAcβ1-4GlcNAcβ–Sp8	335	266	133	79
207	Neu5Acα2-8Neu5Acα2-8Neu5Acα-Sp8	334	135	68	40
115	Galβ1-3(Fucα1-4)GlcNAcβ1-3Galβ1-4(Fucα1-3)GlcNAcβ-Sp0	334	121	61	36
284	Neu5Acα2-3Galβ1-3GlcNAcβ1-3Galβ1-3GlcNAcβ-Sp0	333	304	152	91
52	Galβ1-4GlcNAcβ1-2Manα1-3(Galβ1-4GlcNAcβ1-2Manα1-6)Manβ1-4GlcNAcβ1-4GlcNAcβ-Gly	333	219	109	66
130	Galβ1-3Galβ–Sp8	331	26	13	8
277	Galβ1-3-(Neu5Aα2-3Galβ1-4GlcNacβ1-6)GalNAc-T	330	306	153	93
267	[3OSO3]Galβ1-4[Fucα1-3][6OSO3]GlcNAc-Sp8	328	172	86	52
184	GlcAβ-Sp8	326	108	54	33
86	GalNAcα1-3Galβ–Sp8	326	94	47	29
192	Manα1-6(Manα1-2Manα1-3)Manα1-6(Manα2Manα1-3)Manβ1-4GlcNAcβ1-4GlcNAcβ-N	324	143	71	44
180	Glcβ1-4Glcβ-Sp8	324	235	117	72
153	Galβ1-4GlcNAcβ–Sp8	323	75	38	23
94	Galα1-2Galβ–Sp8	323	238	119	74
56	Fucα1-2Galβ1-3GalNAcβ1-3Galα1-4Galβ1-4Glcβ-Sp9	319	85	43	27
88	GalNAcβ1-3GalNAca–Sp8	319	96	48	30
75	Fucα1-3GlcNAcβ-Sp8	317	127	63	40
132	Galβ1-3GlcNAcβ1-3Galβ1-4Glcβ–Sp10	317	87	43	27
121	Galβ1-3(GlcNAcβ1-6)GalNAcα-Sp8	315	107	54	34
127	Galβ1-3GalNAcβ1-3Galα1-4Galβ1-4Glcβ-Sp0	312	59	30	19
76	Fucα1-3GlcNAcβ-Sp8	311	126	63	40
172	(GlcNAcβ1-4)5β-Sp8	307	113	57	37
129	Galβ1-3GalNAcβ1-4Galβ1-4Glcβ–Sp8	305	78	39	25
95	Galα1-3(Fucα1-2)Galβ1-3GlcNAcβ-Sp0	303	112	56	37
175	GlcNAcβ1-6GalNAcα–Sp8	302	178	89	59
232	Neu5Acα2-3Galβ1-4(Fucα1-3)GlcNAcβ1-3Galβ-Sp8	302	189	95	63
252	Neu5Acα2-8Neu5Acα-Sp8	301	213	106	71

#	Glycan Name	Mean RFU (n=4)*	STDEV	SEM	% CV
241	Neu5Acα2-6(Galβ1-3)GalNAcα–Sp8	300	75	38	25
137	Galβ1-4(Fucα1-3)GlcNAcβ1-4Galβ1-4(Fucα1-3)GlcNAcβ-Sp0	300	71	36	24
230	Neu5Acα2-3Galβ1-4(Fucα1-3)GlcNAcβ–Sp0	299	136	68	45
100	Galα1-3(Galα1-4)Galβ1-4GlcNAcβ-Sp8	299	141	71	47
118	Galβ1-3(Fucα1-4)GlcNAc–Sp8	292	21	11	7
234	Neu5Acα2-3Galβ1-4GlcNAcβ1-3Galβ1-4(Fucα1-3)GlcNAc-Sp0	291	187	94	64
21	β-GlcNAc–Sp0	290	147	74	51
18	β-D-Glc–Sp8	289	97	48	33
159	GlcNAcβ1-3(GlcNAcβ1-6)GalNAcα–Sp8	287	82	41	29
145	Galβ1-4GlcNAcβ1-3Galβ1-4(Fucα1-3)GlcNAcβ1-3Galβ1-4(Fucα1-3)GlcNAcβ-Sp0	285	76	38	27
166	GlcNAcβ1-3Galβ1-4GlcNAcβ1-3Galβ1-4GlcNAcβ-Sp0	280	133	66	47
104	Galα1-3Galβ1-3GlcNAcβ-Sp0	278	65	33	24
205	Neu5Acα2-8Neu5Acα2-8Neu5Acα2-3Galβ1-4Glcβ–Sp0	277	171	85	62
187	KDNα2-3Galβ1-3GlcNAcβ–Sp0	277	68	34	25
186	GlcAβ1-6Galβ-Sp8	277	137	68	49
164	GlcNAcβ1-3Galβ1-4GlcNAcβ–Sp0	276	140	70	51
101	Galα1-3GalNAcα-Sp8	275	96	48	35
173	GlcNAcβ1-4GlcNAcβ1-4GlcNAcβ–Sp8	274	97	49	36
5	Fibrinogen	272	144	72	53
204	Neu5Acα2-8Neu5Acα2-8Neu5Acα2-3(GalNAcβ1-4)Galβ1-4Glcβ-Sp0	271	212	106	78
156	GlcNAcα1-3Galβ1-4GlcNAcβ-Sp8	270	146	73	54
140	Galβ1-4[6OSO3]Glcβ–Sp8	270	53	27	20
22	β-GlcNAc–Sp8	268	161	80	60
117	Galβ1-3(Fucα1-4)GlcNAc–Sp0	262	63	31	24
78	Fucβ1-3GlcNAcβ-Sp8	262	187	94	72
157	GlcNAcα1-6Galβ1-4GlcNAcβ-Sp8	260	112	56	43
91	GalNAcβ1-4(Fucα1-3)GlcNAcβ-Sp0	260	109	54	42
196	Manα1-3(Manα1-2Manα1-2Manα1-6)Manα-Sp9	256	131	65	51
147	Galβ1-4GlcNAcβ1-3Galβ1-4GlcNAcβ–Sp0	256	52	26	20
185	GlcAβ1-3Galβ-Sp8	255	173	86	68
154	Galβ1-4Glcβ–Sp0	255	126	63	49
138	Galβ1-4(Fucα1-3)GlcNAcβ1-4Galβ1-4(Fucα1-3)GlcNAcβ1-4Galβ1-4(Fucα1-3)GlcNAcβ–Sp0	254	86	43	34
110	Galα1-4Galβ1-4GlcNAcβ–Sp8	251	35	18	14
99	Galα1-3(Fucα1-2)Galβ–Sp8	250	208	104	83

#	Glycan Name	Mean RFU (n=4)*	STDEV	SEM	% CV
51	GlcNAcβ1-2Manα1-3(GlcNAcβ1-2Manα1-6)Manβ1-4GlcNAcβ1-4GlcNAcβ-Gly	250	90	45	36
31	[3OSO3]Galβ1-3(Fucα1-4)GlcNAcβ–Sp8	249	167	84	67
144	Galβ1-4GlcNAcβ1-3GalNAcα–Sp8	248	117	59	47
270	Fucα1-2Galβ1-4[6OSO3]GlcNAc-Sp8	245	155	78	63
148	Galβ1-4GlcNAcβ1-3Galβ1-4Glcβ–Sp0	244	105	53	43
57	Fucα1-2Galβ1-3(Fucα1-4)GlcNAcβ–Sp8	243	81	41	33
177	Glcα1-4Glcβ–Sp8	241	144	72	60
149	Galβ1-4GlcNAcβ1-3Galβ1-4Glcβ–Sp8	241	156	78	65
256	Neu5Acβ2-6(Galβ1-3)GalNAcα–Sp8	239	98	49	41
198	Manα1-6(Manα1-3)Manα1-6(Manα1-3)Manβ1-4GlcNAcβ1-4 GlcNAcβ-N	237	181	91	77
266	[3OSO3]Galβ1-4(Fucα1-3)Glc-Sp0	235	87	43	37
282	Galβ1-4(Fucα1-3)GlcNAcβ1-3Galβ1-3(Fucα1-4)GlcNAcβ-Sp0	234	84	42	36
190	Manα1-2Manα1-3(Manα1-2Manα1-6)Manα-Sp9	234	129	65	55
155	Galβ1-4Glcβ–Sp8	231	60	30	26
89	GalNAcβ1-3(Fucα1-2)Galβ-Sp8	230	145	73	63
125	Galβ1-3GalNAcα-Sp8	229	118	59	52
217	Neu5Acα2-3Galβ1-3(Fucα1-4)GlcNAcβ–Sp8	228	65	33	29
174	GlcNAcβ1-6(Galβ1-3)GalNAcα–Sp8	227	135	68	60
98	Galα1-3(Fucα1-2)Galβ1-4Glcβ-Sp0	226	104	52	46
87	GalNAcα1-4(Fucα1-2)Galβ1-4GlcNAcβ-Sp8	223	129	65	58
215	Neu5Acα2-3GalNAcβ1-4GlcNAcβ-Sp0	222	77	38	35
199	Man5_9mix N	219	79	40	36
176	GlcNAcβ1-6Galβ1-4GlcNAcβ-Sp8	219	224	112	102
194	Manα1-2Manα1-2Manα1-3(Manα1-2Manα1-3(Manα1-2Manα1-6)Manα1-6)Manβ1-4GlcNAcβ1-4GlcNAcβ-N	218	113	57	52
243	Neu5Acα2-6GalNAcβ1-4GlcNAcβ-Sp0	218	273	136	125
193	Manα1-2Manα1-6(Manα1-3)Manα1-6(Manα2Manα2Manα1-3)Manβ1-4GlcNAcβ1-4GlcNAcβ-N	216	89	44	41
161	GlcNAcβ1-3GalNAcα–Sp8	214	72	36	34
208	Neu5Acα2-3(6-O-Su)Galβ1-4(Fucα1-3)GlcNAcβ–Sp8	213	83	41	39
244	Neu5Acα2-6Galβ1-4[6OSO3]GlcNAcβ-Sp8	213	70	35	33
141	Galβ1-4GalNAcα1-3(Fucα1-2)Galβ1-4GlcNAcβ-Sp8	212	110	55	52
239	Neu5Acα2-3Galβ1-4Glcβ–Sp0	211	187	94	89
163	GlcNAcβ1-3Galβ1-3GalNAcα-Sp8	209	46	23	22
108	Galα1-4(Fucα1-2)Galβ1-4GlcNAcβ-Sp8	206	67	33	33

#	Glycan Name	Mean RFU (n=4)*	STDEV	SEM	% CV
126	Galβ1-3GalNAcβ–Sp8	205	49	25	24
134	Galβ1-3GlcNAcβ–Sp8	202	72	36	36
158	GlcNAcβ1-2Galβ1-3GalNAcα–Sp8	196	53	27	27
142	Galβ1-4GalNAcβ1-3(Fucα1-2)Galβ1-4GlcNAcβ-Sp8	195	35	17	18
8	α-D-Glc–Sp8	195	129	64	66
253	Neu5Acα2-8Neu5Acα2-3Galβ1-4Glcβ–Sp0	194	72	36	37
179	Glcα1-6Glcα1-6Glcβ-Sp8	191	104	52	54
102	Galα1-3GalNAcβ–Sp8	191	42	21	22
203	NeuAcα2-8NeuAcα2-8NeuAcα2-3(GalNAcβ1-4)Galβ1-4Glcβ-Sp0	188	116	58	62
181	Glcβ1-6Glcβ-Sp8	188	79	39	42
143	Galβ1-4GlcNAcβ1-3(Galβ1-4GlcNAcβ1-6)GalNAcα-Sp8	186	100	50	54
97	Galα1-3(Fucα1-2)Galβ1-4GlcNAc-Sp0	186	80	40	43
171	(GlcNAcβ1-4)6β-Sp8	185	90	45	48
276	Galβ1-3(GlcNacβ1-6)GalNAc-T	185	101	50	54
24	$(Galβ1-4GlcNAcβ)_2$-3,6-GalNAcα–Sp8	182	106	53	58
280	Galβ1-4[Fucα1-3][6OSO3]GlcNAc-Sp0	180	115	57	64
254	Neu5Acβ2-6GalNAcα–Sp8	179	138	69	77
11	α-L-Fuc–Sp8	178	123	62	69
61	Fucα1-2Galβ1-3GlcNAcβ1-3Galβ1-4Glcβ–Sp10	178	89	44	50
23	β-GlcN(Gc)-Sp8	176	119	60	68
183	GlcAα-Sp8	174	198	99	113
162	GlcNAcβ1-3Galβ-Sp8	174	105	53	60
169	GlcNAcβ1-4(GlcNAcβ1-6)GalNAcα-Sp8	174	164	82	94
245	Neu5Acα2-6Galβ1-4GlcNAcβ–Sp0	173	129	65	75
77	Fucα1-4GlcNAcβ–Sp8	172	65	33	38
28	[3OSO3]Galβ1-4Glcβ-Sp8	170	93	46	55
272	Fucα1-2-(6OSO3)-Galβ1-4Glc-Sp0	170	32	16	19
135	Galβ1-4(Fucα1-3)GlcNAcβ–Sp0	170	110	55	65
182	Sorbitol-Sp8	166	79	39	47
16	β-Neu5Ac-Sp8	160	74	37	46
68	Fucα1-2Galβ1-4(Fucα1-3)GlcNAcβ–Sp8	159	110	55	69
274	Galβ1-3(Fucα1-4)GlcNAcβ1-3Galβ1-3(Fucα1-4)GlcNAcβ-Sp0	158	66	33	42
139	Galβ1-4[6OSO3]Glcβ–Sp0	158	102	51	65
165	GlcNAcβ1-3Galβ1-4GlcNAcβ-Sp8	157	30	15	19

#	Glycan Name	Mean RFU (n=4)*	STDEV	SEM	% CV
41	6-H_2PO_3Manα–Sp8	156	37	18	23
268	[3OSO3]Galβ1-4[Fucα1-3]GlcNAc-Sp0	155	47	24	31
273	Fucα1-2-Galβ1-4[6OSO3]Glc-Sp0	154	124	62	80
281	Galβ1-4[Fucα1-3][6OSO3]Glc-Sp0	149	79	39	53
167	GlcNAcβ1-3Galβ1-4Glcβ–Sp0	148	49	24	33
216	Neu5Acα2-3Galβ1-3(6OSO3)GlcNAc-Sp8	140	98	49	70
50	Manα1-3(Manα1-6)Manβ1-4GlcNAcβ1-4GlcNAcβ-Gly	139	53	26	38
283	Galβ1-4GlcNAcβ1-3Galβ1-3GlcNAcβ-Sp0	138	102	51	74
271	Fucα1-2[6OSO3]Galβ1-4[6OSO3]Glc-Sp0	136	67	34	49
229	Neu5Acα2-3Galβ1-4(Fucα1-3)GlcNAcβ1-3Galβ1-4(Fucα1-3)GlcNAcβ1-3Galβ1-4(Fucα1-3) GlcNAcβ–Sp0	133	104	52	78
200	Manβ1-4GlcNAcβ-Sp0	130	82	41	63
160	GlcNAcβ1-3(GlcNAcβ1-6)Galβ1-4GlcNAcβ–Sp8	128	118	59	92
119	Galβ1-3(Fucα1-4)GlcNAcβ–Sp8	125	110	55	88
178	Glcα1-4Glcα–Sp8	125	70	35	56
168	GlcNAcβ1-4MDPLys	121	86	43	71
131	Galβ1-3GlcNAcβ1-3Galβ1-4GlcNAcβ-Sp0	117	110	55	94
150	Galβ1-4GlcNAcβ1-6(Galβ1-3)GalNAcα–Sp8	113	40	20	35
214	Neu5Acα2-3GalNAcα–Sp8	112	24	12	22
206	Neu5Acα2-8Neu5Acα2-3(GalNAcβ1-4)Galβ1-4Glcβ–Sp0	107	58	29	55
269	Fucα1-2[6OSO3]Galβ1-4GlcNAc-Sp0	104	38	19	37
275	Galβ1-3-(Galβ1-4GlcNacβ1-6)GalNAc-T	76	39	20	52
19	β-D-Man–Sp8	71	29	15	41
279	Galβ1-3GlcNAcβ1-3Galβ1-3GlcNAcβ-Sp0	53	19	9	35

* Although six spots are tested for each glycan, data are mean fluorescence for four spots, after discarding the two spots with the highest and lowest values. Sp#: spacer. Spacer structures can be found at http://www.functionalglycomics.org/. STDEV: standard deviation. SEM: standard error about the mean. CV: coefficient of variation.

APPENDIX B
PUBLICATIONS

B.1 Publications

Publications emanating from this thesis are listed below with the corresponding manuscripts provided on the following pages.

Byres E., Paton, A. W., Paton, J. C., Löfling J. C., Smith, D. F., Wilce, M. C. J., Talbot, U. M., Chong, D. C., Yu, H., Huang, S., Chen, X., Varki, N. M., Varki, A., Rossjohn, J. & Beddoe, T. (in press) Incorporation of a non-human glycan mediates human susceptibility to a bacterial toxin. **Nature**, doi:10.1038/nature07428

Chong, D. C., Paton, J. C., Thorpe, C. M. & Paton, A. W. (2008) Clathrin-dependent trafficking of subtilase cytotoxin, a novel AB_5 toxin that targets the endoplasmic reticulum chaperone BiP. **Cellular Microbiology**, 10, 795-806.

Byres, E., Paton, A. W., Paton, J. C., Löfling J. C., Smith, D. F., Wilce, M. C. J., Talbot, U. M., Chong, D. C., Yu, H., Huang, S., Chen, X., Varki, N. M., Varki, A., Rossjohn, J. & Beddoe, T. (2008) Incorporation of a non-human glycan mediates human susceptibility to a bacterial toxin.
Nature, v. 456, pp. 648-652

Chong, D. C., Paton, J. C., Thorpe, C. M. & Paton, A. W. (2008) Clathrin-dependent trafficking of subtilase cytotoxin, a novel AB_5 toxin that targets the endoplasmic reticulum chaperone BiP.
Cellular Microbiology, v. 10(3), pp. 795-806

References

ACHESON, D. W., MOORE, R., DE BREUCKER, S., LINCICOME, L., JACEWICZ, M., SKUTELSKY, E. & KEUSCH, G. T. (1996) Translocation of Shiga toxin across polarized intestinal cells in tissue culture. *Infect Immun,* 64**,** 3294-300.

AHMED, S. & DONAGHY, M. (1998) An Outbreak of *Escherichia coli* O157:H7 in Central Scotland. IN KAPER, J. B. & O'BRIEN, A. D. (Eds.) Escherichia coli *O157:H7 and other Shiga toxin-producing* E. coli *strains. (Presentations and Discussions of the 3rd International Symposium held 22-26 June 1997, in Baltimore, Maryland.).* Washington, DC., American Society for Microbiology Press.

ARAB, S. & LINGWOOD, C. A. (1998) Intracellular targeting of the endoplasmic reticulum/nuclear envelope by retrograde transport may determine cell hypersensitivity to verotoxin via globotriaosyl ceramide fatty acid isoform traffic. *J Cell Physiol,* 177**,** 646-60.

AROSIO, D., VRASIDAS, I., VALENTINI, P., LISKAMP, R. M., PIETERS, R. J. & BERNARDI, A. (2004) Synthesis and cholera toxin binding properties of multivalent GM1 mimics. *Org Biomol Chem,* 2**,** 2113-24.

BAST, D. J., BANERJEE, L., CLARK, C., READ, R. J. & BRUNTON, J. L. (1999) The identification of three biologically relevant globotriaosyl ceramide receptor binding sites on the Verotoxin 1 B subunit. *Mol Microbiol,* 32**,** 953-60.

BATES, S. R., TAO, J. Q., SCHALLER, S., FISHER, A. B. & SHUMAN, H. (2000) Lamellar body membrane turnover is stimulated by secretagogues. *Am J Physiol Lung Cell Mol Physiol,* 278**,** L443-52.

BEGAUD, E. & GERMANI, Y. (1992) Detection of enterotoxigenic *Escherichia coli* in faecal specimens by acetylaminofluorene-labelled DNA probes. *Res Microbiol,* 143**,** 315-25.

BELL, B. P., GOLDOFT, M., GRIFFIN, P. M., DAVIS, M. A., GORDON, D. C., TARR, P. I., BARTLESON, C. A., LEWIS, J. H., BARRETT, T. J., WELLS, J. G. & ET AL. (1994) A multistate outbreak of *Escherichia coli* O157:H7-associated bloody diarrhea and hemolytic uremic syndrome from hamburgers. The Washington experience. *Jama,* 272**,** 1349-53.

BELLIS, S. L. (2004) Variant glycosylation: an underappreciated regulatory mechanism for beta1 integrins. *Biochim Biophys Acta,* 1663**,** 52-60.

BERNARDI, K. M., FORSTER, M. L., LENCER, W. I. & TSAI, B. (2007) Derlin-1 facilitates the retro-translocation of cholera toxin. *Mol Biol Cell.*

BEUTIN, L., GEIER, D., STEINRUCK, H., ZIMMERMANN, S. & SCHEUTZ, F. (1993) Prevalence and some properties of verotoxin (Shiga-like toxin)-producing *Escherichia coli* in seven different species of healthy domestic animals. *J Clin Microbiol,* 31**,** 2483-8.

BOKETE, T. N., O'CALLAHAN, C. M., CLAUSEN, C. R., TANG, N. M., TRAN, N., MOSELEY, S. L., FRITSCHE, T. R. & TARR, P. I. (1993) Shiga-like toxin-producing *Escherichia coli* in Seattle children: a prospective study. *Gastroenterology,* 105**,** 1724-31.

BOPP, C. A., GREENE, K. D., DOWNES, F. P., SOWERS, E. G., WELLS, J. G. & WACHSMUTH, I. K. (1987) Unusual verotoxin-producing *Escherichia coli* associated with hemorrhagic colitis. *J Clin Microbiol,* 25**,** 1486-9.

BOYD, B. & LINGWOOD, C. (1989) Verotoxin receptor glycolipid in human renal tissue. *Nephron,* 51**,** 207-10.

BOYD, B., MAGNUSSON, G., ZHIUYAN, Z. & LINGWOOD, C. A. (1994) Lipid modulation of glycolipid receptor function. Availability of Gal(alpha 1-4)Gal disaccharide for verotoxin binding in natural and synthetic glycolipids. *Eur J Biochem,* 223**,** 873-8.

BRIAN, M. J., FROSOLONO, M., MURRAY, B. E., MIRANDA, A., LOPEZ, E. L., GOMEZ, H. F. & CLEARY, T. G. (1992) Polymerase chain reaction for diagnosis of enterohemorrhagic *Escherichia coli* infection and hemolytic-uremic syndrome. *J Clin Microbiol,* 30**,** 1801-6.

BROMANDER, A., HOLMGREN, J. & LYCKE, N. (1991) Cholera toxin stimulates IL-1 production and enhances antigen presentation by macrophages in vitro. *J Immunol,* 146**,** 2908-14.

BUCHKOVICH, N. J., MAGUIRE, T. G., YU, Y., PATON, A. W., PATON, J. C. & ALWINE, J. C. (2008) Human cytomegalovirus specifically controls the levels of the endoplasmic reticulum chaperone BiP/GRP78, which is required for virion assembly. *J Virol,* 82**,** 31-9.

CAMPOS, E. A., NAMIKOSHI, J., MAEBA, S., YAMAMOTO, M., FUKUMOTO, M. & YAMAMOTO, H. (2003) Nasally administered cholera toxin A-subunit acts as a mucosal adjuvant. *J Oral Sci,* 45**,** 25-31.

CAPRIOLI, A. & TOZZI, A. E. (1998) Epidemiology of Shiga Toxin-Producing *Escherichia coli* Infections in Continental Europe. IN KAPER, J. B. & O'BRIEN, A. D. (Eds.) Escherichia coli *O157:H7 and other Shiga toxin-producing* E. coli *strains. (Presentations and Discussions of the 3rd International Symposium held 22-26 June 1997, in Baltimore, Maryland.).* Washington, DC., American Society for Microbiology Press.

CHARLWOOD, P. A., HATTON, M. W. & REGOECZI, E. (1976) The physicochemical and chemical properties of alpha 1-acid glycoproteins from mammalian and avian plasmas. *Biochim Biophys Acta,* 453**,** 81-92.

CHEN, K. S. & STROBER, W. (1990) Cholera holotoxin and its B subunit enhance Peyer's patch B cell responses induced by orally administered influenza virus: disproportionate cholera toxin enhancement of the IgA B cell response. *Eur J Immunol,* 20**,** 433-6.

CHERLA, R. P., LEE, S. Y. & TESH, V. L. (2003) Shiga toxins and apoptosis. *FEMS Microbiol Lett,* 228**,** 159-66.

CHINNAPEN, D. J., CHINNAPEN, H., SASLOWSKY, D. & LENCER, W. I. (2007) Rafting with cholera toxin: endocytosis and trafficking from plasma membrane to ER. *FEMS Microbiol Lett,* 266**,** 129-37.

CHOU, H. H., HAYAKAWA, T., DIAZ, S., KRINGS, M., INDRIATI, E., LEAKEY, M., PAABO, S., SATTA, Y., TAKAHATA, N. & VARKI, A. (2002) Inactivation of CMP-N-acetylneuraminic acid hydroxylase occurred prior to brain expansion during human evolution. *Proc Natl Acad Sci U S A,* 99**,** 11736-41.

CHOU, H. H., TAKEMATSU, H., DIAZ, S., IBER, J., NICKERSON, E., WRIGHT, K. L., MUCHMORE, E. A., NELSON, D. L., WARREN, S. T. & VARKI, A. (1998) A mutation in human CMP-sialic acid hydroxylase occurred after the Homo-Pan divergence. *Proc Natl Acad Sci U S A,* 95**,** 11751-6.

CONG, Y., OLIVER, A. O. & ELSON, C. O. (2001) Effects of cholera toxin on macrophage production of co-stimulatory cytokines. *Eur J Immunol,* 31**,** 64-71.

CONG, Y., WEAVER, C. T. & ELSON, C. O. (1997) The mucosal adjuvanticity of cholera toxin involves enhancement of costimulatory activity by selective up-regulation of B7.2 expression. *J Immunol,* 159**,** 5301-8.

COX, E., VERDONCK, F., VANROMPAY, D. & GODDEERIS, B. (2006) Adjuvants modulating mucosal immune responses or directing systemic responses towards the mucosa. *Vet Res,* 37**,** 511-39.

CROOK, S. J., BOGGS, J. M., VISTNES, A. I. & KOSHY, K. M. (1986) Factors affecting surface expression of glycolipids: influence of lipid environment and ceramide composition on antibody recognition of cerebroside sulfate in liposomes. *Biochemistry,* 25**,** 7488-94.

DE BRABANDER, M. J., VAN DE VEIRE, R. M., AERTS, F. E., BORGERS, M. & JANSSEN, P. A. (1976) The effects of methyl (5-(2-thienylcarbonyl)-1H-benzimidazol-2-yl) carbamate, (R 17934; NSC 238159), a new synthetic antitumoral drug interfering with microtubules, on mammalian cells cultured in vitro. *Cancer Res,* 36**,** 905-16.

DEGRANDIS, S., LAW, H., BRUNTON, J., GYLES, C. & LINGWOOD, C. A. (1989) Globotetraosylceramide is recognized by the pig edema disease toxin. *J Biol Chem,* 264**,** 12520-5.

DEL GIUDICE, G. & RAPPUOLI, R. (1999) Genetically derived toxoids for use as vaccines and adjuvants. *Vaccine,* 17 Suppl 2**,** S44-52.

DENNIS, J. W., GRANOVSKY, M. & WARREN, C. E. (1999) Protein glycosylation in development and disease. *Bioessays,* 21**,** 412-21.

DEVINE, P. L., CLARK, B. A., BIRRELL, G. W., LAYTON, G. T., WARD, B. G., ALEWOOD, P. F. & MCKENZIE, I. F. (1991) The breast tumor-associated epitope defined by monoclonal antibody 3E1.2 is an O-linked mucin carbohydrate containing N-glycolylneuraminic acid. *Cancer Res,* 51**,** 5826-36.

DIXIT, G., MIKORYAK, C., HAYSLETT, T., BHAT, A. & DRAPER, R. K. (2008) Cholera toxin up-regulates endoplasmic reticulum proteins that correlate with sensitivity to the toxin. *Exp Biol Med (Maywood),* 233**,** 163-75.

DONNENBERG, M. S., KAPER, J. B. & FINLAY, B. B. (1997) Interactions between enteropathogenic *Escherichia coli* and host epithelial cells. *Trends Microbiol,* 5**,** 109-14.

DONTA, S. T., BERISTAIN, S. & TOMICIC, T. K. (1993) Inhibition of heat-labile cholera and *Escherichia coli* enterotoxins by brefeldin A. *Infect Immun,* 61**,** 3282-6.

DOUCE, G., FONTANA, M., PIZZA, M., RAPPUOLI, R. & DOUGAN, G. (1997) Intranasal immunogenicity and adjuvanticity of site-directed mutant derivatives of cholera toxin. *Infect Immun,* 65**,** 2821-8.

DOUCE, G., GIANNELLI, V., PIZZA, M., LEWIS, D., EVEREST, P., RAPPUOLI, R. & DOUGAN, G. (1999) Genetically detoxified mutants of heat-labile toxin from *Escherichia coli* are able to act as oral adjuvants. *Infect Immun,* 67**,** 4400-6.

DOUCE, G., TURCOTTE, C., CROPLEY, I., ROBERTS, M., PIZZA, M., DOMENGHINI, M., RAPPUOLI, R. & DOUGAN, G. (1995) Mutants of *Escherichia coli* heat-labile toxin lacking ADP-ribosyltransferase activity act as nontoxic, mucosal adjuvants. *Proc Natl Acad Sci U S A,* 92**,** 1644-8.

DULBECCO, R. & FREEMAN, G. (1959) Plaque production by the Polyoma Virus. *Virology,* 8**,** 396-7.

EDELMAN, R., KARMALI, M. A. & FLEMING, P. A. (1988) From the National Institutes of Health. Summary of the International Symposium and Workshop on Infections due to Verocytotoxin (Shiga-like toxin)-producing *Escherichia coli*. *J Infect Dis,* 157**,** 1102-4.

ELLIOTT, E. J., ROBINS-BROWNE, R. M., O'LOUGHLIN, E. V., BENNETT-WOOD, V., BOURKE, J., HENNING, P., HOGG, G. G., KNIGHT, J., POWELL, H. & REDMOND, D. (2001) Nationwide study of haemolytic uraemic syndrome: clinical, microbiological, and epidemiological features. *Arch Dis Child,* 85**,** 125-31.

ENDO, Y., TSURUGI, K., YUTSUDO, T., TAKEDA, Y., OGASAWARA, T. & IGARASHI, K. (1988) Site of action of a Vero toxin (VT2) from *Escherichia coli* O157:H7 and of Shiga toxin on eukaryotic ribosomes. RNA N-glycosidase activity of the toxins. *Eur J Biochem,* 171**,** 45-50.

ERIKSSON, K., FREDRIKSSON, M., NORDSTROM, I. & HOLMGREN, J. (2003) Cholera toxin and its B subunit promote dendritic cell vaccination with different influences on Th1 and Th2 development. *Infect Immun,* 71**,** 1740-7.

ESQUIVEL-PEREZ, R. & MORENO-FIERROS, L. (2005) Mucosal and systemic adjuvant effects of cholera toxin and Cry1Ac protoxin on the specific antibody response to HIV-1 C4/V3 peptides are different and depend on the antigen co-administered. *Viral Immunol,* 18**,** 695-708.

EVANS, S. V. & ROGER MACKENZIE, C. (1999) Characterization of protein-glycolipid recognition at the membrane bilayer. *J Mol Recognit,* 12**,** 155-68.

EYRE, N. S., CLELAND, L. G., TANDON, N. N. & MAYRHOFER, G. (2006) Involvement of the C-terminal cytoplasmic domain in the plasma membrane localization of FAT/CD36 and its ability to mediate long-chain fatty acid uptake. *J Lipid Res.*

FALGUIERES, T. & JOHANNES, L. (2006) Shiga toxin B-subunit binds to the chaperone BiP and the nucleolar protein B23. *Biol Cell,* 98**,** 125-34.

FALGUIERES, T., MALLARD, F., BARON, C., HANAU, D., LINGWOOD, C., GOUD, B., SALAMERO, J. & JOHANNES, L. (2001) Targeting of Shiga toxin B-subunit to retrograde transport route in association with detergent-resistant membranes. *Mol Biol Cell,* 12**,** 2453-68.

FAN, E., MERRITT, E. A., VERLINDE, C. L. & HOL, W. G. (2000) AB_5 toxins: structures and inhibitor design. *Curr Opin Struct Biol,* 10**,** 680-6.

FISHMAN, P. H. (1982) Role of membrane gangliosides in the binding and action of bacterial toxins. *J Membr Biol,* 69**,** 85-97.

FISHMAN, P. H. & ORLANDI, P. A. (2003) Cholera toxin internalization and intoxication. *J Cell Sci,* 116**,** 431-2; author reply 432-3.

FOCARETA, A., PATON, J. C., MORONA, R., COOK, J. & PATON, A. W. (2006) A recombinant probiotic for treatment and prevention of cholera. *Gastroenterology,* 130**,** 1688-95.

FOLCH, J., ASCOLI, I., LEES, M., MEATH, J. A. & LE, B. N. (1951) Preparation of lipide extracts from brain tissue. *J Biol Chem,* 191**,** 833-41.

FRANCIS, D. H., COLLINS, J. E. & DUIMSTRA, J. R. (1986) Infection of gnotobiotic pigs with an *Escherichia coli* O157:H7 strain associated with an outbreak of hemorrhagic colitis. *Infect Immun,* 51**,** 953-6.

FRASER, M. E., CHERNAIA, M. M., KOZLOV, Y. V. & JAMES, M. N. (1994) Crystal structure of the holotoxin from *Shigella dysenteriae* at 2.5 A resolution. *Nat Struct Biol,* 1**,** 59-64.

FRASER, M. E., FUJINAGA, M., CHERNEY, M. M., MELTON-CELSA, A. R., TWIDDY, E. M., O'BRIEN, A. D. & JAMES, M. N. (2004) Structure of shiga toxin type 2 (Stx2) from *Escherichia coli* O157:H7. *J Biol Chem,* 279**,** 27511-7.

FUJII, J., MATSUI, T., HEATHERLY, D. P., SCHLEGEL, K. H., LOBO, P. I., YUTSUDO, T., CIRAOLO, G. M., MORRIS, R. E. & OBRIG, T. (2003) Rapid apoptosis induced by Shiga toxin in HeLa cells. *Infect Immun,* 71**,** 2724-35.

FUJINAGA, Y., WOLF, A. A., RODIGHIERO, C., WHEELER, H., TSAI, B., ALLEN, L., JOBLING, M. G., RAPOPORT, T., HOLMES, R. K. & LENCER, W. I. (2003)

Gangliosides that associate with lipid rafts mediate transport of cholera and related toxins from the plasma membrane to endoplasmic reticulm. *Mol Biol Cell,* 14**,** 4783-93.

FUKUTA, S., MAGNANI, J. L., TWIDDY, E. M., HOLMES, R. K. & GINSBURG, V. (1988) Comparison of the carbohydrate-binding specificities of cholera toxin and *Escherichia coli* heat-labile enterotoxins LTh-I, LT-IIa, and LT-IIb. *Infect Immun,* 56**,** 1748-53.

GAGLIARDI, M. C., SALLUSTO, F., MARINARO, M., LANGENKAMP, A., LANZAVECCHIA, A. & DE MAGISTRIS, M. T. (2000) Cholera toxin induces maturation of human dendritic cells and licences them for Th2 priming. *Eur J Immunol,* 30**,** 2394-403.

GAGLIARDI, M. C., SALLUSTO, F., MARINARO, M., VENDETTI, S., RICCOMI, A. & DE MAGISTRIS, M. T. (2002) Effects of the adjuvant cholera toxin on dendritic cells: stimulatory and inhibitory signals that result in the amplification of immune responses. *Int J Med Microbiol,* 291**,** 571-5.

GALILI, U., SHOHET, S. B., KOBRIN, E., STULTS, C. L. & MACHER, B. A. (1988) Man, apes, and Old World monkeys differ from other mammals in the expression of alpha-galactosyl epitopes on nucleated cells. *J Biol Chem,* 263**,** 17755-62.

GANNON, V. P., TEERLING, C., MASRI, S. A. & GYLES, C. L. (1990) Molecular cloning and nucleotide sequence of another variant of the *Escherichia coli* Shiga-like toxin II family. *J Gen Microbiol,* 136 (Pt 6)**,** 1125-35.

GARRED, O., VAN DEURS, B. & SANDVIG, K. (1995) Furin-induced cleavage and activation of Shiga toxin. *J Biol Chem,* 270**,** 10817-21.

GEORGE-CHANDY, A., ERIKSSON, K., LEBENS, M., NORDSTROM, I., SCHON, E. & HOLMGREN, J. (2001) Cholera toxin B subunit as a carrier molecule promotes antigen presentation and increases CD40 and CD86 expression on antigen-presenting cells. *Infect Immun,* 69**,** 5716-25.

GETHING, M. J. (1999) Role and regulation of the ER chaperone BiP. *Semin Cell Dev Biol,* 10**,** 465-72.

GILL, D. M. (1975) Involvement of nicotinamide adenine dinucleotide in the action of cholera toxin in vitro. *Proc Natl Acad Sci U S A,* 72**,** 2064-8.

GILL, D. M. & RICHARDSON, S. H. (1980) Adenosine diphosphate-ribosylation of adenylate cyclase catalyzed by heat-labile enterotoxin of *Escherichia coli*: comparison with cholera toxin. *J Infect Dis,* 141**,** 64-70.

GLENN, G. M., RAO, M., MATYAS, G. R. & ALVING, C. R. (1998a) Skin immunization made possible by cholera toxin. *Nature,* 391**,** 851.

GLENN, G. M., SCHARTON-KERSTEN, T., VASSELL, R., MALLETT, C. P., HALE, T. L. & ALVING, C. R. (1998b) Transcutaneous immunization with cholera toxin protects mice against lethal mucosal toxin challenge. *J Immunol,* 161**,** 3211-4.

GLENN, G. M., TAYLOR, D. N., LI, X., FRANKEL, S., MONTEMARANO, A. & ALVING, C. R. (2000) Transcutaneous immunization: a human vaccine delivery strategy using a patch. *Nat Med,* 6**,** 1403-6.

GOCKEL, C. M., BAO, S. & BEAGLEY, K. W. (2000) Transcutaneous immunization induces mucosal and systemic immunity: a potent method for targeting immunity to the female reproductive tract. *Mol Immunol,* 37**,** 537-44.

GORDEN, J. & SMALL, P. L. (1993) Acid resistance in enteric bacteria. *Infect Immun,* 61**,** 364-7.

GRIFFIN, P. M. (1998) Epidemiology of Shiga Toxin-Producing *Escherichia coli* Infections in Humans in the United States. IN KAPER, J. B. & O'BRIEN, A. D. (Eds.) Escherichia coli *O157:H7 and other Shiga toxin-producing* E. coli *strains. (Presentations and Discussions of the 3rd International Symposium held 22-26 June 1997, in Baltimore, Maryland.).* Washington, DC., American Society for Microbiology Press.

GRIFFITHS, S. L., FINKELSTEIN, R. A. & CRITCHLEY, D. R. (1986) Characterization of the receptor for cholera toxin and *Escherichia coli* heat-labile toxin in rabbit intestinal brush borders. *Biochem J,* 238**,** 313-22.

GU, J. & TANIGUCHI, N. (2004) Regulation of integrin functions by N-glycans. *Glycoconj J,* 21**,** 9-15.

GYLES, C. L. (1992) *Escherichia coli* cytotoxins and enterotoxins. *Can J Microbiol,* 38**,** 734-46.

GYLES, C. L., DE GRANDIS, S. A., MACKENZIE, C. & BRUNTON, J. L. (1988) Cloning and nucleotide sequence analysis of the genes determining verocytotoxin production in a porcine edema disease isolate of *Escherichia coli*. *Microb Pathog,* 5**,** 419-26.

Haicheur, N., Bismuth, E., Bosset, S., Adotevi, O., Warnier, G., Lacabanne, V., Regnault, A., Desaymard, C., Amigorena, S., Ricciardi-Castagnoli, P., Goud, B., Fridman, W. H., Johannes, L. & Tartour, E. (2000) The B subunit of Shiga toxin

fused to a tumor antigen elicits CTL and targets dendritic cells to allow MHC class I-restricted presentation of peptides derived from exogenous antigens. *J Immunol,* 165**,** 3301-8.

HAMMAN, B. D., HENDERSHOT, L. M. & JOHNSON, A. E. (1998) BiP maintains the permeability barrier of the ER membrane by sealing the lumenal end of the translocon pore before and early in translocation. *Cell,* 92**,** 747-58.

HANSEN, G. H., DALSKOV, S. M., RASMUSSEN, C. R., IMMERDAL, L., NIELS-CHRISTIANSEN, L. L. & DANIELSEN, E. M. (2005) Cholera toxin entry into pig enterocytes occurs via a lipid raft- and clathrin-dependent mechanism. *Biochemistry,* 44**,** 873-82.

HAVTON, L. A. & BROMAN, J. (2005) Systemic administration of cholera toxin B subunit conjugated to horseradish peroxidase in the adult rat labels preganglionic autonomic neurons, motoneurons, and select primary afferents for light and electron microscopic studies. *J Neurosci Methods,* 149**,** 101-9.

HAYAKAWA, K., HIRAMATSU, N., OKAMURA, M., YAO, J., PATON, A. W., PATON, J. C. & KITAMURA, M. (2008) Blunted activation of NF-kappaB and NF-kappaB-dependent gene expression by geranylgeranylacetone: involvement of unfolded protein response. *Biochem Biophys Res Commun,* 365**,** 47-53.

Hayashi, T., Makino, K., Ohnishi, M., Kurokawa, K., Ishii, K., Yokoyama, K., Han, C. G., Ohtsubo, E., Nakayama, K., Murata, T., Tanaka, M., Tobe, T., Iida, T., Takami, H., Honda, T., Sasakawa, C., Ogasawara, N., Yasunaga, T., Kuhara, S., Shiba, T., Hattori, M. & Shinagawa, H. (2001) Complete genome sequence of enterohemorrhagic *Escherichia coli* O157:H7 and genomic comparison with a laboratory strain K-12. *DNA Res,* 8**,** 11-22.

HEDLUND, M., TANGVORANUNTAKUL, P., TAKEMATSU, H., LONG, J. M., HOUSLEY, G. D., KOZUTSUMI, Y., SUZUKI, A., WYNSHAW-BORIS, A., RYAN, A. F., GALLO, R. L., VARKI, N. & VARKI, A. (2007) N-glycolylneuraminic acid deficiency in mice: implications for human biology and evolution. *Mol Cell Biol,* 27**,** 4340-6.

HEINRICHS, D. E., YETHON, J. A., AMOR, P. A. & WHITFIELD, C. (1998) The assembly system for the outer core portion of R1- and R4-type lipopolysaccharides of Escherichia coli. The R1 core-specific beta-glucosyltransferase provides a novel attachment site for O-polysaccharides. *J Biol Chem,* 273**,** 29497-505.

HENDERSHOT, L. M. (2004) The ER function BiP is a master regulator of ER function. *Mt Sinai J Med,* 71**,** 289-97.

HERMENTIN, P., WITZEL, R., DOENGES, R., BAUER, R., HAUPT, H., PATEL, T., PAREKH, R. B. & BRAZEL, D. (1992) The mapping by high-pH anion-exchange chromatography with pulsed amperometric detection and capillary electrophoresis of the carbohydrate moieties of human plasma alpha 1-acid glycoprotein. *Anal Biochem,* 206**,** 419-29.

HIGASHI, H., NAIKI, M., MATUO, S. & OKOUCHI, K. (1977) Antigen of "serum sickness" type of heterophile antibodies in human sera: indentification as gangliosides with N-glycolylneuraminic acid. *Biochem Biophys Res Commun,* 79**,** 388-95.

HIRABAYASHI, Y., KASAKURA, H., MATSUMOTO, M., HIGASHI, H., KATO, S., KASAI, N. & NAIKI, M. (1987) Specific expression of unusual GM_2 ganglioside with Hanganutziu-Deicher antigen activity on human colon cancers. *Jpn J Cancer Res,* 78**,** 251-60.

HIRAI, T., HASHIGUCHI, S., TORIGOE, N., TODA, Y., ITO, Y. & SUGIMUR, K. (2000) Intranasal sensitization of Japanese cedar pollen by the co-administration of low doses of cholera toxin but not its recombinant B subunit to mice. *Microbiol Immunol,* 44**,** 259-66.

HOLMGREN, J. & CZERKINSKY, C. (2005) Mucosal immunity and vaccines. *Nat Med,* 11**,** S45-53.

HOLMGREN, J., CZERKINSKY, C., ERIKSSON, K. & MHARANDI, A. (2003) Mucosal immunisation and adjuvants: a brief overview of recent advances and challenges. *Vaccine,* 21 Suppl 2**,** S89-95.

HOLMGREN, J., LYCKE, N. & CZERKINSKY, C. (1993) Cholera toxin and cholera B subunit as oral-mucosal adjuvant and antigen vector systems. *Vaccine,* 11**,** 1179-84.

HOPKINS, C. R. (1983) Intracellular routing of transferrin and transferrin receptors in epidermoid carcinoma A431 cells. *Cell,* 35**,** 321-30.

HUGHES, A. K., STRICKLETT, P. K. & KOHAN, D. E. (1998) Shiga toxin-1 regulation of cytokine production by human proximal tubule cells. *Kidney Int,* 54**,** 1093-106.

HUGHES, A. K., STRICKLETT, P. K. & KOHAN, D. E. (2001) Shiga toxin-1 regulation of cytokine production by human glomerular epithelial cells. *Nephron,* 88**,** 14-23.

ITO, H., TERAI, A., KURAZONO, H., TAKEDA, Y. & NISHIBUCHI, M. (1990) Cloning and nucleotide sequencing of Vero toxin 2 variant genes from *Escherichia coli*

O91:H21 isolated from a patient with the hemolytic uremic syndrome. *Microb Pathog,* 8**,** 47-60.

JACEWICZ, M. S., MOBASSALEH, M., GROSS, S. K., BALASUBRAMANIAN, K. A., DANIEL, P. F., RAGHAVAN, S., MCCLUER, R. H. & KEUSCH, G. T. (1994) Pathogenesis of Shigella diarrhea: XVII. A mammalian cell membrane glycolipid, Gb3, is required but not sufficient to confer sensitivity to Shiga toxin. *J Infect Dis,* 169**,** 538-46.

JACKSON, M. P., NEILL, R. J., O'BRIEN, A. D., HOLMES, R. K. & NEWLAND, J. W. (1987) Nucleotide sequence analysis and comparison of the structural genes for Shiga-like toxin I and Shiga-like toxin II encoded by bacteriophages from Escherichia coli 933. *FEMS Microbiol Lett,* 44**,** 109-14.

JOBLING, M. G. & HOLMES, R. K. (1990) Construction of vectors with the p15a replicon, kanamycin resistance, inducible lacZ alpha and pUC18 or pUC19 multiple cloning sites. *Nucleic Acids Res,* 18**,** 5315-6.

JOBLING, M. G. & HOLMES, R. K. (1991) Analysis of structure and function of the B subunit of cholera toxin by the use of site-directed mutagenesis. *Mol Microbiol,* 5**,** 1755-67.

JOHNSON, W. M., LIOR, H. & BEZANSON, G. S. (1983) Cytotoxic *Escherichia coli* O157:H7 associated with haemorrhagic colitis in Canada. *Lancet,* 1**,** 76.

KANNAGI, R., NUDELMAN, E. & HAKOMORI, S. (1982) Possible role of ceramide in defining structure and function of membrane glycolipids. *Proc Natl Acad Sci U S A,* 79**,** 3470-4.

KAPER, J. B., NATARO, J. P. & MOBLEY, H. L. (2004) Pathogenic *Escherichia coli*. *Nat Rev Microbiol,* 2**,** 123-40.

KARLSSON, K. A. (1998) Meaning and therapeutic potential of microbial recognition of host glycoconjugates. *Mol Microbiol,* 29**,** 1-11.

KARMALI, M. A. (1989) Infection by verocytotoxin-producing *Escherichia coli*. *Clin Microbiol Rev,* 2**,** 15-38.

KARMALI, M. A., PETRIC, M., LIM, C., FLEMING, P. C., ARBUS, G. S. & LIOR, H. (1985) The association between idiopathic hemolytic uremic syndrome and infection by verotoxin-producing *Escherichia coli*. *J Infect Dis,* 151**,** 775-82.

KAWASAKI, T., KOYAMA, J. & YAMASHINA, I. (1966) Isolation and characterization of alpha 1-acid glycoprotein from rat serum. *J Biochem (Tokyo),* 60**,** 554-60.

KELM, S. & SCHAUER, R. (1997) Sialic acids in molecular and cellular interactions. *Int Rev Cytol,* 175**,** 137-240.

KENNY, B., DEVINNEY, R., STEIN, M., REINSCHEID, D. J., FREY, E. A. & FINLAY, B. B. (1997) Enteropathogenic *E. coli* (EPEC) transfers its receptor for intimate adherence into mammalian cells. *Cell,* 91**,** 511-20.

KEUSCH, G. T., GRADY, G. F., MATA, L. J. & MCIVER, J. (1972) The pathogenesis of Shigella diarrhea. I. Enterotoxin production by *Shigella dysenteriae* I. *J Clin Invest,* 51**,** 1212-8.

KHINE, A. A., TAM, P., NUTIKKA, A. & LINGWOOD, C. A. (2004) Brefeldin A and filipin distinguish two globotriaosyl ceramide/verotoxin-1 intracellular trafficking pathways involved in Vero cell cytotoxicity. *Glycobiology,* 14**,** 701-12.

KIARASH, A., BOYD, B. & LINGWOOD, C. A. (1994) Glycosphingolipid receptor function is modified by fatty acid content. Verotoxin 1 and verotoxin 2c preferentially recognize different globotriaosyl ceramide fatty acid homologues. *J Biol Chem,* 269**,** 11138-46.

KIM, P. S. & ARVAN, P. (1998) Endocrinopathies in the family of endoplasmic reticulum (ER) storage diseases: disorders of protein trafficking and the role of ER molecular chaperones. *Endocr Rev,* 19**,** 173-202.

KITOV, P. I., SADOWSKA, J. M., MULVEY, G., ARMSTRONG, G. D., LING, H., PANNU, N. S., READ, R. J. & BUNDLE, D. R. (2000) Shiga-like toxins are neutralized by tailored multivalent carbohydrate ligands. *Nature,* 403**,** 669-72.

KNUTTON, S., BALDWIN, T., WILLIAMS, P. H. & MCNEISH, A. S. (1989) Actin accumulation at sites of bacterial adhesion to tissue culture cells: basis of a new diagnostic test for enteropathogenic and enterohemorrhagic *Escherichia coli*. *Infect Immun,* 57**,** 1290-8.

KONOWALCHUK, J., SPEIRS, J. I. & STAVRIC, S. (1977) Vero response to a cytotoxin of *Escherichia coli*. *Infect Immun,* 18**,** 775-9.

KOVBASNJUK, O., EDIDIN, M. & DONOWITZ, M. (2001) Role of lipid rafts in Shiga toxin 1 interaction with the apical surface of Caco-2 cells. *J Cell Sci,* 114**,** 4025-31.

LAEMMLI, U. K. (1970) Cleavage of structural proteins during the assembly of the head of bacteriophage T4. *Nature,* 227**,** 680-5.

LAI, L. C., WAINWRIGHT, L. A., STONE, K. D. & DONNENBERG, M. S. (1997) A third secreted protein that is encoded by the enteropathogenic *Escherichia coli* pathogenicity island is required for transduction of signals and for attaching and effacing activities in host cells. *Infect Immun,* 65**,** 2211-7.

LAUVRAK, S. U., WALCHLI, S., IVERSEN, T. G., SLAGSVOLD, H. H., TORGERSEN, M. L., SPILSBERG, B. & SANDVIG, K. (2006) Shiga toxin regulates its entry in a Syk-dependent manner. *Mol Biol Cell,* 17**,** 1096-109.

LE, P. U. & NABI, I. R. (2003) Distinct caveolae-mediated endocytic pathways target the Golgi apparatus and the endoplasmic reticulum. *J Cell Sci,* 116**,** 1059-71.

LEE, A. S. (2005) The ER chaperone and signaling regulator GRP78/BiP as a monitor of endoplasmic reticulum stress. *Methods,* 35**,** 373-81.

LEE, A. S. (2007) GRP78 induction in cancer: therapeutic and prognostic implications. *Cancer Res,* 67**,** 3496-9.

LENCER, W. I., CONSTABLE, C., MOE, S., JOBLING, M. G., WEBB, H. M., RUSTON, S., MADARA, J. L., HIRST, T. R. & HOLMES, R. K. (1995) Targeting of cholera toxin and *Escherichia coli* heat labile toxin in polarized epithelia: role of COOH-terminal KDEL. *J Cell Biol,* 131**,** 951-62.

LENCER, W. I., CONSTABLE, C., MOE, S., RUFO, P. A., WOLF, A., JOBLING, M. G., RUSTON, S. P., MADARA, J. L., HOLMES, R. K. & HIRST, T. R. (1997) Proteolytic activation of cholera toxin and *Escherichia* coli labile toxin by entry into host epithelial cells. Signal transduction by a protease-resistant toxin variant. *J Biol Chem,* 272**,** 15562-8.

LENCER, W. I. & SASLOWSKY, D. (2005) Raft trafficking of AB_5 subunit bacterial toxins. *Biochim Biophys Acta,* 1746**,** 314-21.

LENCER, W. I. & TSAI, B. (2003) The intracellular voyage of cholera toxin: going retro. *Trends Biochem Sci,* 28**,** 639-45.

LIN, Z., YAMASAKI, S., KURAZONO, H., OHMURA, M., KARASAWA, T., INOUE, T., SAKAMOTO, S., SUGANAMI, T., TAKEOKA, T., TANIGUCHI, Y. & ET AL. (1993) Cloning and sequencing of two new Verotoxin 2 variant genes of *Escherichia coli* isolated from cases of human and bovine diarrhea. *Microbiol Immunol,* 37**,** 451-9.

LING, H., BOODHOO, A., HAZES, B., CUMMINGS, M. D., ARMSTRONG, G. D., BRUNTON, J. L. & READ, R. J. (1998) Structure of the shiga-like toxin I B-pentamer complexed with an analogue of its receptor Gb3. *Biochemistry,* 37**,** 1777-88.

LINGWOOD, C. A. (1996) Role of verotoxin receptors in pathogenesis. *Trends Microbiol,* 4**,** 147-53.

LINGWOOD, C. A. (2000) A holistic approach to glycolipid function: is the lipid moiety important? *Trends in Glycoscience and Glycotechnology,* 12**,** 7-16.

LINGWOOD, C. A., BOYD, B. & NUTIKKA, A. (2000) Analysis of interactions between glycosphingolipids and microbial toxins. *Methods Enzymol,* 312**,** 459-73.

LINGWOOD, C. A., LAW, H., RICHARDSON, S., PETRIC, M., BRUNTON, J. L., DE GRANDIS, S. & KARMALI, M. (1987) Glycolipid binding of purified and recombinant *Escherichia coli* produced verotoxin in vitro. *J Biol Chem,* 262**,** 8834-9.

LIPPINCOTT-SCHWARTZ, J., DONALDSON, J. G., SCHWEIZER, A., BERGER, E. G., HAURI, H. P., YUAN, L. C. & KLAUSNER, R. D. (1990) Microtubule-dependent retrograde transport of proteins into the ER in the presence of brefeldin A suggests an ER recycling pathway. *Cell,* 60**,** 821-36.

LIPPINCOTT-SCHWARTZ, J., YUAN, L., TIPPER, C., AMHERDT, M., ORCI, L. & KLAUSNER, R. D. (1991) Brefeldin A's effects on endosomes, lysosomes, and the TGN suggest a general mechanism for regulating organelle structure and membrane traffic. *Cell,* 67**,** 601-16.

LÓPEZ, E. L., CONTRINI, M. M. & DE ROSA, M. F. (1998) Epidemiology of Shiga Toxin-Producing *Escherichia coli* in South America. IN KAPER, J. B. & O'BRIEN, A. D. (Eds.) Escherichia coli *O157:H7 and other Shiga toxin-producing* E. coli *strains. (Presentations and Discussions of the 3rd International Symposium held 22-26 June 1997, in Baltimore, Maryland.).* Washington, DC., American Society for Microbiology Press.

LOUISE, C. B., KAYE, S. A., BOYD, B., LINGWOOD, C. A. & OBRIG, T. G. (1995) Shiga toxin-associated hemolytic uremic syndrome: effect of sodium butyrate on sensitivity of human umbilical vein endothelial cells to Shiga toxin. *Infect Immun,* 63**,** 2766-9.

LU, X., CLEMENTS, J. D. & KATZ, J. M. (2002) Mutant *Escherichia coli* heat-labile enterotoxin [LT(R192G)] enhances protective humoral and cellular immune responses to orally administered inactivated influenza vaccine. *Vaccine,* 20**,** 1019-29.

LYCKE, N. & HOLMGREN, J. (1986) Strong adjuvant properties of cholera toxin on gut mucosal immune responses to orally presented antigens. *Immunology,* 59**,** 301-8.

MAGNANI, J. L., SMITH, D. F. & GINSBURG, V. (1980) Detection of gangliosides that bind cholera toxin: direct binding of 125I-labeled toxin to thin-layer chromatograms. *Anal Biochem,* 109**,** 399-402.

MAJOUL, I., SCHMIDT, T., POMASANOVA, M., BOUTKEVICH, E., KOZLOV, Y. & SOLING, H. D. (2002) Differential expression of receptors for Shiga and Cholera toxin is regulated by the cell cycle. *J Cell Sci,* 115**,** 817-26.

MALLARD, F., ANTONY, C., TENZA, D., SALAMERO, J., GOUD, B. & JOHANNES, L. (1998) Direct pathway from early/recycling endosomes to the Golgi apparatus revealed through the study of shiga toxin B-fragment transport. *J Cell Biol,* 143**,** 973-90.

MALYKH, Y. N., SCHAUER, R. & SHAW, L. (2001) N-Glycolylneuraminic acid in human tumours. *Biochimie,* 83**,** 623-34.

MASSOL, R. H., LARSEN, J. E., FUJINAGA, Y., LENCER, W. I. & KIRCHHAUSEN, T. (2004) Cholera toxin toxicity does not require functional Arf6- and dynamin-dependent endocytic pathways. *Mol Biol Cell,* 15**,** 3631-41.

MAYOR, S. & RIEZMAN, H. (2004) Sorting GPI-anchored proteins. *Nat Rev Mol Cell Biol,* 5**,** 110-20.

MCGUIRE, C., CHAN, W. C. & WAKELIN, D. (2002) Nasal immunization with homogenate and peptide antigens induces protective immunity against *Trichinella spiralis*. *Infect Immun,* 70**,** 7149-52.

MCKENZIE, S. J. & HALSEY, J. F. (1984) Cholera toxin B subunit as a carrier protein to stimulate a mucosal immune response. *J Immunol,* 133**,** 1818-24.

MERRICK, J. M., ZADARLIK, K. & MILGROM, F. (1978) Characterization of the Hanganutziu-Deicher (serum-sickness) antigen as gangliosides containing N-glycolylneuraminic acid. *Int Arch Allergy Appl Immunol,* 57**,** 477-80.

MERRITT, E. A. & HOL, W. G. (1995) AB_5 toxins. *Curr Opin Struct Biol,* 5**,** 165-71.

MERRITT, E. A., KUHN, P., SARFATY, S., ERBE, J. L., HOLMES, R. K. & HOL, W. G. (1998) The 1.25 A resolution refinement of the cholera toxin B-pentamer: evidence of peptide backbone strain at the receptor-binding site. *J Mol Biol,* 282**,** 1043-59.

MERRITT, E. A., SARFATY, S., VAN DEN AKKER, F., L'HOIR, C., MARTIAL, J. A. & HOL, W. G. (1994) Crystal structure of cholera toxin B-pentamer bound to receptor GM1 pentasaccharide. *Protein Sci,* 3**,** 166-75.

MERRITT, E. A., ZHANG, Z., PICKENS, J. C., AHN, M., HOL, W. G. & FAN, E. (2002) Characterization and crystal structure of a high-affinity pentavalent receptor-binding inhibitor for cholera toxin and *E. coli* heat-labile enterotoxin. *J Am Chem Soc,* 124**,** 8818-24.

MEYER, T., KARCH, H., HACKER, J., BOCKLAGE, H. & HEESEMANN, J. (1992) Cloning and sequencing of a Shiga-like toxin II-related gene from *Escherichia coli* O157:H7 strain 7279. *Zentralbl Bakteriol,* 276**,** 176-88.

MICHINO, H., ARAKI, K., MINAMI, S., NAKAYAMA, T., EJIMA, Y., HIROE, K., TANAKA, H., FUJITA, N., USAMI, S., YONEKAWA, M., SADAMOTO, K., TAKAYA, S. & SAKAI, N. (1998) Recent Outbreaks of Infections Caused by *Escherichia coli* O157:H7 in Japan. IN KAPER, J. B. & O'BRIEN, A. D. (Eds.) Escherichia coli *O157:H7 and other Shiga toxin-producing* E. coli *strains. (Presentations and Discussions of the 3rd International Symposium held 22-26 June 1997, in Baltimore, Maryland.).* Washington, DC., American Society for Microbiology Press.

MIDDLEBROOK, J. L. & DORLAND, R. B. (1984) Bacterial toxins: cellular mechanisms of action. *Microbiol Rev,* 48**,** 199-221.

MILLS, S. D. & FINLAY, B. B. (1994) Comparison of *Salmonella typhi* and *Salmonella typhimurium* invasion, intracellular growth and localization in cultured human epithelial cells. *Microb Pathog,* 17**,** 409-23.

MONNENS, L. A., SAVAGE, C. O. & TAYLOR, C. M. (1998) Pathophysiology of Hemolytic-Uremic Syndrome. IN KAPER, J. B. & O'BRIEN, A. D. (Eds.) Escherichia coli *O157:H7 and other Shiga toxin-producing* E. coli *strains. (Presentations and Discussions of the 3rd International Symposium held 22-26 June 1997, in Baltimore, Maryland.).* Washington, DC., American Society for Microbiology Press.

MONTECUCCO, C., PAPINI, E. & SCHIAVO, G. (1994) Bacterial protein toxins penetrate cells via a four-step mechanism. *FEBS Lett,* 346**,** 92-8.

MONTENEGRO, M. A., BULTE, M., TRUMPF, T., ALEKSIC, S., REUTER, G., BULLING, E. & HELMUTH, R. (1990) Detection and characterization of fecal verotoxin-producing *Escherichia coli* from healthy cattle. *J Clin Microbiol,* 28**,** 1417-21.

MORINAGA, N., YAHIRO, K., MATSUURA, G., MOSS, J. & NODA, M. (2008) Subtilase cytotoxin, produced by Shiga-toxigenic *Escherichia coli*, transiently inhibits protein synthesis of Vero cells via degradation of BiP and induces cell cycle arrest at G1 by downregulation of cyclin D1. *Cell Microbiol,* 10**,** 921-9.

MORINAGA, N., YAHIRO, K., MATSUURA, G., WATANABE, M., NOMURA, F., MOSS, J. & NODA, M. (2007) Two distinct cytotoxic activities of subtilase cytotoxin produced by shiga-toxigenic *Escherichia coli*. *Infect Immun,* 75**,** 488-96.

MUCHMORE, E. A., DIAZ, S. & VARKI, A. (1998) A structural difference between the cell surfaces of humans and the great apes. *Am J Phys Anthropol,* 107**,** 187-98.

MUCHMORE, E. A., MILEWSKI, M., VARKI, A. & DIAZ, S. (1989) Biosynthesis of N-glycolyneuraminic acid. The primary site of hydroxylation of N-acetylneuraminic acid is the cytosolic sugar nucleotide pool. *J Biol Chem,* 264**,** 20216-23.

MULVEY, G., KITOV, P. I., MARCATO, P., BUNDLE, D. R. & ARMSTRONG, G. D. (2001) Glycan mimicry as a basis for novel anti-infective drugs. *Biochimie,* 83**,** 841-7.

MULVEY, G. L., MARCATO, P., KITOV, P. I., SADOWSKA, J., BUNDLE, D. R. & ARMSTRONG, G. D. (2003) Assessment in mice of the therapeutic potential of tailored, multivalent Shiga toxin carbohydrate ligands. *J Infect Dis,* 187**,** 640-9.

NATARO, J. P. & KAPER, J. B. (1998) Diarrheagenic *Escherichia coli*. *Clin Microbiol Rev,* 11**,** 142-201.

NICHOLS, B. J. (2002) A distinct class of endosome mediates clathrin-independent endocytosis to the Golgi complex. *Nat Cell Biol,* 4**,** 374-8.

NICHOLS, B. J., KENWORTHY, A. K., POLISHCHUK, R. S., LODGE, R., ROBERTS, T. H., HIRSCHBERG, K., PHAIR, R. D. & LIPPINCOTT-SCHWARTZ, J. (2001) Rapid cycling of lipid raft markers between the cell surface and Golgi complex. *J Cell Biol,* 153**,** 529-41.

Nishikawa, K., Matsuoka, K., Kita, E., Okabe, N., Mizuguchi, M., Hino, K., Miyazawa, S., Yamasaki, C., Aoki, J., Takashima, S., Yamakawa, Y., Nishijima, M., Terunuma, D., Kuzuhara, H. & Natori, Y. (2002) A therapeutic agent with oriented carbohydrates for treatment of infections by Shiga toxin-producing *Escherichia coli* O157:H7. *Proc Natl Acad Sci U S A,* 99**,** 7669-74.

NISHIKAWA, K., MATSUOKA, K., WATANABE, M., IGAI, K., HINO, K., HATANO, K., YAMADA, A., ABE, N., TERUNUMA, D., KUZUHARA, H. & NATORI, Y. (2005)

Identification of the optimal structure required for a Shiga toxin neutralizer with oriented carbohydrates to function in the circulation. *J Infect Dis,* 191**,** 2097-105.

O'BRIEN, A. D. & HOLMES, R. K. (1987) Shiga and Shiga-like toxins. *Microbiol Rev,* 51**,** 206-20.

O'BRIEN, A. D., MARQUES, L. R., KERRY, C. F., NEWLAND, J. W. & HOLMES, R. K. (1989) Shiga-like toxin converting phage of enterohemorrhagic *Escherichia coli* strain 933. *Microb Pathog,* 6**,** 381-90.

O'BRIEN, A. D., NEWLAND, J. W., MILLER, S. F., HOLMES, R. K., SMITH, H. W. & FORMAL, S. B. (1984) Shiga-like toxin-converting phages from *Escherichia coli* strains that cause hemorrhagic colitis or infantile diarrhea. *Science,* 226**,** 694-6.

O'BRIEN, A. D., THOMPSON, M. R., CANTEY, J. R. & FORMAL, S. B. (1977) Production of a Shigella dysenteriae-like toxin by pathogenic *Escherichia coli,* abstr. B-103. *Abstracts of the 77th Annual Meeting of the American Society for Microbiology 1977.* Washington, D. C., American Society for Microbiology Press.

O'BRIEN, A. O., LIVELY, T. A., CHEN, M. E., ROTHMAN, S. W. & FORMAL, S. B. (1983) Escherichia coli O157:H7 strains associated with haemorrhagic colitis in the United States produce a Shigella dysenteriae 1 (SHIGA) like cytotoxin. *Lancet,* 1**,** 702.

O'NEAL, C. J., AMAYA, E. I., JOBLING, M. G., HOLMES, R. K. & HOL, W. G. (2004) Crystal structures of an intrinsically active cholera toxin mutant yield insight into the toxin activation mechanism. *Biochemistry,* 43**,** 3772-82.

OHASHI, Y., SASABE, T., NISHIDA, T., NISHI, Y. & HIGASHI, H. (1983) Hanganutziu-Deicher heterophile antigen in human retinoblastoma cells. *Am J Ophthalmol,* 96**,** 321-5.

OHMURA-HOSHINO, M., YAMAMOTO, M., YUKI, Y., TAKEDA, Y. & KIYONO, H. (2004) Non-toxic Stx derivatives from *Escherichia coli* possess adjuvant activity for mucosal immunity. *Vaccine,* 22**,** 3751-61.

OHMURA, M., YAMAMOTO, M., TOMIYAMA-MIYAJI, C., YUKI, Y., TAKEDA, Y. & KIYONO, H. (2005) Nontoxic Shiga toxin derivatives from *Escherichia coli* possess adjuvant activity for the augmentation of antigen-specific immune responses via dendritic cell activation. *Infect Immun,* 73**,** 4088-97.

OHTSUBO, M., THEODORAS, A. M., SCHUMACHER, J., ROBERTS, J. M. & PAGANO, M. (1995) Human cyclin E, a nuclear protein essential for the G1-to-S phase transition. *Mol Cell Biol,* 15**,** 2612-24.

OKU, Y., YUTSUDO, T., HIRAYAMA, T., O'BRIEN, A. D. & TAKEDA, Y. (1989) Purification and some properties of a Vero toxin from a human strain of *Escherichia coli* that is immunologically related to Shiga-like toxin II (VT2). *Microb Pathog,* 6**,** 113-22.

ONO, M. & HAKOMORI, S. (2004) Glycosylation defining cancer cell motility and invasiveness. *Glycoconj J,* 20**,** 71-8.

ORLANDI, P. A., CURRAN, P. K. & FISHMAN, P. H. (1993) Brefeldin A blocks the response of cultured cells to cholera toxin. Implications for intracellular trafficking in toxin action. *J Biol Chem,* 268**,** 12010-6.

ORLANDI, P. A. & FISHMAN, P. H. (1993) Orientation of cholera toxin bound to target cells. *J Biol Chem,* 268**,** 17038-44.

ORLANDI, P. A. & FISHMAN, P. H. (1998) Filipin-dependent inhibition of cholera toxin: evidence for toxin internalization and activation through caveolae-like domains. *J Cell Biol,* 141**,** 905-15.

ØRSKOV, F., ØRSKOV, I. & VILLAR, J. A. (1987) Cattle as reservoir of verotoxin-producing *Escherichia col*i O157:H7. *Lancet,* 2**,** 276.

PARK, S. J., CHUN, S. K. & KIM, P. H. (2003) Intraperitoneal delivery of cholera toxin B subunit enhances systemic and mucosal antibody responses. *Mol Cells,* 16**,** 106-12.

PATON, A. W., BEDDOE, T., THORPE, C. M., WHISSTOCK, J. C., WILCE, M. C., ROSSJOHN, J., TALBOT, U. M. & PATON, J. C. (2006a) AB_5 subtilase cytotoxin inactivates the endoplasmic reticulum chaperone BiP. *Nature,* 443**,** 548-52.

PATON, A. W., BEUTIN, L. & PATON, J. C. (1995) Heterogeneity of the amino-acid sequences of *Escherichia coli* Shiga-like toxin type-I operons. *Gene,* 153**,** 71-4.

PATON, A. W., JENNINGS, M. P., MORONA, R., WANG, H., FOCARETA, A., RODDAM, L. F. & PATON, J. C. (2005) Recombinant probiotics for treatment and prevention of enterotoxigenic *Escherichia coli* diarrhea. *Gastroenterology,* 128**,** 1219-28.

PATON, A. W., MORONA, R. & PATON, J. C. (2000a) A new biological agent for treatment of Shiga toxigenic Escherichia coli infections and dysentery in humans. *Nat Med,* 6**,** 265-70.

PATON, A. W., MORONA, R. & PATON, J. C. (2000b) A new biological agent for treatment of Shiga toxigenic *Escherichia coli* infections and dysentery in humans. *Nat Med,* 6**,** 265-70.

PATON, A. W., MORONA, R. & PATON, J. C. (2001a) Neutralization of Shiga toxins Stx1, Stx2c, and Stx2e by recombinant bacteria expressing mimics of globotriose and globotetraose. *Infect Immun,* 69**,** 1967-70.

PATON, A. W., MORONA, R. & PATON, J. C. (2006b) Designer probiotics for prevention of enteric infections. *Nat Rev Microbiol,* 4**,** 193-200.

PATON, A. W. & PATON, J. C. (2005) Multiplex PCR for direct detection of Shiga toxigenic *Escherichia coli* strains producing the novel subtilase cytotoxin. *J Clin Microbiol,* 43**,** 2944-7.

PATON, A. W., PATON, J. C., GOLDWATER, P. N., HEUZENROEDER, M. W. & MANNING, P. A. (1993a) Sequence of a variant Shiga-like toxin type-I operon of *Escherichia coli* O111:H. *Gene,* 129**,** 87-92.

PATON, A. W., PATON, J. C., HEUZENROEDER, M. W., GOLDWATER, P. N. & MANNING, P. A. (1992) Cloning and nucleotide sequence of a variant Shiga-like toxin II gene from *Escherichia coli* OX3:H21 isolated from a case of sudden infant death syndrome. *Microb Pathog,* 13**,** 225-36.

PATON, A. W., PATON, J. C. & MANNING, P. A. (1993b) Polymerase chain reaction amplification, cloning and sequencing of variant *Escherichia coli* Shiga-like toxin type II operons. *Microb Pathog,* 15**,** 77-82.

PATON, A. W., RATCLIFF, R. M., DOYLE, R. M., SEYMOUR-MURRAY, J., DAVOS, D., LANSER, J. A. & PATON, J. C. (1996) Molecular microbiological investigation of an outbreak of hemolytic-uremic syndrome caused by dry fermented sausage contaminated with Shiga-like toxin-producing *Escherichia coli*. *J Clin Microbiol,* 34**,** 1622-7.

PATON, A. W., SRIMANOTE, P., TALBOT, U. M., WANG, H. & PATON, J. C. (2004) A New Family of Potent AB5 Cytotoxins Produced by Shiga Toxigenic Escherichia coli. *J Exp Med,* 200**,** 35-46.

PATON, A. W., SRIMANOTE, P., WOODROW, M. C. & PATON, J. C. (2001b) Characterization of Saa, a novel autoagglutinating adhesin produced by locus of enterocyte effacement-negative Shiga-toxigenic *Escherichia coli* strains that are virulent for humans. *Infect Immun,* 69**,** 6999-7009.

PATON, A. W., WOODROW, M. C., DOYLE, R. M., LANSER, J. A. & PATON, J. C. (1999) Molecular characterization of a Shiga toxigenic *Escherichia coli* O113:H21 strain lacking eae responsible for a cluster of cases of hemolytic-uremic syndrome. *J Clin Microbiol,* 37**,** 3357-61.

PATON, J. C. & PATON, A. W. (1998) Pathogenesis and diagnosis of Shiga toxin-producing *Escherichia coli* infections. *Clin Microbiol Rev,* 11**,** 450-79.

PELLIZZARI, A., PANG, H. & LINGWOOD, C. A. (1992) Binding of verocytotoxin 1 to its receptor is influenced by differences in receptor fatty acid content. *Biochemistry,* 31**,** 1363-70.

Perna, N. T., Plunkett, G., 3rd, Burland, V., Mau, B., Glasner, J. D., Rose, D. J., Mayhew, G. F., Evans, P. S., Gregor, J., Kirkpatrick, H. A., Posfai, G., Hackett, J., Klink, S., Boutin, A., Shao, Y., Miller, L., Grotbeck, E. J., Davis, N. W., Lim, A., Dimalanta, E. T., Potamousis, K. D., Apodaca, J., Anantharaman, T. S., Lin, J., Yen, G., Schwartz, D. C., Welch, R. A. & Blattner, F. R. (2001) Genome sequence of enterohaemorrhagic *Escherichia coli* O157:H7. *Nature,* 409**,** 529-33.

PIZZA, M., GIULIANI, M. M., FONTANA, M. R., MONACI, E., DOUCE, G., DOUGAN, G., MILLS, K. H., RAPPUOLI, R. & DEL GIUDICE, G. (2001) Mucosal vaccines: non toxic derivatives of LT and CT as mucosal adjuvants. *Vaccine,* 19**,** 2534-41.

PLAUT, R. D. & CARBONETTI, N. H. (2008) Retrograde transport of pertussis toxin in the mammalian cell. *Cell Microbiol,* 10**,** 1130-9.

POPOFF, M. R. (1998) Interactions between bacterial toxins and intestinal cells. *Toxicon,* 36**,** 665-85.

PUDYMAITIS, A. & LINGWOOD, C. A. (1992) Susceptibility to verotoxin as a function of the cell cycle. *J Cell Physiol,* 150**,** 632-9.

RAO, R. V., ELLERBY, H. M. & BREDESEN, D. E. (2004) Coupling endoplasmic reticulum stress to the cell death program. *Cell Death Differ,* 11**,** 372-80.

RAPPUOLI, R., PIZZA, M., DOUCE, G. & DOUGAN, G. (1999) Structure and mucosal adjuvanticity of cholera and *Escherichia coli* heat-labile enterotoxins. *Immunol Today,* 20**,** 493-500.

ROBINS-BROWNE, R. M., ELLIOTT, E. J. & DESMARCHELIER, P. (1998) Shiga Toxin-Producing *Escherichia coli* in Australia. IN KAPER, J. B. & O'BRIEN, A. D. (Eds.) Escherichia coli *O157:H7 and other Shiga toxin-producing* E. coli *strains. (Presentations and Discussions of the 3rd International Symposium held 22-26 June 1997, in Baltimore, Maryland.).* Washington, DC., American Society for Microbiology Press.

ROGALSKI, A. A. & SINGER, S. J. (1984) Associations of elements of the Golgi apparatus with microtubules. *J Cell Biol,* 99**,** 1092-100.

ROGERS, T. J., PATON, A. W., MCCOLL, S. R. & PATON, J. C. (2003) Enhanced CXC chemokine responses of human colonic epithelial cells to locus of enterocyte effacement-negative Shiga-toxigenic *Escherichia coli*. *Infect Immun,* 71**,** 5623-32.

ROSE, P. & CHANT, I. (1998) Hematology of Hemolytic-Uremic Syndrome. IN KAPER, J. B. & O'BRIEN, A. D. (Eds.) Escherichia coli *O157:H7 and other Shiga toxin-producing* E. coli *strains. (Presentations and Discussions of the 3rd International Symposium held 22-26 June 1997, in Baltimore, Maryland.).* Washington, DC., American Society for Microbiology Press.

ROTHBERG, K. G., HEUSER, J. E., DONZELL, W. C., YING, Y. S., GLENNEY, J. R. & ANDERSON, R. G. (1992) Caveolin, a protein component of caveolae membrane coats. *Cell,* 68**,** 673-82.

ROWE, P. C., ORRBINE, E., OGBORN, M., WELLS, G. A., WINTHER, W., LIOR, H., MANUEL, D. & MCLAINE, P. N. (1994) Epidemic *Escherichia coli* O157:H7 gastroenteritis and hemolytic-uremic syndrome in a Canadian inuit community: intestinal illness in family members as a risk factor. *J Pediatr,* 124**,** 21-6.

RUSSELL, M. W., MOLDOVEANU, Z., WHITE, P. L., SIBERT, G. J., MESTECKY, J. & MICHALEK, S. M. (1996) Salivary, nasal, genital, and systemic antibody responses in monkeys immunized intranasally with a bacterial protein antigen and the Cholera toxin B subunit. *Infect Immun,* 64**,** 1272-83.

RUTJES, N. W., BINNINGTON, B. A., SMITH, C. R., MALONEY, M. D. & LINGWOOD, C. A. (2002) Differential tissue targeting and pathogenesis of verotoxins 1 and 2 in the mouse animal model. *Kidney Int,* 62**,** 832-45.

SAMUEL, J. E., PERERA, L. P., WARD, S., O'BRIEN, A. D., GINSBURG, V. & KRIVAN, H. C. (1990) Comparison of the glycolipid receptor specificities of Shiga-like toxin type II and Shiga-like toxin type II variants. *Infect Immun,* 58**,** 611-8.

SANCHEZ, J., WALLERSTROM, G., FREDRIKSSON, M., ANGSTROM, J. & HOLMGREN, J. (2002) Detoxification of cholera toxin without removal of its immunoadjuvanticity by the addition of (STa-related) peptides to the catalytic subunit. A potential new strategy to generate immunostimulants for vaccination. *J Biol Chem,* 277**,** 33369-77.

SANDRIN, M. S., VAUGHAN, H. A., DABKOWSKI, P. L. & MCKENZIE, I. F. (1993) Anti-pig IgM antibodies in human serum react predominantly with Gal(alpha 1-3)Gal epitopes. *Proc Natl Acad Sci U S A,* 90**,** 11391-5.

SANDVIG, K., GARRED, O., PRYDZ, K., KOZLOV, J. V., HANSEN, S. H. & VAN DEURS, B. (1992) Retrograde transport of endocytosed Shiga toxin to the endoplasmic reticulum. *Nature,* 358**,** 510-2.

SANDVIG, K., OLSNES, S., BROWN, J. E., PETERSEN, O. W. & VAN DEURS, B. (1989) Endocytosis from coated pits of Shiga toxin: a glycolipid-binding protein from *Shigella dysenteriae* 1. *J Cell Biol,* 108**,** 1331-43.

SANDVIG, K., OLSNES, S., PETERSEN, O. W. & VAN DEURS, B. (1987) Acidification of the cytosol inhibits endocytosis from coated pits. *J Cell Biol,* 105**,** 679-89.

SANDVIG, K., RYD, M., GARRED, O., SCHWEDA, E., HOLM, P. K. & VAN DEURS, B. (1994) Retrograde transport from the Golgi complex to the ER of both Shiga toxin and the nontoxic Shiga B-fragment is regulated by butyric acid and cAMP. *J Cell Biol,* 126**,** 53-64.

SANDVIG, K. & VAN DEURS, B. (1996) Endocytosis, intracellular transport, and cytotoxic action of Shiga toxin and ricin. *Physiol Rev,* 76**,** 949-66.

SANDVIG, K. & VAN DEURS, B. (2002) Membrane traffic exploited by protein toxins. *Annu Rev Cell Dev Biol,* 18**,** 1-24.

SAUKKONEN, K., BURNETTE, W. N., MAR, V. L., MASURE, H. R. & TUOMANEN, E. I. (1992) Pertussis toxin has eukaryotic-like carbohydrate recognition domains. *Proc Natl Acad Sci U S A,* 89**,** 118-22.

SAVAGE, D. C. (1977) Microbial ecology of the gastrointestinal tract. *Annu Rev Microbiol,* 31**,** 107-33.

SAXENA, S. K., O'BRIEN, A. D. & ACKERMAN, E. J. (1989) Shiga toxin, Shiga-like toxin II variant, and ricin are all single-site RNA N-glycosidases of 28 S RNA when microinjected into Xenopus oocytes. *J Biol Chem,* 264**,** 596-601.

SCHENGRUND, C. L. (2003) "Multivalent" saccharides: development of new approaches for inhibiting the effects of glycosphingolipid-binding pathogens. *Biochem Pharmacol,* 65**,** 699-707.

SCHENGRUND, C. L. & RINGLER, N. J. (1989) Binding of Vibrio cholera toxin and the heat-labile enterotoxin of *Escherichia coli* to GM1, derivatives of GM1, and nonlipid oligosaccharide polyvalent ligands. *J Biol Chem,* 264**,** 13233-7.

SCHMIDT, H. (2001) Shiga-toxin-converting bacteriophages. *Res Microbiol,* 152**,** 687-95.

SCHMITT, C. K., MCKEE, M. L. & O'BRIEN, A. D. (1991) Two copies of Shiga-like toxin II-related genes common in enterohemorrhagic *Escherichia coli* strains are responsible for the antigenic heterogeneity of the O157:H- strain E32511. *Infect Immun,* 59**,** 1065-73.

SCHMITZ, A., HERRGEN, H., WINKELER, A. & HERZOG, V. (2000) Cholera toxin is exported from microsomes by the Sec61p complex. *J Cell Biol,* 148**,** 1203-12.

SCOTLAND, S. M., SMITH, H. R., WILLSHAW, G. A. & ROWE, B. (1983) Vero cytotoxin production in strain of *Escherichia coli* is determined by genes carried on bacteriophage. *Lancet,* 2**,** 216.

SHAW, L. & SCHAUER, R. (1988) The biosynthesis of N-glycoloylneuraminic acid occurs by hydroxylation of the CMP-glycoside of N-acetylneuraminic acid. *Biol Chem Hoppe Seyler,* 369**,** 477-86.

SHERMAN, P., SONI, R. & KARMALI, M. (1988) Attaching and effacing adherence of Vero cytotoxin-producing *Escherichia coli* to rabbit intestinal epithelium in vivo. *Infect Immun,* 56**,** 756-61.

SHOGOMORI, H. & FUTERMAN, A. H. (2001) Cholera toxin is found in detergent-insoluble rafts/domains at the cell surface of hippocampal neurons but is internalized via a raft-independent mechanism. *J Biol Chem,* 276**,** 9182-8.

SIEZEN, R. J., DE VOS, W. M., LEUNISSEN, J. A. & DIJKSTRA, B. W. (1991) Homology modelling and protein engineering strategy of subtilases, the family of subtilisin-like serine proteinases. *Protein Eng,* 4**,** 719-37.

SIEZEN, R. J. & LEUNISSEN, J. A. (1997) Subtilases: the superfamily of subtilisin-like serine proteases. *Protein Sci,* 6**,** 501-23.

SIMONS, K. & IKONEN, E. (1997) Functional rafts in cell membranes. *Nature,* 387**,** 569-72.

SINGH, R. D., PURI, V., VALIYAVEETTIL, J. T., MARKS, D. L., BITTMAN, R. & PAGANO, R. E. (2003) Selective caveolin-1-dependent endocytosis of glycosphingolipids. *Mol Biol Cell,* 14**,** 3254-65.

SIXMA, T. K., PRONK, S. E., KALK, K. H., WARTNA, E. S., VAN ZANTEN, B. A., WITHOLT, B. & HOL, W. G. (1991) Crystal structure of a cholera toxin-related heat-labile enterotoxin from E. coli. *Nature,* 351**,** 371-7.

SKINNER, L. M. & JACKSON, M. P. (1997) Investigation of ribosome binding by the Shiga toxin A1 subunit, using competition and site-directed mutagenesis. *J Bacteriol,* 179**,** 1368-74.

SMITH, D. C., LORD, J. M., ROBERTS, L. M. & JOHANNES, L. (2004) Glycosphingolipids as toxin receptors. *Semin Cell Dev Biol,* 15**,** 397-408.

SMITH, H. R., ROWE, B., ADAK, G. K. & REILLY, W. J. (1998) Shiga Toxin (Verocytotoxin)-Producing *Escherichia coli* in the United Kingdom. IN KAPER, J. B. & O'BRIEN, A. D. (Eds.) Escherichia coli *O157:H7 and other Shiga toxin-producing* E. coli *strains. (Presentations and Discussions of the 3rd International Symposium held 22-26 June 1997, in Baltimore, Maryland.).* Washington, DC., American Society for Microbiology Press.

SMITH, H. W., GREEN, P. & PARSELL, Z. (1983) Vero cell toxins in *Escherichia coli* and related bacteria: transfer by phage and conjugation and toxic action in laboratory animals, chickens and pigs. *J Gen Microbiol,* 129 (Pt 10)**,** 3121-37.

SMITH, W. E., KANE, A. V., CAMPBELL, S. T., ACHESON, D. W., COCHRAN, B. H. & THORPE, C. M. (2003) Shiga toxin 1 triggers a ribotoxic stress response leading to p38 and JNK activation and induction of apoptosis in intestinal epithelial cells. *Infect Immun,* 71**,** 1497-504.

SORIANI, M., SANTI, I., TADDEI, A., RAPPUOLI, R., GRANDI, G. & TELFORD, J. L. (2006) Group B Streptococcus crosses human epithelial cells by a paracellular route. *J Infect Dis,* 193**,** 241-50.

SPANGLER, B. D. (1992) Structure and function of cholera toxin and the related *Escherichia coli* heat-labile enterotoxin. *Microbiol Rev,* 56**,** 622-47.

SPIKA, S. J., KHAKHRIA, R., MICHEL, P., MILLEY, D., WILSON, J. & WATERS, J. (1998) Shiga Toxin-Producing Escherichia coli Infections in Canada. IN KAPER, J. B. & O'BRIEN, A. D. (Eds.) Escherichia coli *O157:H7 and other Shiga toxin-producing* E. coli *strains. (Presentations and Discussions of the 3rd International Symposium held 22-26 June 1997, in Baltimore, Maryland.).* Washington, DC., American Society for Microbiology Press.

STEIN, P. E., BOODHOO, A., ARMSTRONG, G. D., COCKLE, S. A., KLEIN, M. H. & READ, R. J. (1994a) The crystal structure of pertussis toxin. *Structure,* 2**,** 45-57.

STEIN, P. E., BOODHOO, A., ARMSTRONG, G. D., HEERZE, L. D., COCKLE, S. A., KLEIN, M. H. & READ, R. J. (1994b) Structure of a pertussis toxin-sugar complex as a model for receptor binding. *Nat Struct Biol,* 1**,** 591-6.

STROCKBINE, N. A., JACKSON, M. P., SUNG, L. M., HOLMES, R. K. & O'BRIEN, A. D. (1988) Cloning and sequencing of the genes for Shiga toxin from *Shigella dysenteriae* type 1. *J Bacteriol,* 170**,** 1116-22.

STROCKBINE, N. A., MARQUES, L. R., NEWLAND, J. W., SMITH, H. W., HOLMES, R. K. & O'BRIEN, A. D. (1986) Two toxin-converting phages from *Escherichia coli* O157:H7 strain 933 encode antigenically distinct toxins with similar biologic activities. *Infect Immun,* 53**,** 135-40.

SUETAKE, K. & YU, R. K. (2003) Thin-layer chromatography; immunostaining of glycolipid antigens; and interpretation of false-positive findings with acidic lipids. *Methods Enzymol,* 363**,** 312-9.

SUN, J. B., HOLMGREN, J. & CZERKINSKY, C. (1994) Cholera toxin B subunit: an efficient transmucosal carrier-delivery system for induction of peripheral immunological tolerance. *Proc Natl Acad Sci U S A,* 91**,** 10795-9.

SVENNERHOLM, L. (Ed.) (1980) *Structure and function of gangliosides,* New York, Plenum Press.

SWINBANKS, D. (1996) Japan shuns radishes after 'possible link' to *E. coli*. *Nature,* 382**,** 567.

TAKANO, M., KOYAMA, Y., NISHIKAWA, H., MURAKAMI, T. & YUMOTO, R. (2004) Segment-selective absorption of lysozyme in the intestine. *Eur J Pharmacol,* 502**,** 149-55.

TAKANO, Y., HIRAMATSU, N., OKAMURA, M., HAYAKAWA, K., SHIMADA, T., KASAI, A., YOKOUCHI, M., SHITAMURA, A., YAO, J., PATON, A. W., PATON, J. C. &

KITAMURA, M. (2007) Suppression of cytokine response by GATA inhibitor K-7174 via unfolded protein response. *Biochem Biophys Res Commun,* 360**,** 470-5.

TAKAO, T., TANABE, T., HONG, Y. M., SHIMONISHI, Y., KURAZONO, H., YUTSUDO, T., SASAKAWA, C., YOSHIKAWA, M. & TAKEDA, Y. (1988) Identity of molecular structure of Shiga-like toxin I (VT1) from *Escherichia coli* O157:H7 with that of Shiga toxin. *Microb Pathog,* 5**,** 57-69.

TAKIZAWA, C. G. & MORGAN, D. O. (2000) Control of mitosis by changes in the subcellular location of cyclin-B1-Cdk1 and Cdc25C. *Curr Opin Cell Biol,* 12**,** 658-65.

TALBOT, U. M., PATON, J. C. & PATON, A. W. (2005) Protective immunization of mice with an active-site mutant of subtilase cytotoxin of Shiga toxin-producing Escherichia coli. *Infect Immun,* 73**,** 4432-6.

TANGVORANUNTAKUL, P., GAGNEUX, P., DIAZ, S., BARDOR, M., VARKI, N., VARKI, A. & MUCHMORE, E. (2003) Human uptake and incorporation of an immunogenic nonhuman dietary sialic acid. *Proc Natl Acad Sci U S A,* 100**,** 12045-50.

TETER, K., ALLYN, R. L., JOBLING, M. G. & HOLMES, R. K. (2002) Transfer of the cholera toxin A1 polypeptide from the endoplasmic reticulum to the cytosol is a rapid process facilitated by the endoplasmic reticulum-associated degradation pathway. *Infect Immun,* 70**,** 6166-71.

THOMPSON, J. P. & SCHENGRUND, C. L. (1997) Oligosaccharide-derivatized dendrimers: defined multivalent inhibitors of the adherence of the cholera toxin B subunit and the heat labile enterotoxin of *E. coli* to GM1. *Glycoconj J,* 14**,** 837-45.

TOCHIKUBO, K., ISAKA, M., YASUDA, Y., KOZUKA, S., MATANO, K., MIURA, Y. & TANIGUCHI, T. (1998) Recombinant cholera toxin B subunit acts as an adjuvant for the mucosal and systemic responses of mice to mucosally co-administered bovine serum albumin. *Vaccine,* 16**,** 150-5.

TOWBIN, H., STAEHELIN, T. & GORDON, J. (1979) Electrophoretic transfer of proteins from polyacrylamide gels to nitrocellulose sheets: procedure and some applications. *Proc Natl Acad Sci U S A,* 76**,** 4350-4.

TROY, F. A., 2ND (1992) Polysialylation: from bacteria to brains. *Glycobiology,* 2**,** 5-23.

TSAI, B. & RAPOPORT, T. A. (2002) Unfolded cholera toxin is transferred to the ER membrane and released from protein disulfide isomerase upon oxidation by Ero1. *J Cell Biol,* 159**,** 207-16.

TSAI, B., RODIGHIERO, C., LENCER, W. I. & RAPOPORT, T. A. (2001) Protein disulfide isomerase acts as a redox-dependent chaperone to unfold cholera toxin. *Cell,* 104**,** 937-48.

TURNER, J. R. & TARTAKOFF, A. M. (1989) The response of the Golgi complex to microtubule alterations: the roles of metabolic energy and membrane traffic in Golgi complex organization. *J Cell Biol,* 109**,** 2081-8.

TUTTLE, J., GOMEZ, T., DOYLE, M. P., WELLS, J. G., ZHAO, T., TAUXE, R. V. & GRIFFIN, P. M. (1999) Lessons from a large outbreak of *Escherichia coli* O157:H7 infections: insights into the infectious dose and method of widespread contamination of hamburger patties. *Epidemiol Infect,* 122**,** 185-92.

VAN DE KAR, N. C., KOOISTRA, T., VERMEER, M., LESSLAUER, W., MONNENS, L. A. & VAN HINSBERGH, V. W. (1995) Tumor necrosis factor alpha induces endothelial galactosyl transferase activity and verocytotoxin receptors. Role of specific tumor necrosis factor receptors and protein kinase C. *Blood,* 85**,** 734-43.

VAN DE KAR, N. C., MONNENS, L. A., KARMALI, M. A. & VAN HINSBERGH, V. W. (1992) Tumor necrosis factor and interleukin-1 induce expression of the verocytotoxin receptor globotriaosylceramide on human endothelial cells: implications for the pathogenesis of the hemolytic uremic syndrome. *Blood,* 80**,** 2755-64.

VAN DEURS, B., TONNESSEN, T. I., PETERSEN, O. W., SANDVIG, K. & OLSNES, S. (1986) Routing of internalized ricin and ricin conjugates to the Golgi complex. *J Cell Biol,* 102**,** 37-47.

VAN GINKEL, F. W., JACKSON, R. J., YUKI, Y. & MCGHEE, J. R. (2000) Cutting edge: the mucosal adjuvant cholera toxin redirects vaccine proteins into olfactory tissues. *J Immunol,* 165**,** 4778-82.

VARKI, A. (1992) Diversity in the sialic acids. *Glycobiology,* 2**,** 25-40.

VARKI, A. (1993) Biological roles of oligosaccharides: all of the theories are correct. *Glycobiology,* 3**,** 97-130.

VARKI, A. (1998) Factors controlling the glycosylation potential of the Golgi apparatus. *Trends Cell Biol,* 8**,** 34-40.

VERMA, A., DAVIS, G. E. & IHLER, G. M. (2000) Infection of human endothelial cells with *Bartonella bacilliformis* is dependent on Rho and results in activation of Rho. *Infect Immun,* 68**,** 5960-9.

VIEIRA, J. & MESSING, J. (1991) New pUC-derived cloning vectors with different selectable markers and DNA replication origins. *Gene,* 100**,** 189-94.

WANG, H., PATON, J. C. & PATON, A. W. (2007) Pathologic changes in mice induced by subtilase cytotoxin, a potent new *Escherichia coli* AB_5 toxin that targets the endoplasmic reticulum. *J Infect Dis,* 196**,** 1093-101.

WANG, L. H., ROTHBERG, K. G. & ANDERSON, R. G. (1993) Mis-assembly of clathrin lattices on endosomes reveals a regulatory switch for coated pit formation. *J Cell Biol,* 123**,** 1107-17.

WATANABE, M., MATSUOKA, K., KITA, E., IGAI, K., HIGASHI, N., MIYAGAWA, A., WATANABE, T., YANOSHITA, R., SAMEJIMA, Y., TERUNUMA, D., NATORI, Y. & NISHIKAWA, K. (2004) Oral therapeutic agents with highly clustered globotriose for treatment of Shiga toxigenic *Escherichia coli* infections. *J Infect Dis,* 189**,** 360-8.

WATERS, J. R., SHARP, J. C. & DEV, V. J. (1994) Infection caused by *Escherichia coli* O157:H7 in Alberta, Canada, and in Scotland: a five-year review, 1987-1991. *Clin Infect Dis,* 19**,** 834-43.

WEINSTEIN, D. L., JACKSON, M. P., SAMUEL, J. E., HOLMES, R. K. & O'BRIEN, A. D. (1988) Cloning and sequencing of a Shiga-like toxin type II variant from *Escherichia coli* strain responsible for edema disease of swine. *J Bacteriol,* 170**,** 4223-30.

WELLS, J. G., SHIPMAN, L. D., GREENE, K. D., SOWERS, E. G., GREEN, J. H., CAMERON, D. N., DOWNES, F. P., MARTIN, M. L., GRIFFIN, P. M., OSTROFF, S. M. & ET AL. (1991) Isolation of *Escherichia coli* serotype O157:H7 and other Shiga-like-toxin-producing *E. coli* from dairy cattle. *J Clin Microbiol,* 29**,** 985-9.

WILLIAMS, N. A., HIRST, T. R. & NASHAR, T. O. (1999) Immune modulation by the cholera-like enterotoxins: from adjuvant to therapeutic. *Immunol Today,* 20**,** 95-101.

WILLIAMS, S. J. & DAVIES, G. J. (2001) Protein--carbohydrate interactions: learning lessons from nature. *Trends Biotechnol,* 19**,** 356-62.

WOLF, A. A., FUJINAGA, Y. & LENCER, W. I. (2002) Uncoupling of the cholera toxin-GM1 ganglioside receptor complex from endocytosis, retrograde Golgi trafficking, and downstream signal transduction by depletion of membrane cholesterol. *J Biol Chem,* 277**,** 16249-56.

WOLF, A. A., JOBLING, M. G., WIMER-MACKIN, S., FERGUSON-MALTZMAN, M., MADARA, J. L., HOLMES, R. K. & LENCER, W. I. (1998) Ganglioside structure dictates signal transduction by cholera toxin and association with caveolae-like membrane domains in polarized epithelia. *J Cell Biol,* 141**,** 917-27.

YAHIRO, K., MORINAGA, N., SATOH, M., MATSUURA, G., TOMONAGA, T., NOMURA, F., MOSS, J. & NODA, M. (2006) Identification and characterization of receptors for vacuolating activity of subtilase cytotoxin. *Mol Microbiol,* 62**,** 480-90.

YAMAMOTO, M., BRILES, D. E., YAMAMOTO, S., OHMURA, M., KIYONO, H. & MCGHEE, J. R. (1998) A nontoxic adjuvant for mucosal immunity to pneumococcal surface protein A. *J Immunol,* 161**,** 4115-21.

YAMAMOTO, S., TAKEDA, Y., YAMAMOTO, M., KURAZONO, H., IMAOKA, K., YAMAMOTO, M., FUJIHASHI, K., NODA, M., KIYONO, H. & MCGHEE, J. R. (1997) Mutants in the ADP-ribosyltransferase cleft of cholera toxin lack diarrheagenicity but retain adjuvanticity. *J Exp Med,* 185**,** 1203-10.

YE, J., KITAJIMA, K., INOUE, Y., INOUE, S. & TROY, F. A., 2ND (1994) Identification of polysialic acids in glycoconjugates. *Methods Enzymol,* 230**,** 460-84.

YU, M. & HASLAM, D. B. (2005) Shiga toxin is transported from the endoplasmic reticulum following interaction with the luminal chaperone HEDJ/ERdj3. *Infect Immun,* 73**,** 2524-32.

ZHANG, Z., MERRITT, E. A., AHN, M., ROACH, C., HOU, Z., VERLINDE, C. L., HOL, W. G. & FAN, E. (2002) Solution and crystallographic studies of branched multivalent ligands that inhibit the receptor-binding of cholera toxin. *J Am Chem Soc,* 124**,** 12991-8.

ZHU, A. & HURST, R. (2002) Anti-N-glycolylneuraminic acid antibodies identified in healthy human serum. *Xenotransplantation,* 9**,** 376-81.

Zopf, D. & Roth, S. (1996) Oligosaccharide anti-infective agents. Lancet, 347, 1017-21.